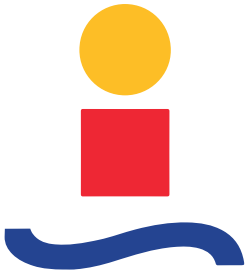

Resumen en castellano del proyecto: "Battery Swapping Station management supported by Intelligent Transport Systems: an MPC approach."

Ezequiel G. Debada

Eduardo F. Camacho

June 11, 2015

Contents

Resumen

Para lograr la completa integración del vehículo eléctrico (EV), es necesario solucionar varios problemas relacionados con el proceso de carga. Recientemente las "Battery Swapping Stations" o estaciones de intercambio de batería han surgido como una alternativa prometedora al planteamiento tradicional de las estaciones de carga de baterías (Battery Charging Stations). No obstante, las BSSs no están exentas de problemas que han de ser resueltos para que dicha estructura sea operacionalmente factible. Este proyecto propone un MPC como método de control de una BSS. En paralelo, este trabajo analiza la influencia de la precisión de la predicción de la demanda en el desempeño del control en términos de calidad de serivio (QoS) y beneficios; presenta un "Sistema de Transporte Inteligente" (ITS de sus siglas en inglés) para que las estaciones de carga tengan informacián en tiempo real de la congestión de tráfico y de su estado en los alrededores; y propone una estrategia de predicción basada en dicha información que posee un alto grado de robustez. Además, se desarrolla un entorno de simulación configurable que se utilizará como herramienta para testear las estrategias de control y de predicción de demanda presentados. Los resultados muestran el propio funcionamiento del algoritmo de control propuesto, la importancia de la exactitud de la predicción y detalla las ventajas que acarrea el uso de información en tiempo real en esos términos.

Chapter 1 Introducción

La electromovilidad está destinada a tener un fuerte impacto en muchos aspectos de nuestra vida diaria: fomentando nuevos hábitos de desplazamiento, proponiendo nuevos modelos de negocio y abriendo la puerta a nuevas configuraciones de vehículos imposibles con motores de combustión [1].

El cambio de paradigma del uso de los combustibles fósiles a la electricidad presenta algunas dificultades. El principal reto está relacionado con la red, que sería testigo de un drástico cambio en la forma y comportamiento de la curva de consumo. Sin embargo, incluso en esos términos, el control parcial de los EVs puede usarse como apoyo a la integración de puntos de generación distribuidas, equilibrado de fuentes renovables intermitentes, estabilización de la propia red etc [2].

Los largos tiempos de recarga, el coste de reemplazo y la autonomía de las baterías son los principales causantes de los problemas de integración y por ello, los principales focos de atención para la comunidad científica. Las BSSs surgen como una alternativa de recarga con amplias posibilidades técnicas [3, 4, 5, 6, 7] y empresariales. En la literatura pueden encontrarse trabajos centrados en la ventaja de tener control sobre los hábitos de grandes flotas de EVs, y estas conclusiones son extrapolables a las BSSs, además de que la flexibilidad de operación de esta configuración en cuanto a la (des)carga de las baterías, supondría precios más competitivos, menor degradación de las baterías etc.

La mayor dificultad que acompaña a esta novedosa configuración es el hecho de que las baterías a servir deben ser recargas con anterioridad a la llegada de los clientes, por lo que se requiere una estimación veraz de esa futura demanda. Los retos propuestos por esta condición pueden reducirse si se considera la utilización de ITSs [8], un nuevo concepto de uso e intercambio de información entre vehículos muy popular los últimos años [9] (como demuestra el reciente proyecto *INRIX* [10] presentado por *BMW*). Esto supondría la disponibilidad en tiempo real de información sobre la densidad de tráfico y los estados de las baterías que podría utilizarse para reducir el error de predicción.

Por otro lado, la ausencia de infraestructuras reales y la falta de datos en general supone una dificultad añadida. A pesar de ello, puesto que la propia factibilidad de la integración de los EVs está estrechamente relacionada con el rendimiento de su operación, la investigación en esta dirección debe continuar.

Este artículo estudia alguno de los retos asociados a las BSSs, más concretamente, aquellos relacionados con su gestión en general así como con la influencia de la predicción de la demanda en su rendimiento. Siendo las principales contribuciones, la formulación de un MPC para el control de una BSSs y la propuesta de un simple ITS empleado para la generación de predicciones de demanda adecuadas.

El resto de este artículo se organiza como sigue: La Sección 2 presenta el simulador, describe el sistema y detalla los métodos de control y predicción. La Sección 6 muestra los principales resultados que serán posteriormente discutidos en la Sección 7, donde también se recogen posibles líneas de trabajos futuros.

Chapter 2 Simulador

El simulador que se presenta en esta sección está inspirado en el utilizado por Jenniferen Johnson et al. en [11] cuya principal característica es la simplicidad. Como puede verse en la Figura 2.1, dicha simplicidad se refiere a la ausencia de mapas y en consecuencia, la sencillez del cálculo de rutas o el posicionamiento de las estaciones de carga.

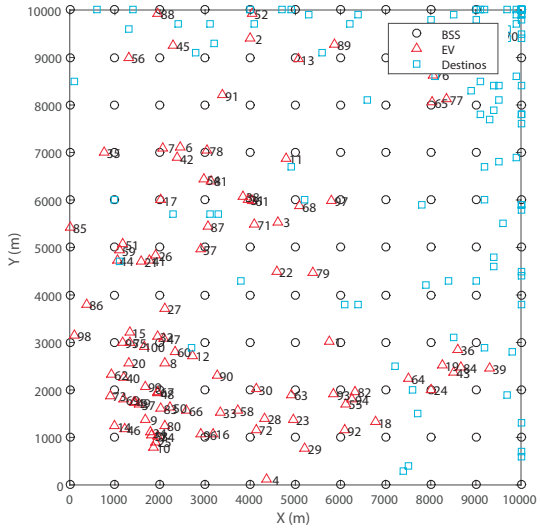

Figure 2.1: Vista general del simulador

Para definir su funcionamiento, se han de cubrir los siguientes aspectos:

- Consideraciones geométricas
- Comportamiento EVs
- Operación de BSSs
- Información en tiempo real (ITS).

2.0.1 Consideraciones geométricas

Las consideraciones geométricas engloban la dimensione del escenario, la posición de las estaciones y la generación de los puntos de partida y destino que corresponderán a las rutas de los EVs.

Geometría del escenario

Se considera un escenario cuadrado de dimensiones $SC_{Heigh} \times SC_{Width}$ m, con nCS estaciones de carga homogéneamente distribuidas con una separación de $CS_{Spacing}$ m. Valores que pueden ser modificados para influir indirectamente en los niveles de congestión alcanzados en las estaciones, el número de eventos de recarga etc.

Inicio/Final de ruta

Si se pretenden contrastar técnicas de predicción de demanda con este simulador, es deseable conseguir un cierto grado de repetibilidad en relación al desplazamiento de los vehículos. Esto se consigue generando los puntos de

inicio y fin de ruta atendiendo a una cierta Función de Densidad Probabilidad (PDF) de forma similar a como se hace en [12]. Donde la probabilidad de que un punto (x, y) sea considerado punto de inicio/final de ruta viene dado por las probabilidades $P^{Dep}(x, y)$ y $P^{Arr}(x, d)$ respectivamente.

$$P^{Dep}(x, y) = P^{Dep}(x)P^{Dep}(y) \tag{2.1}$$
$$P^{Arr}(x, y) = P^{Arr}(x)P^{Arr}(y) \tag{2.2}$$

Donde

$$P^{Dep}(x) = 1 - P^{Arr}(x) = \frac{(SC_{Width} - x)^3}{x(SC_{Width} - \frac{x^3}{4})} \tag{2.3}$$
$$P^{Dep}(y) = 1 - P^{Arr}(y) = \frac{(SC_{Height} - y)^3}{y(SC_{Height} - \frac{y^3}{4})} \tag{2.4}$$

En la Figura 2.2 se observa un conjunto de puntos de inicio y destino generados de esta manera.

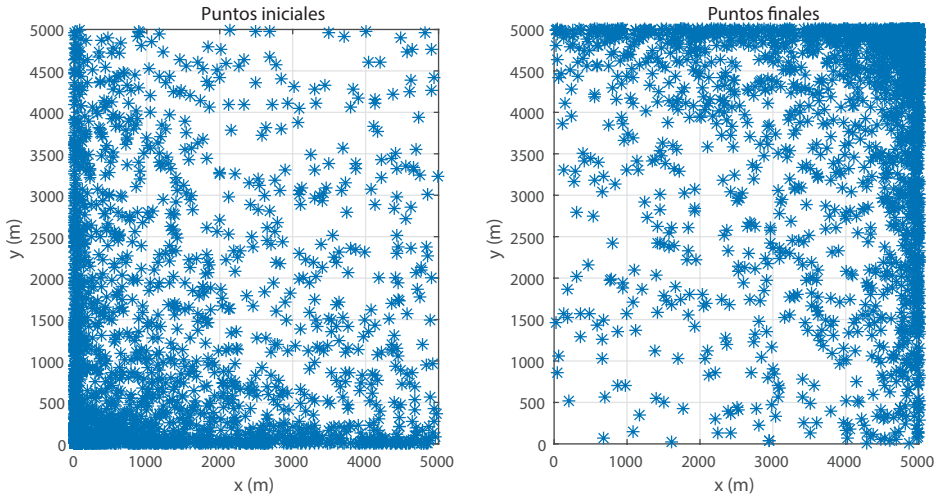

Figure 2.2: Distribución de posiciones de inicio y final de ruta

2.0.2 Comportamiento de EVs

Puesto que la materia a estudio en este trabajo no requiere un comportamiento complejo por parte de los clientes, la racionalidad supuesta a los EVs será muy simple.

Características de los EVs

Los vehículos se limitarán a desplazarse desde los puntos iniciales a los finales en línea recta y a velocidad *vel* m/s. Los estados de carga iniciales de las baterías (SoC) se generarán aleatoriamente y las características de las baterías (capacidad, flujo de potencia máxima etc) se asumen comunes a todos los vehículos.

Gestión de recarga.

Los EVs decidirán dirigirse hacia una BSS cuando su SoC está por debajo de SoC_{charge} y la BSS será seleccionada atendiendo al criterio de mínima distancia.

2.0.3 BSS

La operación de la BSS es el objeto de análisis de este artículo por lo que, el funcionamiento detallado de estas se expone en las siguientes secciones.

2.0.4 Información en tiempo real

Se propone un sistema de para generar información en tiempo real con la que se consiga tener una visión general del estado del tráfico manejando una cantidad reducida de datos y sin atentar contra la privacidad de los conductores. Para ello se divide el mapa en celdas, y a cada celda se le asocian dos datos:

- Cantidad de vehículos en la celda EV_{cell}.
- El SoC medio de los vehículos en la celda SoC_{cell}.

De esta forma, no es posible conocer con certeza ningún tipo de información personal de ningún usuario y el número de datos a manejar sólo de penderá de la extensión de terreno de la que se requiera información.

2.1 Resumen de parámetros.

En la Tabla 2.1 se presentan los valores típicos utilizados en la configuración del simulador en este trabajo.

Parámetros	**Valor**
nEV	100
Tamaño de escenario	500×500 m
Espaciado entre BSSs	500 m
Velocidad de EVs	20 m/s
Tamaño de celdas de información	500 m

Table 2.1: Relación de parámetros del simulador.

Chapter 3 Arquitectura del Sistema

El modelo completo de una BSS puede dividirse en dos módulos principales (Figura 3.1): una cola de recepción abierta a la que llegan los nuevos clientes, y le BSS propiamente dice que contiene un conjunto de baterías a gestionar y puestos de intercambio de baterías (SSs de sus siglas en inglés).

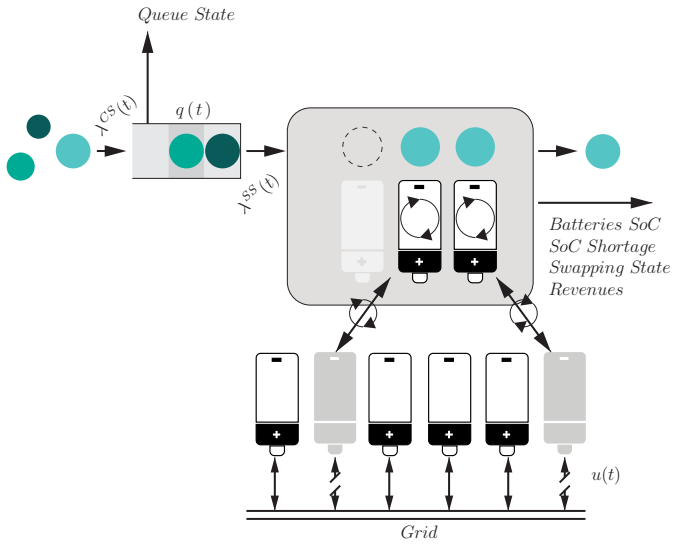

Figure 3.1: Arquitectura de una BSS

Modelo de cola

La cola de recepción se encarga de albergar a aquellos clientes que no pueden ser servidos por no haber puestos de intercambio libres (Figura 3.2).

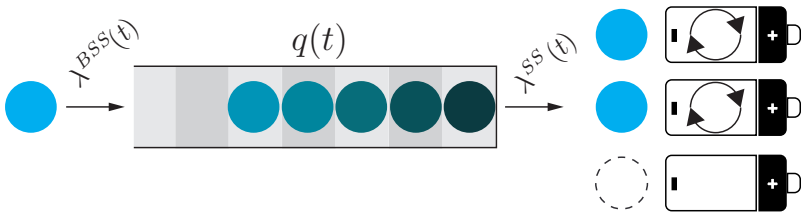

Figure 3.2: Cola de recepción

La presencia de la cola de recepción hace que el ratio de llegada de clientes a la BSS ($\lambda^{BSS}(t)$) sea distinto del ratio de clientes tomando los puestos de intercambio ($\lambda^{SS}(t)$). La relación entre ambos viene dada por el modelo de la cola que resulta de aplicar ecuaciones de balance a la misma.

$$\sum_{\tau=1}^{t\in T}(\lambda^{BSS}(\tau) - \lambda^{SS}(\tau)) = nEV_Q(\tau) \tag{3.1}$$

$$nEV_Q(t+1) = nEV_Q(t) + \lambda^{BSS}(t) - \lambda^{SS}(t) \tag{3.2}$$

donde $nEV_Q(t)$ representa el número de Electric Vehicles (EVs) en cola en el instante t y donde se cumple que $\lambda^{SS}(\tau) \leq nSS$.

BSS

La BSS propiamente dicha engloba un cierto número de baterías y puestos de intercambio y su objetivo consiste en gestionar el estado de carga de las baterías para maximizar los beneficios.

La propia naturaleza de esta configuración conlleva algunas características particulares: la operación de cambio de batería tiene una duración fija, los usuarios no puedes solicitar un SoC personalizado puesto que las baterías deben estar listas antes de la llegada de los clientes y precisamente por esto último, el rendimiento de una BSS está condicionado a la precisión de su predicción.

El hecho de que las BSSs no estén obligadas a cargar las baterías en el menor tiempo posible les permite aplicar señales de control suaves o incluso vender la energía almacenada en ellas si resulta beneficioso.

Además, se asume que todas las baterías están conectadas directamente a la red así como que la operación de intercambio de batería comienza en el preciso instante en el que un cliente toma el puesto de intercambio.

Parámetros

El tamaño de una BSS viene dado por el número de baterías $nBat \in \mathbb{N}^+$ y el número de puestos de intercambio $nSS \in \mathbb{N}^+$, mientras que el proceso de carga queda definido por la potencia máxima que admiten las baterías $P^M_{Ch} \in \mathbb{R}$ kW, la potencia máxima que puede consumir la estación P^M_{CS} kW, la capacidad de las baterías E^M_{Bat} kWh y el tiempo necesario para completar la operación de intercambio $TSwap$min.

Parámetros	Valores
$nBat$	5
nSS	4
P^M_{Ch}	80 kW
P^M_{CS}	160 kW
E^M_{Bat}	30 kWh
$TSwap$	15 min

Table 3.1: Valor típico de los parámetros

Estados del sistema

El estado del sistema viene definido por el SoC de las baterías modelado como:

$$SoC(t+1) = SoC(t) + \frac{P_i \Delta t}{E^M_{Bat}} \tag{3.3}$$

Donde P_i es la potencia aplicada a la batería, Δt el tiempo de muestreo y $Swap_j = (SS^c_j ont)/TSwap \forall j \in [1, nSS]$ el progreso de las operaciones de intercambios (si $SS^c_j ont$ un contador asociado a la SS-j).

Por otro lado se definen algunos estados binarios que serán utilizado en la formulación del MPC. En concreto una primera variable $Y_{b,j} \in \{0, 1\}$ que indica si la batería b está ocupando el puesto de intercambio j (1) o no (0) y una segunda variable $SoC^{LB} \in \{0, 1\}$ que se activa cuando el State of Charge (SoC) de la batería b se encuentra por debajo de un mínimo fijado.

Señales de control

Pueden diferenciarse dos conjuntos de señales de control. Un primer grupo que comanda la (des)carga de las baterías $u_i(t) \in \mathbb{R} : [0, 1]$ y un segundo grupo de señales de control binarias que da comienzo al proceso de cambio $x_{ij} \in 0, 1$.

La señal de control $u_i(t)$ es un valor normalizado de la potencia aplicada en el proceso de carga de forma que se cumple que

$$P_b(t) = U_b(t) P^M_{Ch}(t) \tag{3.4}$$

Señales externas

Finalmente, la llegada de usuarios a la BSS $\lambda^{BSS}(t) \in \mathbb{N}^+$ se considera una señal externa que está relacionada con el ratio de llegada a los postes de intercambio $\lambda^{SS}(t)$ a través del modelo de la cola.

Chapter 4 Control de BSS

Como se ha comentado anteriormente, un controlador de una BSS debería gestionar la (des)carga de las baterías, dar comienzo el proceso de intercambio, y generar la asignación de baterías-usuarios a servir. Este trabajo propone un MPC como método de control basado en [4].

MPC

La formulación del MPC está basado en el problema de optimización presentado por Mushfiqur R. Sarker et al. en [4]. La formulación ha sido cambiada para simplificar algunos aspectos (la consideración de varios tipos de baterías) e incluir otros (la duración del proceso de cambio, mínimo SoC deseado etc). La formulación propuesta es la siguiente:

Maximize

$$-\Big(\sum_{t\in T}\sum_{b\in B}\left(x_{b,t}-SoC_{b,t}^{\text{Short}}\right)-\sum_{t\in T}pr_t\left(e_t\right)- \\ -200\Big(\sum_{t\in T}D_t-\sum_{b\in B}x_{b,t}\Big)-9\sum_{t\in T}\sum_{b\in B}SoC_{b,t}^{Low} \tag{4.1}$$

Subject to

$$SoC_{b,t}=\left(SoC_{b,t-1}+\frac{TP_b^M}{E_b^M}\left(u_{b,t}^{ch}-u_{b,t}^{ds}\right)\right)\left(1-x_{b,t}\right)+ \\ +SoC_{b,t}^{ini}x_{b,t}\ \forall b\in B,t\in T \tag{4.2}$$

$$SoC_{b,t-1}+SoC_{b,t}^{\text{short}}\geq x_{b,t}\ \forall b\in B,t\in T \tag{4.3}$$

$$\sum_{b\in B}x_{b,t}+bat_t^{\text{short}}=\hat{\lambda}_t^{SS}\ \forall t\in T \tag{4.4}$$

$$e_t^{\text{buy}}-e_t^{\text{sell}}=TP_{Ch}^M\sum_{b\in B}\left(u_{b,t}^{\text{ch}}-u_{b,t}^{\text{ds}}\right)\ \forall t\in T \tag{4.5}$$

$$y_{b,t}\leq\sum_{t-\text{TSwap}}^{t}x_{b,t} \tag{4.6}$$

$$y_{b,t}\geq\frac{1}{\text{TSwap}}\sum_{t-\text{Swap Time}}^{t}x_{b,t} \tag{4.7}$$

$$0\leq u_{b,t}^{\text{ch}}\leq\left(1-y_{b,t}\right)\forall b\in B,t\in T \tag{4.8}$$

$$0\leq u_{b,t}^{\text{ds}}\leq\left(1-y_{b,t}\right)\forall b\in B,t\in T \tag{4.9}$$

$$SoC_{b,t}^{Low}\leq\left(1-SoC^{LB}\right)+SoC_{b,t} \tag{4.10}$$

$$SoC_{b,t}^{Low}\geq SoC_{b,t}-1-SoC^{LB} \tag{4.11}$$

$$P_{Ch}^{\text{M}}\sum_{b\in B}u_{b,t}^{\text{ch}}\leq P_{CS}^M \tag{4.12}$$

$$0\leq SoC_{i,t}\leq 1\ \forall b\in B,t\in T \tag{4.13}$$

$$0\leq SoC_{i,t}^{\text{short}}\leq 1\ \forall b\in B,t\in T \tag{4.14}$$

$$u_{b,t}^{\text{ch}}\leq 1\alpha_{b,t}\ \forall b\in B,t\in T \tag{4.15}$$

La restricción 4.2 implementa el modelo de carga de las baterías, donde la variable binaria $x_{b,t}$ es usada para resetear el SoC de las baterías cada vez que tiene lugar un intercambio. Las restricciones 4.3 y 4.4 sirven para cuantificar el

número de baterías no servidas y la falta de estado de carga de aquellas baterías servidas parcialmente cargadas. La Ecuación 4.5 registra la cantidad de energía comprada/vendida. Las restricciones 4.6 y 4.7 relacionan la variable binaria $y_{b,t}$ (que indica que una batería está siendo intercambiada) con la señal binaria de inicio de operación de cambio $x_{b,t}$. El bloqueo operacional impuesto a las baterías por el propio proceso de cambio se introduce con las Ecuaciones 4.8 y 4.9. Las restricciones 4.10 y 4.11 activan la variable binaria $SoC_{b,t}^{Low}$ cuando el SoC de la batería b se encuentra por debajo del nivel de seguridad previamente establecido. La Ecuación 4.13 asegura que la potencia utilizada no supera a la contratada por la BSS. Finalmente, las restricciones 4.13, 4.14 y 4.15 establecen el limite superior y inferior de las variables de decisión $u_{b,t}$, $SoC_{b,t}$ y $SoC_{b,t}^{\text{Short}}$.

La función objetivo 4.1 maximiza beneficios y penaliza el hecho de servir baterías parcialmente cargadas, le cantidad de energía comprada/vendida, las baterías no servidas, así como la violación del nivel mínimo de seguridad impuesto a las baterías.

El problema formulado corresponde a un Mixed integer nonlinear programming (MINLP) debido a la no linealidad introducida por la restricción 4.2. En este caso es posible deshacer la no linealidad mediante la introducción de variables intermedias $V_{b,t}^1, V_{b,t}^2, V_{b,t}^3$ (tal como se muestra en [14]). La reescritura de la restricción queda:

$$\begin{aligned} SoC_{b,t} =& SoC_{b,t-1} + TP_b^{\text{M}} \left(u_{b,t}^{\text{ch}} - u_{b,t}^{\text{ds}}\right) - V_{b,t}^1 - \\ & - TP_b^{\text{M}} \left(V_{b,t}^2 - V_{b,t}^3\right) + SoC_{b,t}^{ini} x_{b,t} \end{aligned} \tag{4.16}$$

Donde a las variables intermedias denotadas por V se les asocian la siguientes restricciones.

$$V_{b,t}^1 \leq SoC_{b,t-1} \tag{4.17}$$
$$V_{b,t}^1 \geq SoC_{b,t-1} - M(1 - x_{b,t}) \tag{4.18}$$
$$V_{b,t}^1 \leq M x_{b,t} \tag{4.19}$$

$$V_{b,t}^2 \leq u_{b,t}^{\text{ch}} \tag{4.20}$$
$$V_{b,t}^2 \geq u_{b,t}^{\text{ch}} - M(1 - x_{b,t}) \tag{4.21}$$
$$V_{b,t}^2 \leq M x_{b,t} \tag{4.22}$$

$$V_{b,t}^3 \leq u_{b,t}^{\text{ds}} \tag{4.23}$$
$$V_{b,t}^3 \geq u_{b,t}^{\text{ds}} - M(1 - x_{b,t}) \tag{4.24}$$
$$V_{b,t}^3 \leq M x_{b,t} \tag{4.25}$$

Problema que se ha resuelto mediante el solver *Cplex*.

Para estar en disposición de resolver el problema, queda aclarar algunos aspectos acerca del término $\hat{\lambda}_t^{SS}$ presente en la restricción 4.4, que será el tema a tratar en la próxima sección.

Chapter 5 Demanda

La predicción de demanda juega un papel importante en el rendimiento de las Battery Swapping Stations (BSSs) . Manejar una predicción precisa supone plantear mejores estrategias de mercado, proveer mejor Quality of Service (QoS) , gestionar de forma más eficiente las baterías etc. Este artículo propone usar un Intelligent Transport System (ITS) como herramienta para disminuir el error de predicción. El hecho de tener información del tráfico en tiempo real, precios de las BSS vecinas etc, supondría una ventaja en el desarrollo de técnicas avanzadas de predicción. En aras de comparación, este trabajo presentas dos posibles métodos que serán comparados en la sección 6.0.2: una estrategia basada en datos históricos, y otra que emplea la información del ITS .

Datos históricos

Esta primera opción hace uso de datos históricos para generar un patrón de llegada de usuarios probable $\lambda_{HD}^{BSS} = [l_i^{BSS,hd}]$. Dado un registro del patrón de demanda $\lambda_{Reg\#i}^{BSS} = [l_j^{cs,reg\#i}]\ \forall i \in [1,\cdots,N^{Reg}]\ \forall j \in [1,\cdots,N_2]$ con N^{Reg} muestras , los elementos del patrón vienen dados por:

$$l_i^{cs,hd} = \max(l_j^{cs,rg\#i})\ \forall i \in (1,\cdots,N^{Reg}) \tag{5.1}$$

Que equivale a considera en cada instante el máximo valor registrado en el pasado.

Planteamiento ITS

Se pretende obtener una predicción razonable de los clientes que llegarán en el futuro próximo a partir de los datos extraídos del ITS propuesto en la sección 2.0.4 que son básicamente:

$$SoC_{Cell} = \frac{\sum SoC}{nEV_{Cell}} \tag{5.2}$$

$$Ev_{Cell} = \frac{nEV_{Cell}}{nEV_{Tot}} \tag{5.3}$$

Se pretende por tanto estimar en t la llegada de usuarios a una BSS en $t+K$ ($\lambda^{BSS}(t+k|t)$) a partir de la información de las celdas ITS . Dada una celda, es posible obtener un rango ($[SoC_m, SoC_M]$) tal que, cualquier cliente en la celda con un SoC comprendido en el podría llegar a la BSS considerada en el instante $t+K$. Con ese rango, puede obtenerse una cota superior del número de usuarios que llegarán en $t+K$ provenientes de esa celda en particular.

Haciendo lo anterior con las celdas cercanas a la BSS, se tendría una estimación apropiada.

Rango de SoC Asumiendo la velocidad a la que se desplazan los EVs , puede calcularse una distancia (d_{path} m) asociada al instante de predicción de interés $t+K$ como:

$$d_{path} = K \cdot vel \tag{5.4}$$

Por tanto, d_{path} representa la distancia que un EV en la celda tiene que ser capaz de recorrer para llegar en el instante $t+K$. Asumiendo que los vehículos sólo describen líneas rectas (suposición válida para este trabajo), el lugar geométrico de los puntos cuya suma de distancias a la BSS y a la posición de la celda es igual a d_{path} viene dada por una elipse de focos coincidentes con la BSS y la celda.

Dicha elipse representa los puntos donde los EVs cambiarían de dirección, que en el escenario considerado, corresponde con el lugar en el que deciden ir a cargar.

Teniendo en cuenta la ecuación en polares de la elipse relativa a uno de sus focos (Ecuación 5.5), pueden obtenerse fácilmente los puntos más cercanos (asociado con SoC_m) y más alejados (SoC_M) a la celda donde puede darse la decisión de ir a cargar.

$$r(\theta) = \frac{a(1-e^2)}{1+e\cos(\theta)} \tag{5.5}$$

Tales puntos pueden calcularse haciendo $\frac{dr(\theta)}{d\theta} = 0$, identifica el punto $(0, a)$ como el más cercano, y el $(0, -a)$ como el más lejano. Con esto, los SoC que delimitan el rango serían:

$$SoC_m = SoC_{Charge} + (a - \frac{dist(CS, CELL)}{2})\frac{1}{Max\_Range} \tag{5.6}$$

$$SoC_M = SoC_{Charge} + \frac{a + dist(CS, CELL)}{Max\_Range} \tag{5.7}$$

Máximo número de usuarios posibles Conocido la SoC medio y el número de usuarios en una celda, puede obtenerse una cota superior del número de usuarios en la celda con un SoC concreto. Para un SoC objetivo de SoC $= SoC^*$ dicha cota superior ($nEV^M_{SoC^*}$) es:

$$nEV^M_{SoC^*} = \frac{nEV_{Cell}(1 - SoC_{Cell})}{1 - SoC^*} \tag{5.8}$$

si $SoC^* \leq SoC_{Cell}$ y

$$nEV^M_{SoC^*} = \frac{nEV_{Cell} SoC_{Cell}}{SoC^*} \tag{5.9}$$

si $SoC^* \geq SoC_{Cell}$.

La Figura 5.1 muestra la representación de dicha cota para todo el rango de SoC dado diferentes SoC_{Cell} (lineas discontinuas verticales) y el número de EVs en la celda nEV_{Cell} (Línea horizontal).

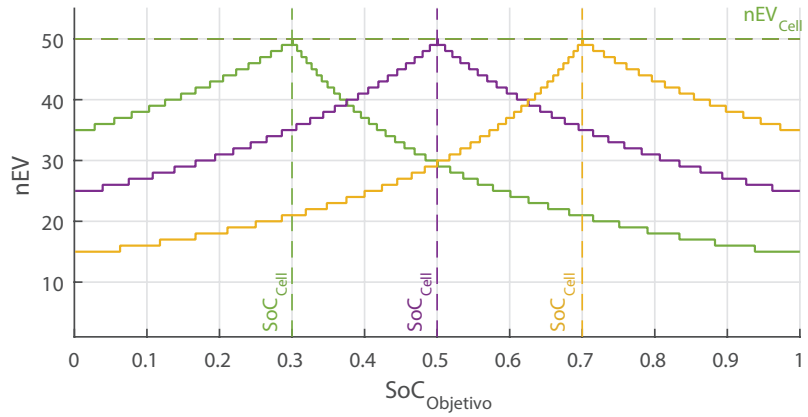

Figure 5.1: Cota superior de vehículos en la celda según el SoC de interés (eje x) para distintos valores de SoC_{Cell} (líneas discontinuas verticales)

Cuando lo que se considera es un rango de SoC , el máximo se obtiene evaluando los usuarios asociados a los SoC de los extremos y seleccionando el mayor de ellos. El extremo escogido depende de uno de los siguientes casos (Figura 5.2).

1. SoC_m si $SoC_m > SoC_{Cell}$ y $SoC_M > SoC_{Cell}$.
2. SoC_{Cell} si $SoC_m < SoC_{Cell}$ y $SoC_M > SoC_{Cell}$.
3. SoC_M si $SoC_m < SoC_{Cell}$ y $SoC_M < SoC_{Cell}$.

Consideraciones Adicionales La elipse comentada anteriormente, podría contener puntos fuera de la zona de influencia de la BSS , entendiendo por zona de influencia aquellos puntos del mapa cuya BSS más cercana es la considerada. Estos puntos han de ser ignorados puesto que un EV que toma la decisión de ir a cargar en ellos, no optará por conducir a la BSS evaluada.

Finalmente debe notarse que, en general, un EV en la región podría describir diferentes caminos antes de llegar a la BSS y por tanto, un mismo usuario podría llegar a la BSS en diferentes instantes futuros. Si esto no se tiene en cuenta, puede resultar una predicción muy sobredimensionada. Dadas dos elipses, la única forma de asegurar

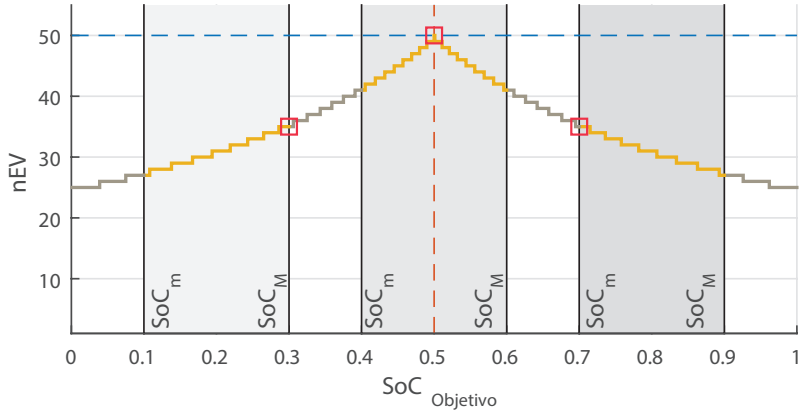

Figure 5.2: Casos según la posición del rango respecto a SoC_{Cell}

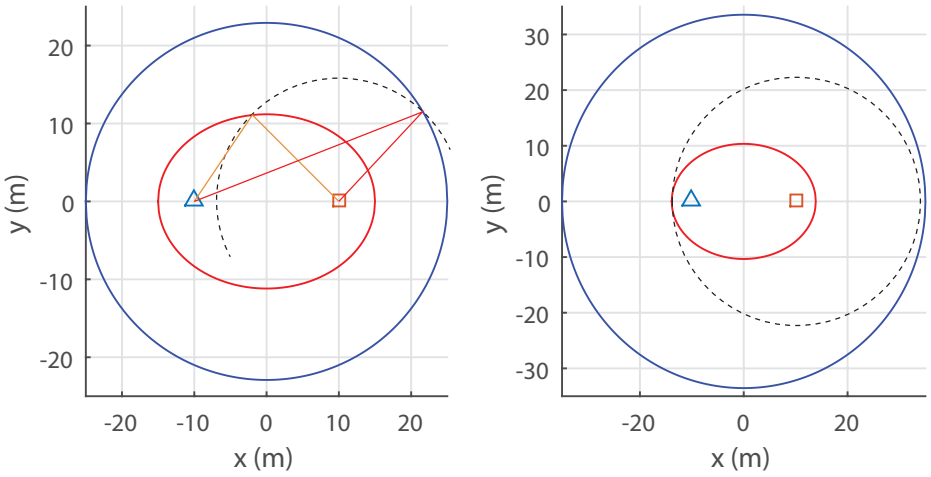

Figure 5.3: Solapamiento de elipses.

que los grupos de usuarios asociados a cada una de ellas son mutuamente excluyentes es evitando el "solapamiento de las elipses". Entendiéndose por solapamiento la existencia de un par de puntos (uno perteneciente a la elipse-1 y otro a la elipse-2) a la misma distancia de la celda (Figura 5.3).

Una solución a este problema sería no hacer predicciones en instantes futuros sucesivo sino, cuantizar dichos instantes de tal forma que se evite el solapamiento. La relación que deben tener dos elipses sucesivas (y por tanto sus instantes de predicción asociados) para no estar solapada es función de la distancia entre BSS y celda $dist(CS, CELL)$:

$$a_{ellipse\ j+1} = a_{ellipse\ j} + dist(CS, CELL) \tag{5.10}$$

$$T_j = T_{j-1} + \frac{2dist(CS, CELL)}{vel} \tag{5.11}$$

Chapter 6 Resultados

Esta sección presenta los resultados asociados a los métodos de control (Sección 6.0.1) y predicción (Sección 6.0.2) presentados. Tras comprobar su funcionamiento aislado, se integran en un un conjunto de pruebas apoyadas sobre el simulador.

6.0.1 Control de BSS

Para observar el funcionamiento del MPC formulado se utilizará la evolución de precios de la Figura 6.1 (cuya forma permitirá ver claramente su influencia), y diferentes perfiles de llegada de usuarios: (i) un perfil de congestión bajo, (ii) un segundo caso con congestión media, (iii) y un tercero caso alto (Figuras 6.2, 6.3 y 6.4 respectivamente).

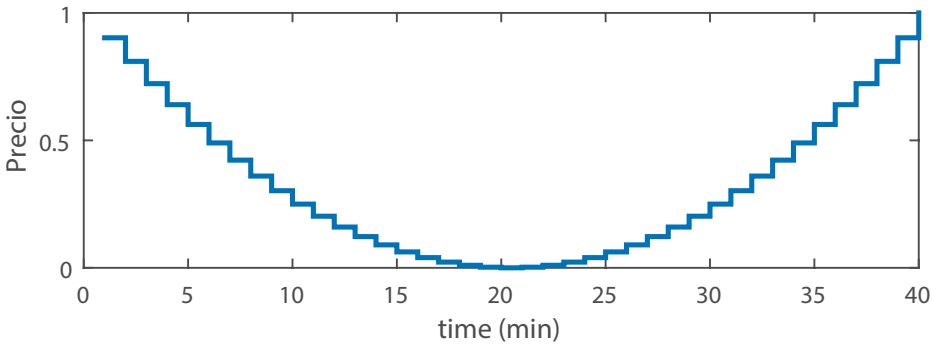

Figure 6.1: Perfil de precio

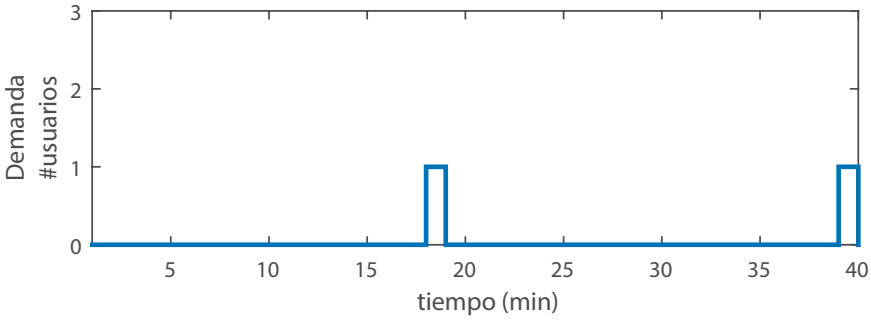

Figure 6.2: Perfil de demanda de baja congestión.

Antes de continuar, se expone brevemente la interpretación de las señales contenidas en los gráficos de resultados. Si se observa alguna de estas figuras (por ejemplo la Figura 6.6) puede verse una línea gris que corresponde a la señal de control, una azul representando el SoC y una discontinua de color rojo que corresponde con la señal binaria que dispara las operaciones de cambio.

MPC

La aplicación del MPC sobre las señales de entrada presentadas da como resultados las Figuras 6.5, 6.6 y 6.7.

En el caso de tener poca demanda, (Figure 6.5) se observa cómo el algoritmo selecciona las baterías número 1 y 6 para ser intercambiadas. Además se observa cómo el resto de baterías se terminan de cargar cuando el precio

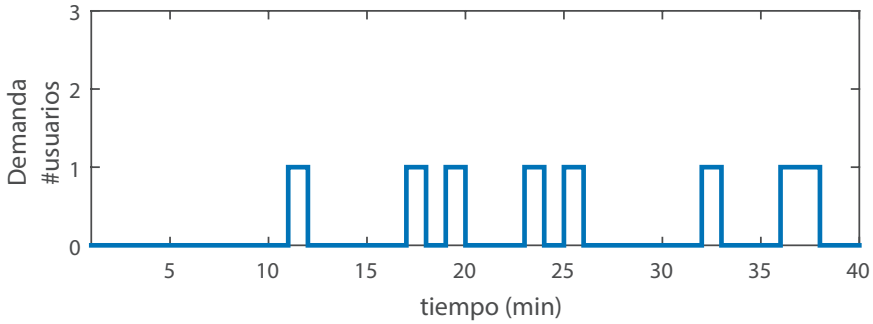

Figure 6.3: Perfil de demanda de congestión media.

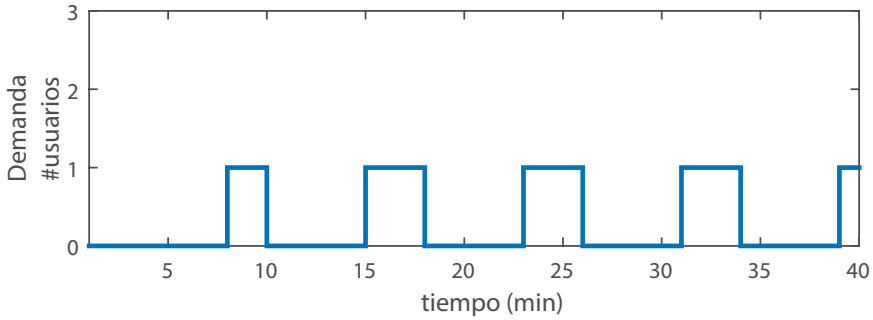

Figure 6.4: Perfil de demanda de congestión alta.

es bajo, y en los últimos instantes cuando el precio es alto, se vende la energía almacenada. En este caso el control funciona perfectamente puesto que no hay ningún problema en relación a la potencia utilizada.

Cuando el número de usuarios incrementa (Figuras 6.6 y 6.7), el algoritmo obtiene una solución óptima que, debido a la limitación de potencia y a la alta frecuencia de llegada de usuarios, no siempre consigue tener baterías totalmente cargadas en reserva.

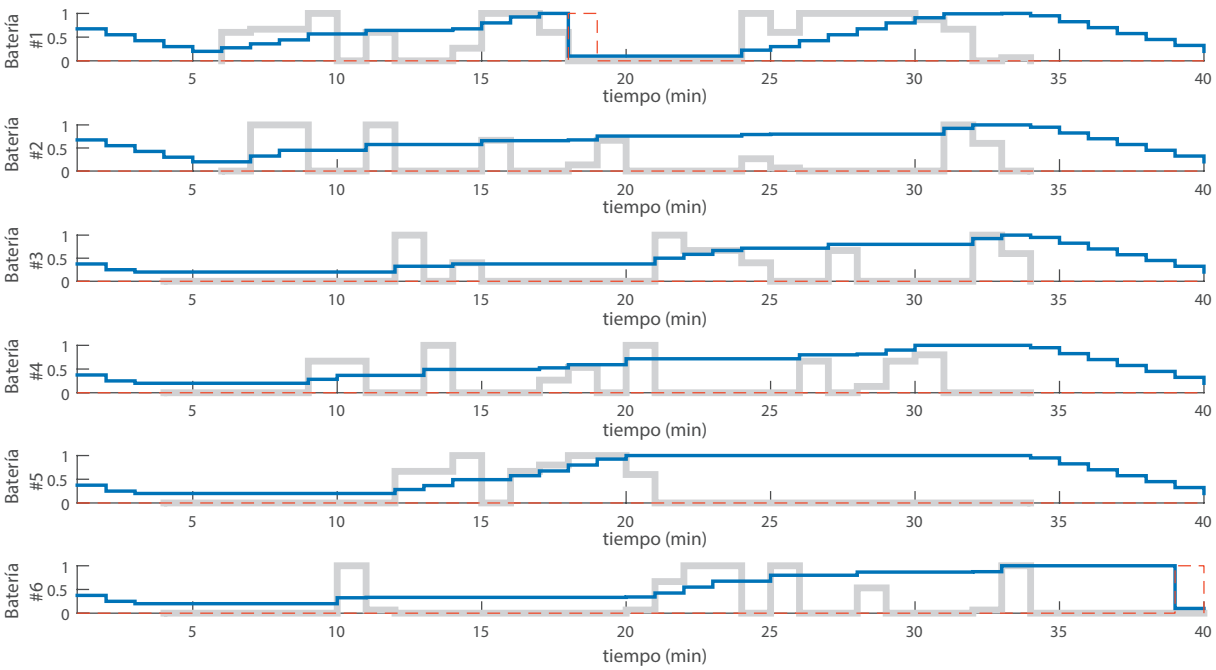

Figure 6.5: Resultado MPC. Evolución de batería de una BSS en zona de congestión baja

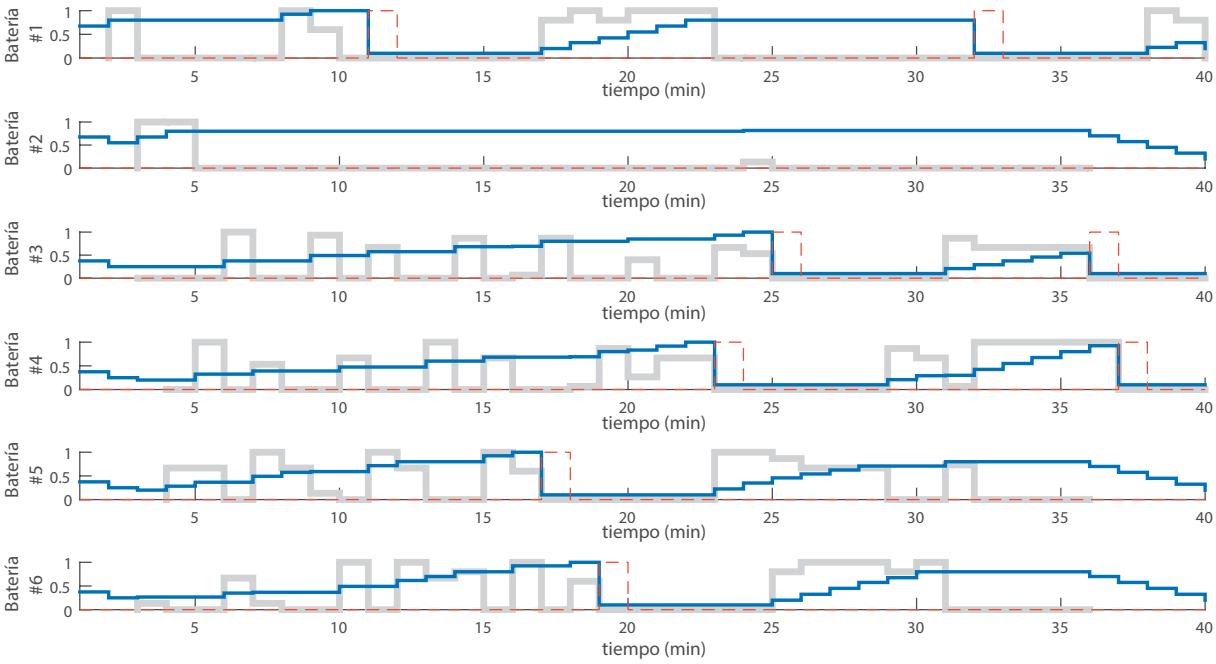

Figure 6.6: Resultado MPC. Evolución de batería de una BSS en zona de congestión media

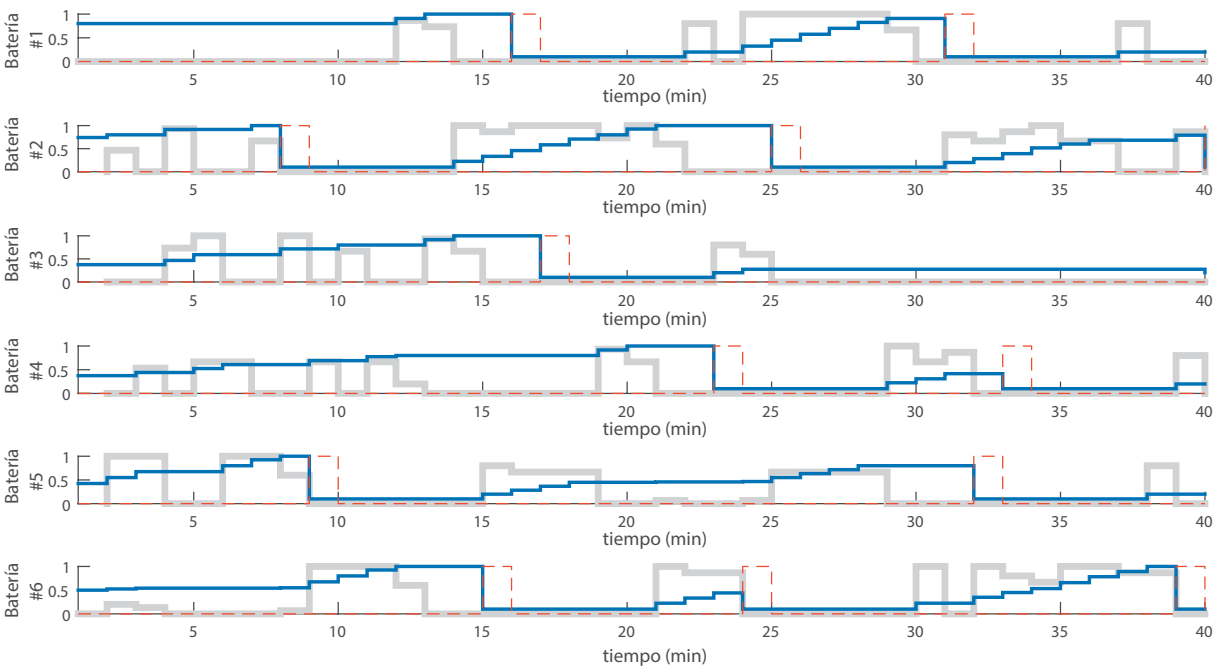

Figure 6.7: Resultado MPC. Evolución de batería de una BSS en zona de congestión alta

6.0.2 Predicción de demanda

Esta sección muestra una comparación entre las técnicas de predicción presentadas en la Sección 5.

Patrón Fijo

Como ya se ha comentado, para obtener un patrón fijo de demanda se necesita una fase inicial de entrenamiento. La cual se lleva a cabo a partir de un set de 50 muestras generadas con el simulador.

Planteamiento ITS

La predicción de demanda que hace uso del ITS no necesita fase de entrenamiento. Merece la pena comentar que esta estrategia calcula en cada instante t una predicción hasta $t + N_2$. Lo que se traduce en que para cualquier momento t^* habrá N_2 predicciones distintas correspondiente a cada uno de los instantes anteriores. Para poder compara esta estrategia con la anterior, los últimos puntos de cada predicción se han ignorado y las primeras muestras se han utilizado para generar un patrón de demanda.

Comparación

La comparación se realizará sobre diferentes BSSs extraídas de una nueva simulación. Se aplicarán ambos métodos y las predicciones resultantes se compararán con la demanda exacta registrada. Cuando se analizan BSSs en zonas de bajo nivel de tráfico (Figura 6.8) se observa que ambos métodos hacen predicciones conservadoras y por tanto, ninguno de ellos experimenta llegadas de usuarios no esperadas. La principal diferencia reside en los falsos positivos detectados. El patrón fijo tiene en cuenta la demanda registrada en el pasado y por ello no puede adaptar su predicción a nuevas circunstancias.

Concretamente en el tramo en el que no llega ningún usuario, la predicción fija tiene en cuenta que alguna vez en el pasado recibió usuarios y por tanto preparara baterías, mientras que el planteamiento ITS observa las proximidades y determina que no llegará ningún cliente.

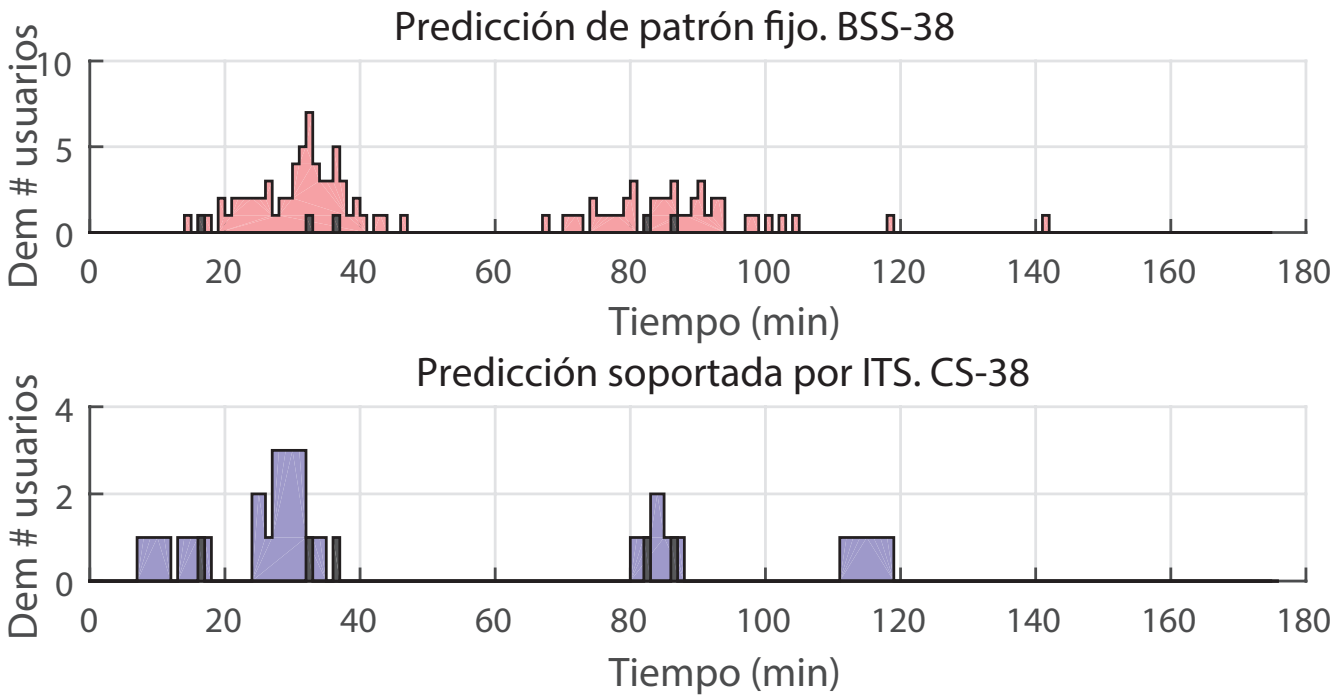

Figure 6.8: Comparación de predicción de demanda de una BSS situada en zona de congestión baja. En negro los eventos de llegada exactos, en rojo la predicción por patrón fijo, y en azul predicción soportada por ITS

Cuando el nivel de tráfico de la región crece (Figura 6.9) , puede aplicarse la misma discusión. Además, puede verse como el ITS comienza a sobrestimar el número de usuarios que llegarán dado que considera todos los vehículos de las zonas cercanas.

Finalmente, en las BSSs situadas en zonas de alta congestión (Figura 6.10) se mantiene la discusión en lo referente al patrón fijo. En relación al planteamiento ITS aparece un nuevo efecto que corresponde a la parte final de las gráficas. Esa predicción mantenida en los últimos instantes es fruto de los vehículos aparcados en las proximidades debido a que el algoritmo considera el SoC de los vehículos aparcados e intenta mantener baterías cargadas para cubrir su posible llegada.

Ambos efectos asociados a la predicción ITS tienen buenas implicaciones respecto a la QoS y no tan buenas en términos de rentabilidad puesto que hay baterías que no pueden ser operadas.

Para comparar numéricamente los métodos, se utilizan las Ecuaciones 6.2 y 6.1 para calcular el margen y el error medio cometido en cada caso. Valores que se recogen en la Tabla 6.1.

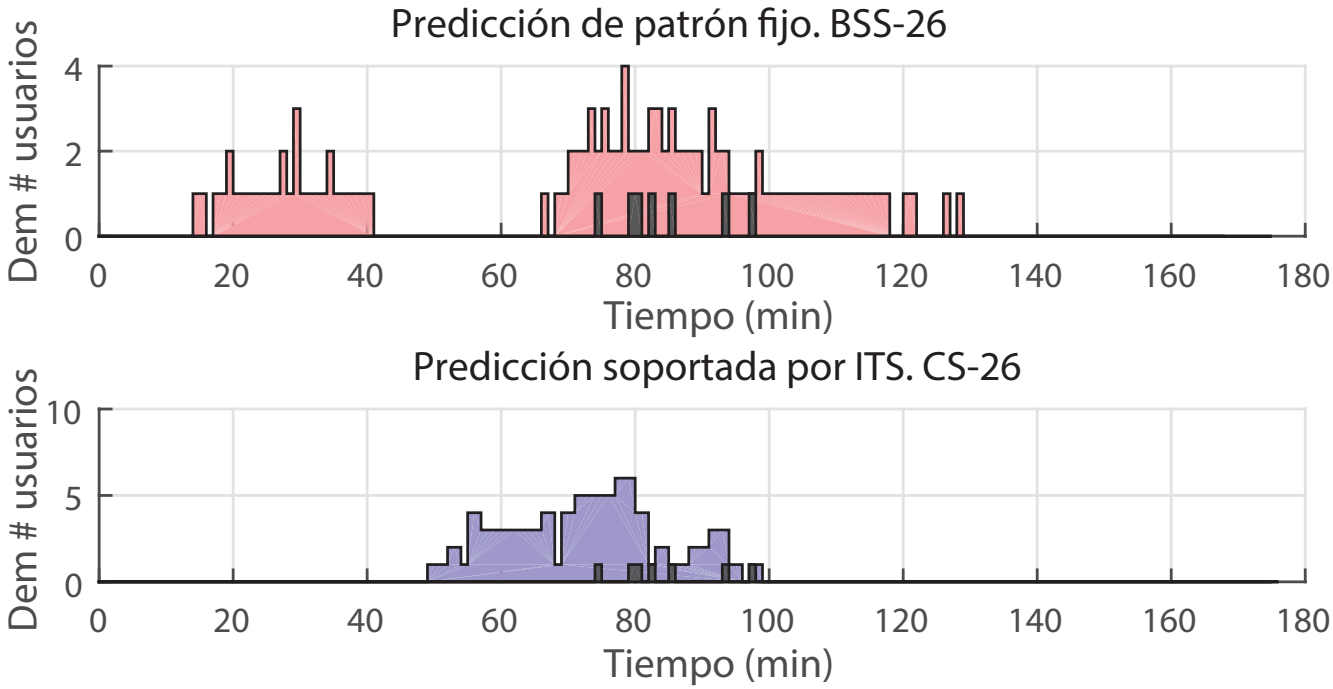

Figure 6.9: Comparación de predicción de demanda de una BSS situada en zona de congestión media. En negro los eventos de llegada exactos, en rojo la predicción por patrón fijo, y en azul predicción soportada por ITS

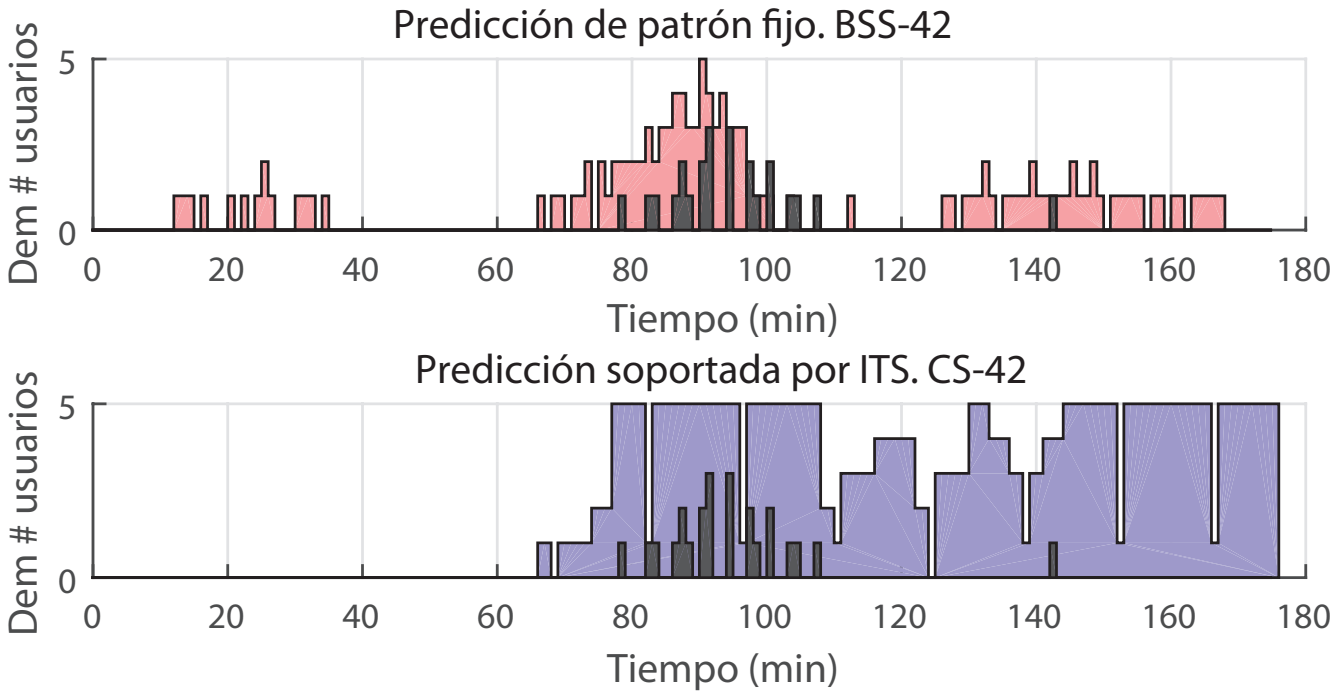

Figure 6.10: Comparación de predicción de demanda de una BSS situada en zona de congestión alta. En negro los eventos de llegada exactos, en rojo la predicción por patrón fijo, y en azul predicción soportada por ITS

$$Error_{BSS} = \overline{\lambda(t) - DFPattern} \tag{6.1}$$

$$Margin_{BSS} = \overline{DFPattern - \lambda(t)} \tag{6.2}$$

Puede verse cómo el planteamiento ITS consigue reducir la tasa de error además de presentar un margen (predicción conservadora) que crece con el nivel de congestión.

Fixed Pattern		
Congestion Level	**Error**	**Margin**
Low	0.341	4.046
Medium	0.25	1.770
High	1	1.397
ITS approach		
Congestion Level	**Error**	**Margin**
Low	0	2.399
Medium	0	3.607
High	0	9.135

Table 6.1: Error/margen registrado según el nivel de congestión

6.0.3 BSS: Test en simulador

Para concluir con los resultados, se implementan las combinaciones de los métodos sobre varias BSSs . A partir de ahora, las posibles combinaciones de control y predicción se denotarán como se muestra en la tabla 6.2. Se denotará como estrategia *miope* a la combinación del MPC y predicción de patrón fijo, y como estrategia *observadora* a la combinación de MPC y predicción soportada sobre ITS y finalmente, estrategia *óptima* a la combinación del MPC asumiendo que la predicción es exacta.

Combinación	**Nombre**
MPC (Sección 6.0.1) + Pred. patrón fijo	Miope
MPC (Sección 6.0.1) + Pred. ITS	Observadora
MPC (Sección 6.0.1) + Pred. Exacta	Óptima

Table 6.2: Notación de la combinación de métodos

Las Figuras 6.11, 6.12 y 6.13 muestran el funcionamiento de cada combinación aplicada sobre una BSS en la que se pueden observar todas las diferencias interesantes entre métodos. En primer lugar se observa cómo la falta de adaptabilidad de la combinación *miope* propicia el servicio de baterías parcialmente cargadas, cosa que no ocurre en el resto de casos. Por otro lado, en los tramos en los que no llega demanda, puede verse cómo el número de ciclos realizados aumenta conforme mejora la predicción de demanda. En este sentido se observa cómo la combinación *observadora* se asemeja más a la *óptima* que la combinación *miope.*. En la tabla 6.3 se recogen las ganancias totales del escenario y medias para las BSS para cada combinación. Evaluando dichas ganancias, se observa claramente la ventaja de la combinación propuesta que, respecto al mejor escenario (combinación óptima), mejora tanto la ganancia total del sistema, como el valor medio ganado por cada estación de forma aislada.

Valor	**Combinación**	**Ganancias**
Total	Miope	613.09
	Observador	638.88
	Óptimo	670.93
Medio	Miope	68.12
	Observador	70.65
	Óptimo	74.55

Table 6.3: Comparación numérica entre escenarios considerados

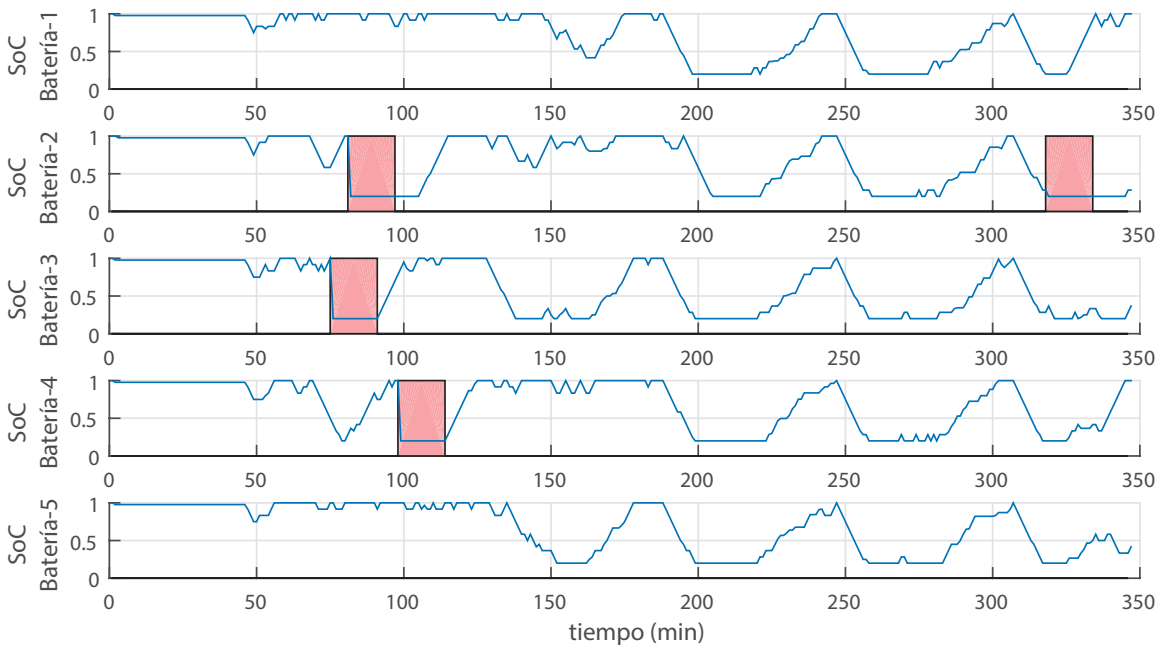

Figure 6.11: Combinación *Miope* aplicada a una BSS en zona de congestión baja.

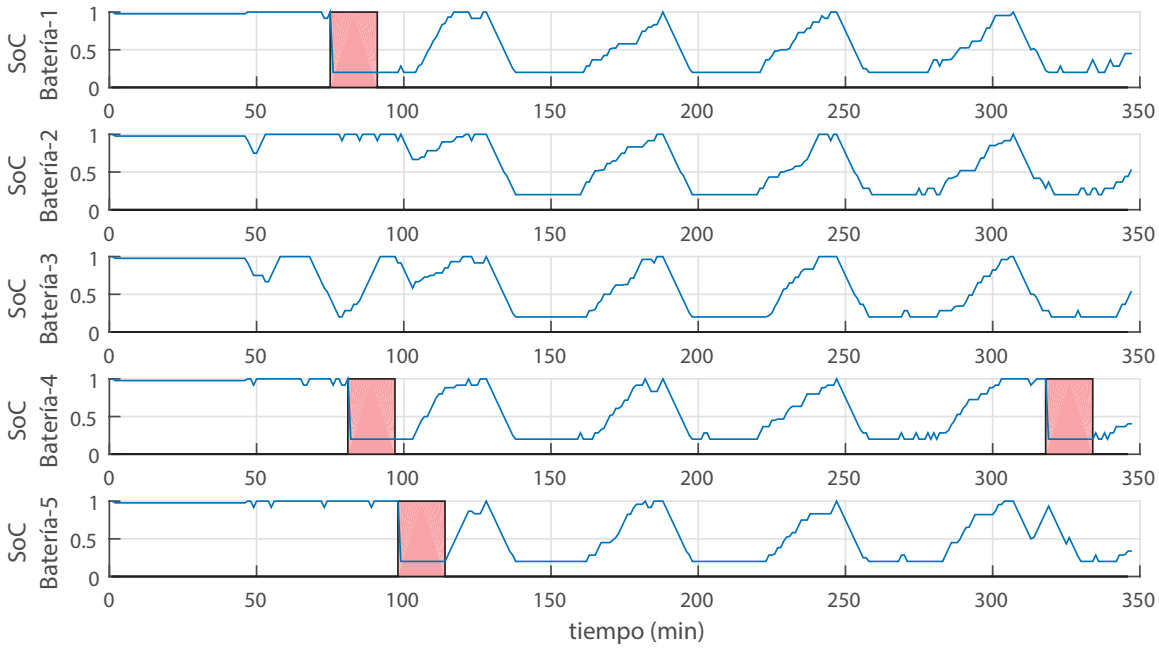

Figure 6.12: Combinación *Observador* aplicada a una BSS en zona de congestión baja.

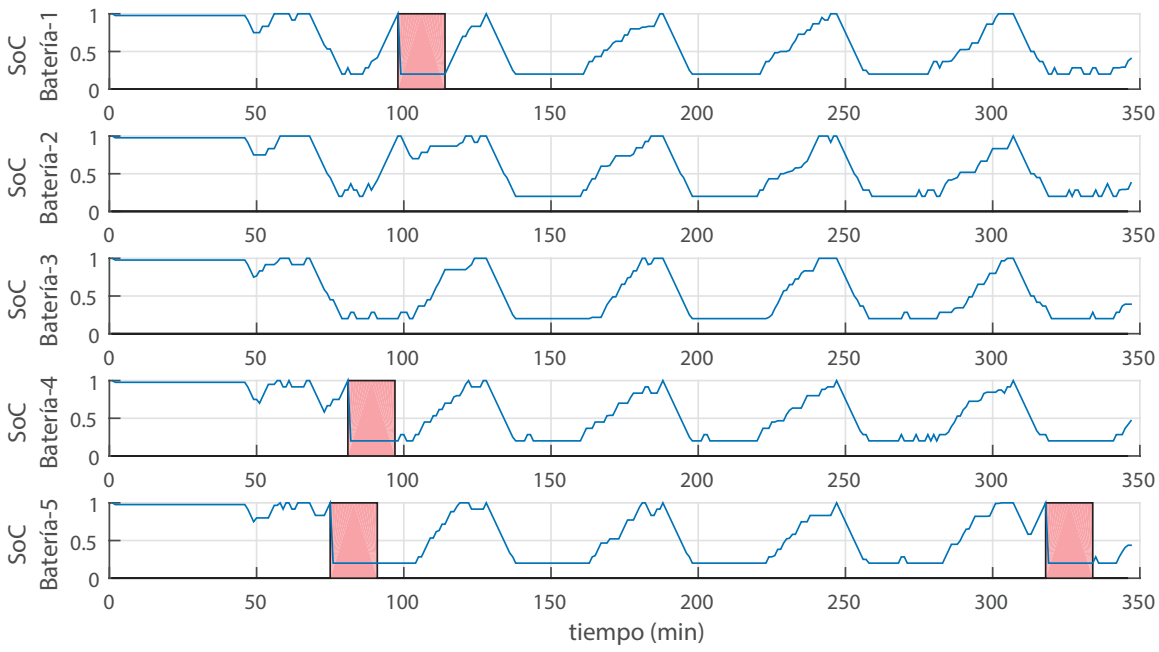

Figure 6.13: Combinación *Óptima* aplicada a una BSS en zona de congestión baja.

Chapter 7 Conclusiones y líneas futuras

Este trabajo presenta un breve estudio sobre la operación de BSSs y el efecto de la precisión de la predicción de demanda. En primer lugar se presenta un simulador que se utiliza como herramienta para testedo. Tras detallar el sistema con el que se va a trabajar, se formula un MPC para operar la estación de la forma más rentable posible. Posteriormente, se discuten las implicaciones de la precisión de la predicción de demanda. La principal contribución de este trabajo consiste en el MPC propuesto, y la materialización del concepto de ITS como herramienta para obtener información en tiempo real del estado de la carretera y predecir la demanda en el futuro próximo de forma más adecuada. Finalmente, el desempeño del control y le predicción se mide en términos de rentabilidad y se observa que el planteamiento presentado supera a otras alternativas planteadas.

Varios líneas futuros pueden nacer a partir de este trabajo. En relación al *entorno de simulación*, podría implementarse un comportamiento de EVs más complejo, se podrían incorporar mapas así como la capacidad de los usuarios responder a ciertos estímulos. En relación a la *arquitectura del sistema* podría asumirse una configuración de estación de carga soportando ambas operaciones (intercambio de baterías y carga directa de baterías de usuarios). Podría por tanto analizarse las implicaciones de suponer una Hybrid Charging Station (HCS) que parece un planteamiento efectivo para cubrir la llegada de usuarios inesperados.

El Propio MPC se presta a algunas extensiones. Podría controlarse el número de ciclos que se le aplican a las baterías, se podría considerar la diferencia de rendimientos propia de la carga y descarga, la frecuencia de conmutación entre carga-descarga se podría limitar, podría añadirse la consideración de varios tipos de baterías, el valor de la potencia usada para cargar podría penalizarse para intentar gestionar las baterías de una forma más amigable etc.

Relacionados también con este trabajo podría considerarse el estudio de mecanismos de Gestión de Respuestas de Demanda para alcanzar un determinado objetivo. Por ejemplo, una BSS podría estar interesada en variar los precios de recarga para reducir/incrementar el nivel de congestión en algunos periodos. Esto resultaría en añadir un modelo de la sensibilidad de usuarios al precio y los precios en sí mismo en el problema de optimización, dando al algoritmo cierto grado de influencia sobre la futura demanda. Una extensión adicional podría consistir en considerar a las BSSs capaces de transmitir información y tomar decisiones sobre sus precios de forma conjunta para alcanzar un objetivo común. Además, considerando el planteamiento del sistema, sería sencilla su extensión para gestionar operaciones de Vehicle to Grid (V2G) en grandes aparcamientos.

En relación a la predicción de demanda, la primera cosa a incorporar serían mecanismos para detectar y corregir los efectos indeseables acarreados por el método ITS . Alternativamente, se podría plantear un sistema de reservas de recargas/intercambios en los que se especificaría la hora de llegada a la estación como medio de reducir la incertidumbre de demanda.

Por último, la información generada por el ITS podría ser modificada ligeramente para intentar reducir la incertidumbre. En lugar de usar el valor medio de SoC o el centro de la celda como la posición real, el SoC_{Cell} podría resultar de una media ponderada en la que se daría más peso a los niveles de batería bajos y la posición de la celda podría ser sustituida por el "centro de masa" de la celda.

Bibliography

[1] J. Wideberg, C. Bordons, P. Luque, D. A. Mántaras, D. Marcos, and H. Kanchwala, "Development and experimental validation of a dynamic model for electric vehicle with in hub motors," *Procedia-Social and Behavioral Sciences*, vol. 160, pp. 84–91, 2014.

[2] P. Xie, B. Qian, D. Shi, J. Chen, and L. Zhu, "Supplementary automatic generation control using electric vehicle battery swapping stations," in *Power and Energy Society General Meeting (PES), 2013 IEEE*, pp. 1–5, IEEE, 2013.

[3] X. Tan, B. Sun, and D. H. Tsang, "Queueing network models for electric vehicle charging station with battery swapping," in *Smart Grid Communications (SmartGridComm), 2014 IEEE International Conference on*, pp. 1–6, IEEE, 2014.

[4] M. R. Sarker, H. Pandzic, and M. A. Ortega-Vazquez, "Optimal operation and services scheduling for an electric vehicle battery swapping station," 2014.

[5] M. R. Sarker, H. Pandzic, and M. A. Ortega-Vazquez, "Electric vehicle battery swapping station: business case and optimization model," in *Connected Vehicles and Expo (ICCVE), 2013 International Conference on*, pp. 289–294, IEEE, 2013.

[6] S. Yang, J. Yao, T. Kang, and X. Zhu, "Dynamic operation model of the battery swapping station for ev (electric vehicle) in electricity market," *Energy*, vol. 65, pp. 544–549, 2014.

[7] L. Xinyi, L. Nian, H. Yangqi, Z. Jianhua, and Z. Nan, "Optimal configuration of ev battery swapping station considering service availability," in *Intelligent Green Building and Smart Grid (IGBSG), 2014 International Conference on*, pp. 1–5, IEEE, 2014.

[8] F. Malandrino, C. Casetti, and C.-F. Chiasserini, "The role of its in charging opportunities for evs," in *Intelligent Transportation Systems-(ITSC), 2013 16th International IEEE Conference on*, pp. 1953–1958, IEEE, 2013.

[9] A. Nkoro and Y. Vershinin, "Current and future trends in applications of intelligent transport systems on cars and infrastructure," in *Intelligent Transportation Systems (ITSC), 2014 IEEE 17th International Conference on*, pp. 514–519, IEEE, 2014.

[10] B. Eisele, D. Schrank, and T. Lomax, "Tti's 2011 congested corridors report powered by inrix traffic data," *Texas Transportation Institute and The Texas A&M University System, USA*, 2011.

[11] J. Johnson, M. Chowdhury, Y. He, and J. Taiber, "Utilizing real-time information transferring potentials to vehicles to improve the fast-charging process in electric vehicles," *Transportation Research Part C: Emerging Technologies*, vol. 26, pp. 352–366, 2013.

[12] I. P. Safak Bayram, George Michailidis and M. Devetsikiotis, "Decentralized control of electric vehicles in a network of fast charging stations," 2013.

[13] T. K. X. Z. Shengjie Yang, Jiangang Yao, "Dynamic operation model of the battery swapping station for ev (electric vehicle) in electricity market," 2014.

[14] C. Guéret, C. Prins, and M. Sevaux, "Applications of optimization with xpress-mp," *contract*, p. 00034, 1999.

[15] J. Lofberg, "Yalmip: A toolbox for modeling and optimization in matlab," in *Computer Aided Control Systems Design, 2004 IEEE International Symposium on*, pp. 284–289, IEEE, 2004.

Battery Swapping Station management supported by Intelligent Transport Systems: an MPC approach.

Ezequiel G. Debada

Eduardo F. Camacho

June 11, 2015

Contents

Acknowledgement

Quiero expresar mi agradecimiento a todas aquellas personas que han contribuido de alguna forma al desarrollo de este trabajo. En especial a mi familia por su apoyo incondicional y su confianza, a Eduardo F. Camacho, por seguir ejerciendo sin obligación el papel de "mentor" que adoptó hace ya algunos años, a Filiberto Fele por sus consejos, su interés y su ayuda en momentos de incertidumbre y a Raquel Zambrano por tender su mano para sortear todos y cada uno de los obstáculos en el camino.

Gracias.

"If I had six hours to chop down a tree,
I'd spend the first four hours sharpening the axe"
Abraham Lincoln

Resumen

Para lograr la completa integración del vehículo eléctrico (EV), es necesario solucionar varios problemas relacionados con el proceso de carga. Recientemente las "Battery Swapping Stations" o estaciones de intercambio de batería han surgido como una alternativa prometedora al planteamiento tradicional de las estaciones de carga de baterías (Battery Charging Stations). No obstante, las BSSs no están exentas de problemas que han de ser resueltos para que dicha estructura sea operacionalmente factible. Este proyecto propone un MPC como método de control de una BSS. En paralelo, este trabajo analiza la influencia de la precisión de la predicción de la demanda en el desempeño del control en términos de calidad de serivio (QoS) y beneficios; presenta un "Sistema de Transporte Inteligente" (ITS de sus siglas en inglés) para que las estaciones de carga tengan informacián en tiempo real de la congestión de tráfico y de su estado en los alrededores; y propone una estrategia de predicción basada en dicha información que posee un alto grado de robustez. Además, se desarrolla un entorno de simulación configurable que se utilizará como herramienta para testear las estrategias de control y de predicción de demanda presentados. Los resultados muestran el propio funcionamiento del algoritmo de control propuesto, la importancia de la exactitud de la predicción y detalla las ventajas que acarrea el uso de información en tiempo real en esos términos.

Chapter 1 Abstract

For a successful Electric Vehicle (EV) integration, it is necessary to cover several problems related to the charging process. Recently, Battery Swapping Station (BSS) strategies are arising as a promising alternative to the traditional Battery Charging Station (BCS) approach since that provides a wider set of business opportunities. However, BSS approach are not exempt from new challenging issues that must be solved for achieving its operationally feasibility. This thesis proposes an MPC to control completely a BSS . In parallel, this work analyses the influence of the demand prediction accuracy in the control performance in terms of Quality of Service (QoS) and revenues; presents an Intelligent Transport System (ITS) for the BSSs to get real time information about the traffic in the surrounding area; and proposes a robust demand prediction strategy built on the aforementioned ITS approach. Furthermore, a configurable simulation environment is developed as a tool to test the strategies and demand prediction methods presented. The results show the proper working of the BSS managing algorithm proposed; the importance of the prediction accuracy, mainly in little congested BSSs ; as well as the advantages provided by using real time information in those terms.

Chapter 2 Introduction

Electromobility technology is destined to have a strong impact in several dimensions of our day a day. From a social point of view, it means to change the way in which we see our mobility. Not only regarding the energy sources but also in relation with new habits, new business opportunities as well as new vehicle configurations that are impossible with combustion engines. Environmentally talking, there is not any doubt that the comparison between electricity and fossil fuels results in favor of electricity; overall when that electricity is generated from renewable sources.

The potential contributions of EVs seem to be countless considering the number of research studies that it motivates.

Obviously, the paradigm shifting from fossil fuel consumption towards electricity also entails some difficulties. The principal challenges are related to the grid, that would experience a significant load shape changing, and would see how the load on the distribution lines increases. However, even in those terms, a proper control of EV at fleet level can be used as a tool to integrate distributed energy sources, balancing intermittent renewable energy sources and it can contribute to stabilize the network.

One of the most popular drawbacks that EVs entail are related to its autonomy, the long battery charging times and high battery replacement cost. That motivates the development of charging facilities suitable for those specific necessities, studies on the best location for BSSs to reduce the driver anxiety, smart systems for selecting the best BSS etc. In contrast to BCSs , BSSs arise as a charging facility architecture that provides several control possibilities. A lot of works in literature have been focused on the advantages reported by the large EV fleet control and, many of those conclusions can be applied to BSS . That is because the fact of owning a certain number of EV batteries, could be seen as a EV fleet completely controllable. Besides, having flexibility regarding when

and how the batteries are charged could result in lower prices, and lower batteries degradation.

The main difficulty introduced by BSSs is the fact that the batteries management depends on an uncertain customer arrival rate and thus, some strategy must be adopted to predict that arrival if the revenues are wanted to be maximized.

The challenges regarding that prediction are reduced if the use of ITS is considered [1]. That would suppose the availability of real time information about the road state and could be used as a good way to bound the prediction error.

A common difficulty to be faced for any research about a futuristic EV framework is the lack of real infrastructure and data in general. Nevertheless, since the own EV feasibility adoption is tightly tied to the performance of its operation, the research in that direction must go on. Probably, that lack of standardization is the reason why EV plays a great deal important role in today's research framework.

This thesis aims to study some of the challenges associated with BSSs . More concretely, concerning the demand prediction accuracy influence. Being the main contributions: a BSS MPC formulation which takes into account the time needed for swapping, a simple ITS that gives information with a reduced amount of data, and a novel prediction method that, supported by the ITS addressed, manages to operate a BSS in a suitable way. A possible scheme of this thesis is shown in Figure 2.1.

The rest of this thesis is organized as follows: Chapter 3 contains a brief overview of the state of the art regarding EV BSS . Chapter 4 presents the simulation environment developed for testing proposes. A detailed system description is included in Chapter 5. Chapter 6 and 7 describe the controller and the demand forecasting methods analyzed later in Chapter 8. And finally, Chapter 9 gathers the conclusions and presents some future works that could be built on this thesis.

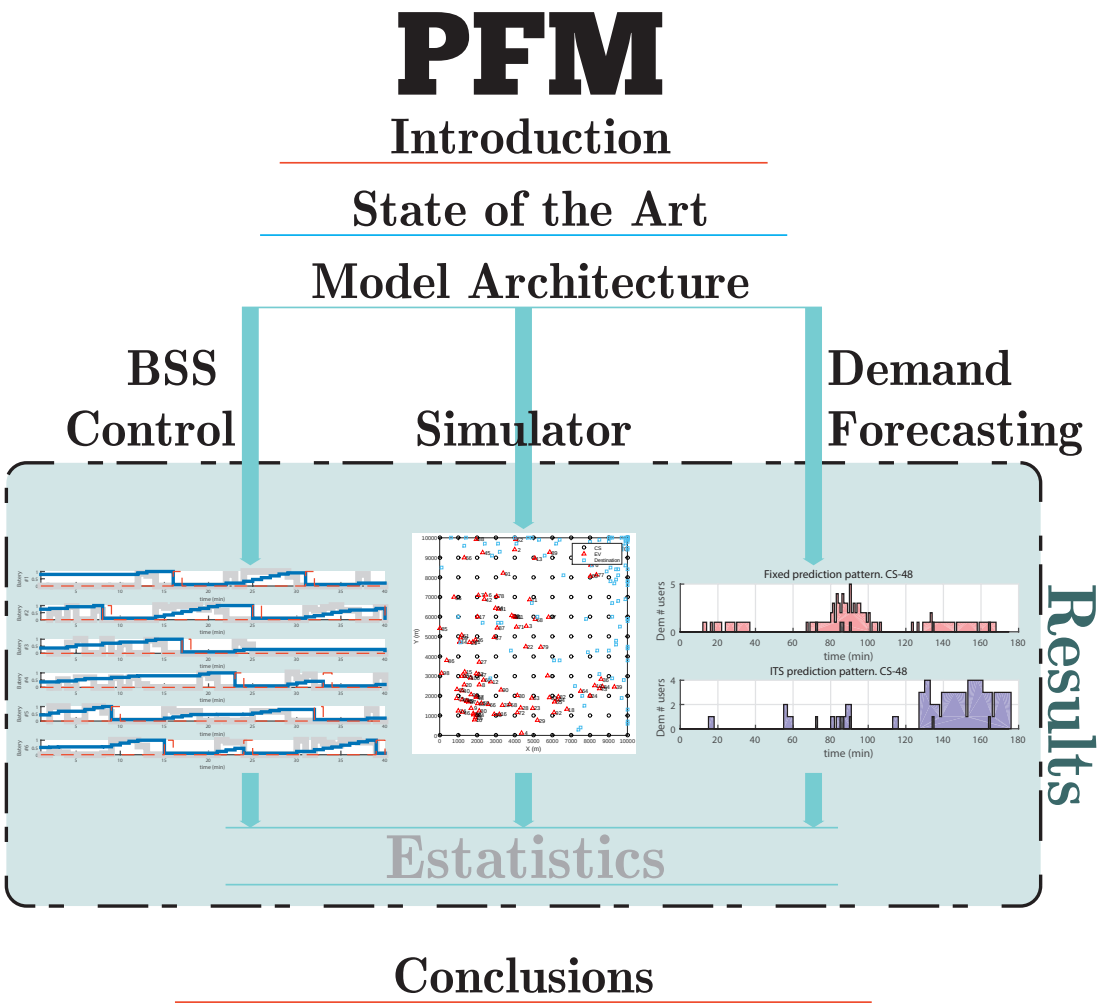

Figure 2.1: Conceptual Scheme

Chapter 3 State of the art

Although the BSS concept is novel, some works related to that topic can be found in the literature. This Section presents some of the most recent works whose content is directly related to BSSs and the topics addressed by this thesis.

BSS placing is one of those topics well studied in literature. Yu Zhen et al. in [2] study the optimal locations where BSS can be installed and operated in distribution systems.

Jun Yang et al. in [3] propose a BSS location routing problem to determine the optimal BSS location and the routing plan of a fleet of EV under battery limitation.

In the absence of standards for BSSs , several works exist proposing different managing methods. Xiaoqi Tan et al. in [4] propose a queuing network model to serve as a performance analysis framework for BSSs . Its target with that work is to provide a benchmark to analyze the performance of BSS approaches.

Mushfiqur R. Sarker et al. in [5] propose an extension of its previous article [6] where they present a detailed BSS model including some aspects regarding its integration within the electricity market and demand uncertainty. However they do not take into account the time needed for swapping the batteries, the maximum power that a BSS can use and do not consider the existence of a queue.

Shengjie Tang et al. in [7] propose a dynamic operation model of BSS in electricity market (formulated as a sequential decision problem) showing that the BSS makes decisions in market environment through tracing the number of batteries in different kinds of states.

Lu Xinyi et al. in [8] present a mathematical model to optimize the number of EV batteries and the number of chargers in a BSS attempting to keep balanced the annual value of the facilities cost.

Bo Sun et al. in [9] aim to obtain the optimal charging policy to minimize the charging cost while ensuring the QoS of the BSS . They formulate the charging

schedule problem as a stochastic control problem and achieve the optimal charging policy by dynamic programming.

BSSs are also a good candidate to provide ancillary services to the grid and some works can be found in that direction. Pingping Xie et al. in [10] study the possibility of providing regulation services by energy storage in BSS in the demand size showing that it can significantly suppress the frequency deviation and tie-line power fluctuations. Besides it introduces the concept of Station to Grid (S2G) to denote the BSS providing services to the grid.

Regarding the load prediction it has to be said that, although general electricity demand forecasting has been treated in the literature, very few works treat the particular case of EV arriving to charging facilities.

Qian Dai et al. in [11] propose a model based on Monte Carlo simulation to estimate uncontrolled energy consumption of the BSS that, since they do not consider real time data available, has a stochastic character.

E. S. Xydas et al. in [12] propose a short-term load forecast model using Support Vector Machines and compare the result with a Monte Carlo forecasting technique.

On the other hand, ITS proposes the existence of a flow information exchange among vehicles, charging Stations, transport authorities, etc. That information exchange can be potentially used to provide valuable extra information in the task of solving transport problems such as congestions, accidents, battery charging efficiency, and more services. A complete review about current and future trends in applications of ITS on cars ca be found in [13] (A.B. Nkoro et al.).

Chapter 4 Simulator

The fact of developing a control strategy for a futuristic EV framework makes necessary the generation of synthetic data for testing and evaluating. Concretely, regarding BSSs operation, the customers arrival pattern needs to be synthetically created. Two alternatives arise:

- Generate an hypothetical EV arrival schedule by hand [14]
- Obtain an arrival schedule as a result of an EV fleet simulator. In this case, the departure/arrival points have to be produced [15].

In this work, both alternatives are used. The first approach is used to test the good BSS control strategy performance, whereas the second one allows to test the combination of the control strategies and different demand prediction methods.

The simulator presented here is inspired on [15] whose main feature is simplicity. Figure 4.1 shows a snapshot of the simulator developed. As it can be seen, the aforementioned simplicity refers to the lack of road maps and the consequences that it entails: such as advantages in terms of EV route calculation or BSS placing.

The aspects that need to be solved to completely define the simulator are:

- Geometrical considerations.

  Size of the scenario and BSSs emplacement.

  EV initial/final locations.

- EV

  Movement characteristics: velocity, consumption, initial battery State of Charge (SoC) .

  Battery management: critical SoC , BSS selection criteria.

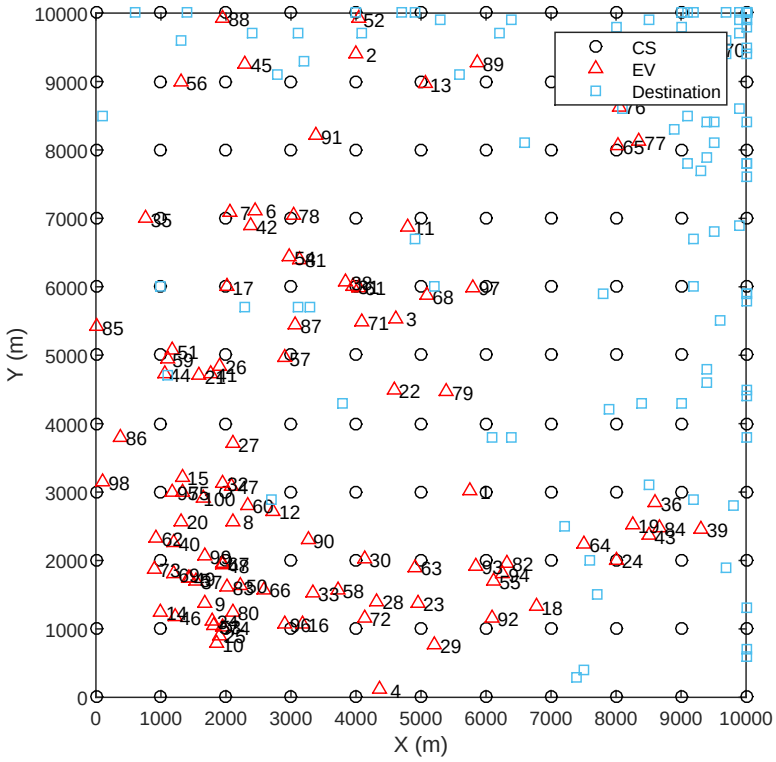

Figure 4.1: Simulator snapshot

- BSS operation
- Real time information

  Real time cells size, kind of information available.

4.1 Geometrical considerations

The geometrical considerations cover the scenario width/height, the BSSs location as well as the way in which the EVs initial/final locations are generated.

Scenario geometry

The scenario consists basically in a square grid ($SC_{Height} \times SC_{Width}$ sized) with BSSs evenly distributed (with $CS_{spacing}$ m between them). These values can be modified to affect indirectly the congestion level reached during the simulations, the number of charging events produced, or even the simulation time needed for every EV reaches its final point. Figure 4.2 shows a couple of scenarios with different CS spacing.

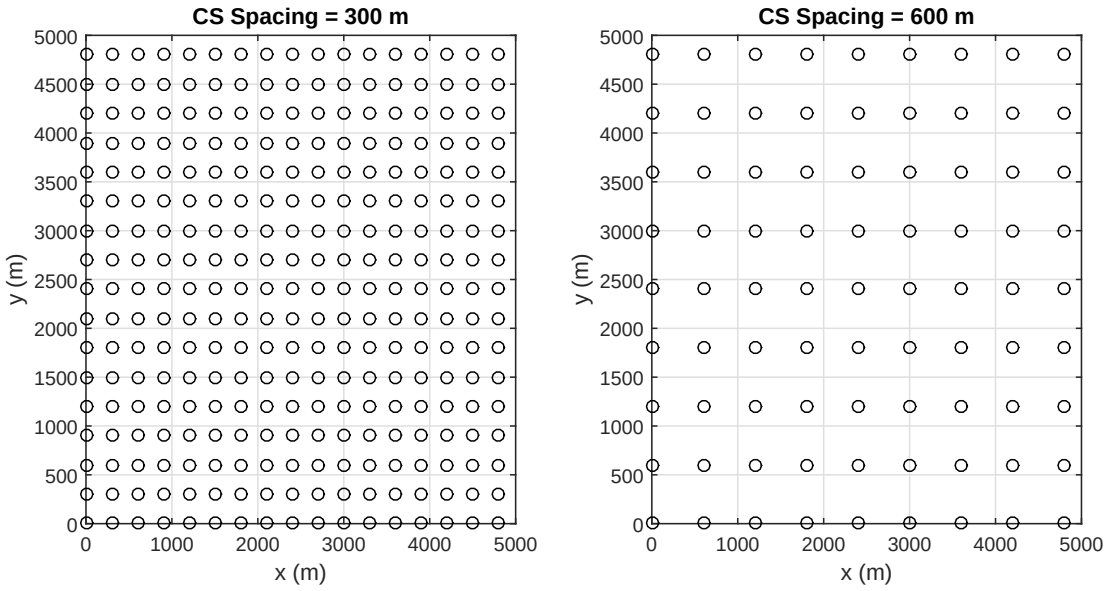

Figure 4.2: Scenarios with different CS spacing

EV Initial/final locations

In some of the prediction strategies addressed, it is necessary to have a customers arrival prediction. Avoiding the way in which that prediction is calculated (that will be detailed in Section 7), for the prediction being possible is required a certain grade of repeatability regarding the EVs displacements. For that, the departure/arrival points generation, in a similar way that it is done in [16], follows the Probability Density Function (PDF) described by Equation 4.1 and 4.2.

$$P^{Dep}(x,y) = P^{Dep}(x)P^{Dep}(y) \tag{4.1}$$
$$P^{Arr}(x,y) = P^{Arr}(x)P^{Arr}(y) \tag{4.2}$$
$$\tag{4.3}$$

Where the probability for the point (x, y) being chosen as a departure or arrival point $P(x, y)$, is given by the product of the probabilities associated to each coordinate (Equations 4.4 and 4.5).

$$P^{Dep}(x) = \frac{(SC_{Width} - x)^3}{x(SC_{Width} - \frac{x^3}{4})} \qquad P^{Dep}(y) = \frac{(SC_{Height} - y)^3}{y(SC_{Height} - \frac{y^3}{4})} \tag{4.4}$$
$$P^{Arr}(x) = 1 - P^{Dep}(x) \qquad P^{Arr}(y) = 1 - P^{Dep}(y) \tag{4.5}$$

Figure 4.3 shows a set of initial/final points generated by that distribution.

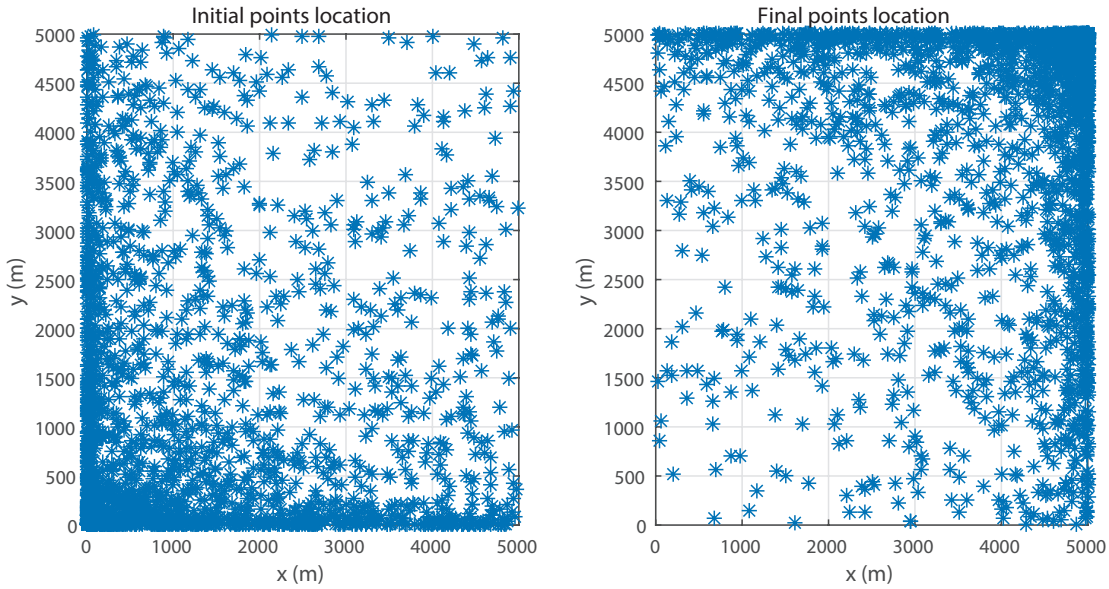

Figure 4.3: Initial/final location distribution

4.2 Electric Vehicle behavior

Since there is no real data available to model the EVs behavior regarding BSS selection, and since this study is not focused on its development, the EV behavior implemented is the simplest one suitable for our propose. This fact is applicable to the EV movement parameters, routes followed, the decision of going to charge and the BSS selection when corresponds.

EV Characteristics

The EV behavior implemented consists in, starting in a given departure point, driving towards an arrival point following a straight trajectory. The velocity $vel \in \mathbb{R}^+$ is assumed to be constant for every EV and the same is assumed for the consumption. For computational reasons, an EV is considered to reach his target when he is less than 100 m far from it. The initial battery SoC is randomly generated within a range previously defined. The EV battery characteristics such as the storage capacity, or the maximum power flow supported are considered also to have the same value for all the EVs . Figures 4.4 and 4.5 show the trajectory and the EV SoC extracted for a simple simulation.

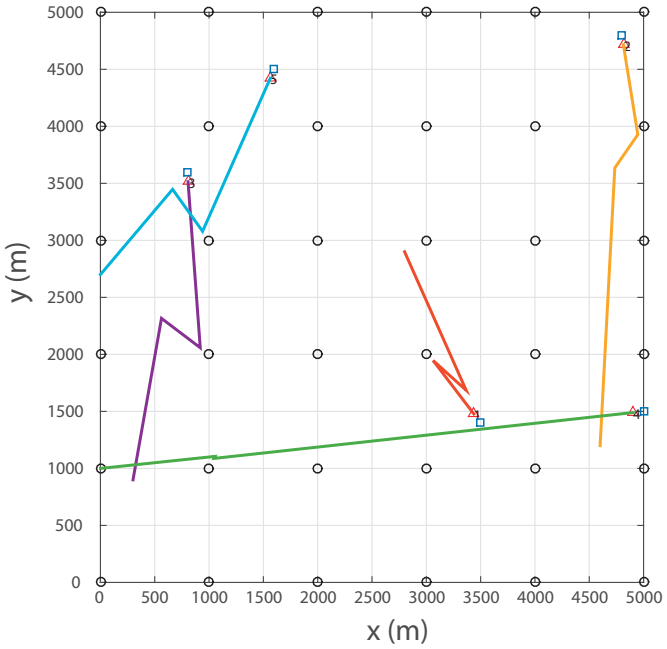

Figure 4.4: Ev routing example

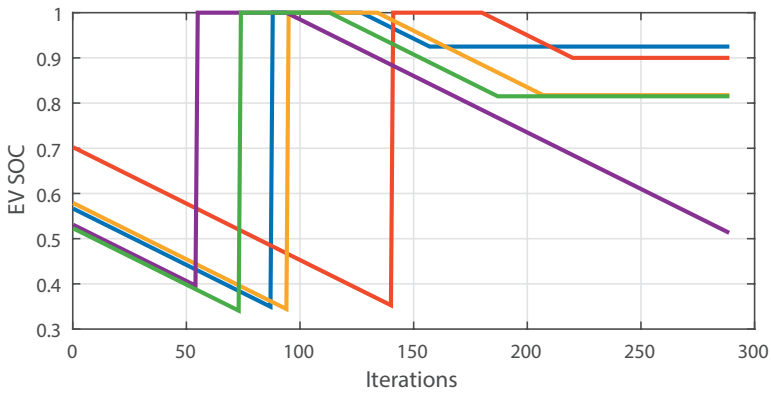

Figure 4.5: EV SoC evolution Example

Battery management

Regarding the charging decisions, an EV decides to go to charge when its battery SoC is lower than a fixed value SoC_{Charge} and the BSS selection follows a minimum distance criteria (Equation 4.6).

$$BSS^* = argmin_{BSS} dist(Ev_{pos}, BSS) \tag{4.6}$$

4.3 BSS

The BSS operation does is actually the subject of this study so a detailed description is presented in the next sections.

4.4 Real Time Information

One of the purposes of using an EV simulator is to evaluate the option of using real time information to increase the demand forecasting accuracy. Consequently, the simulator needs to generate such as information. The method addressed assumes that it is not possible to register the EVs parameters individually due to privacy concerns so that, as Figure 8.16 illustrates, the scenario is divided in cells and each cell provides a mean value of the traffic congestion and the EV SoC .

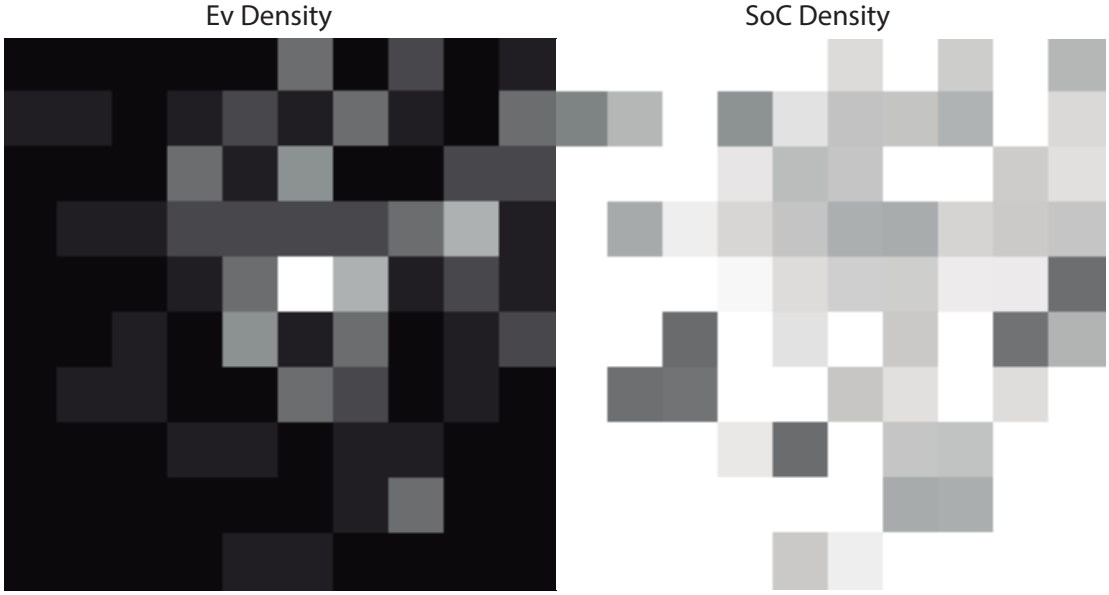

Figure 4.6: Real time information preview. The clearer is the cell, the higher is the value.

- EV Density: measurement of the number of EVs within the cell, referred to the total number of EVs existing.
- EV SoC: mean SoC of the EVs within the cell.

The cells size entails important implications for the demand prediction method proposed in this work. More details are presented in Section 7.3.

4.5 Parameters summary

Table 4.1 gathers all the parameters needed to define the simulator proposed.

Parameter	Value
nEV	100
Scenario Size	$500 \times 500\ m$
BSS Spacing	$500\ m$
Ev Vel	$20\ m/s$
RT Resolution	$500\ m$

Table 4.1: Simulator parameters summary

Chapter 5 System architecture

This chapter presents the BSS architecture and describes the variable and parameters that completely define its operation. The whole system could be divided in three modules: an open queue for receiving the customers arriving, a set of batteries to manage, and some swapping spaces where the swapping operation is performed (Figure 5.1).

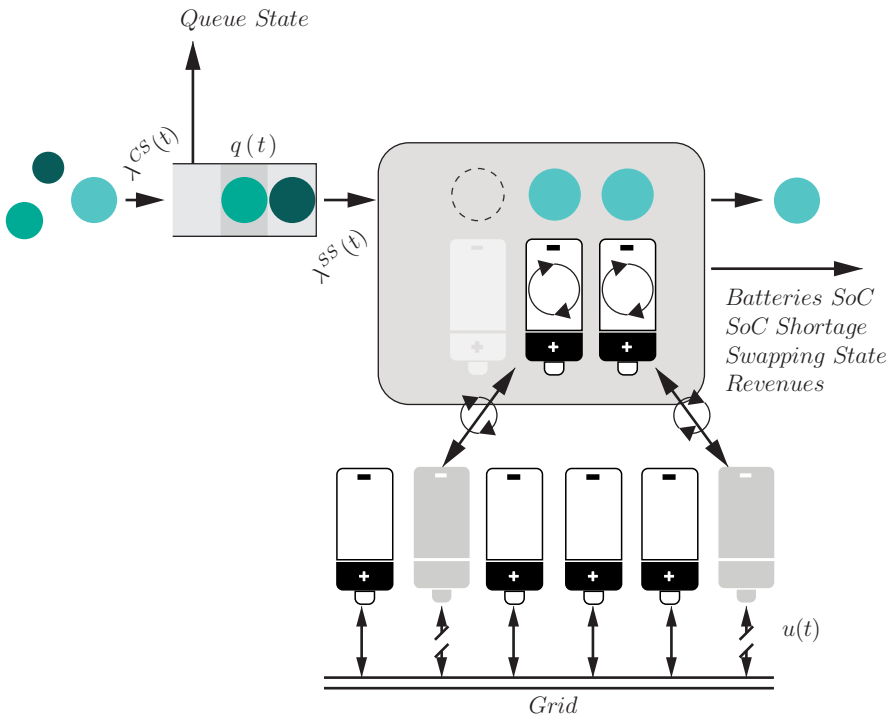

Figure 5.1: BSS Architecture

5.1 Queue model

When a customer arrives to a BSS , if the queue is empty and there is some free Swapping Space (SS) , he can start the swapping process directly. If there is not any free SS , the customer will have to wait before starting the swapping process. Furthermore, it is assumed that the swapping process starts just in the instant in which the SS is taken.

Said that, it has to be noticed that the number of customers arriving at a time t (denoted as $\lambda^{BSS}(t)$), is related but generally different from the number of customer taking the SS and starting the swapping process (given by $\lambda^{SS}(t)$), and the relation between both rates is given by the queue model. The model used is the result of assuring that the same number of customers arriving to the queue is the sum of the number of customers leaving it and the EVs within the queue.

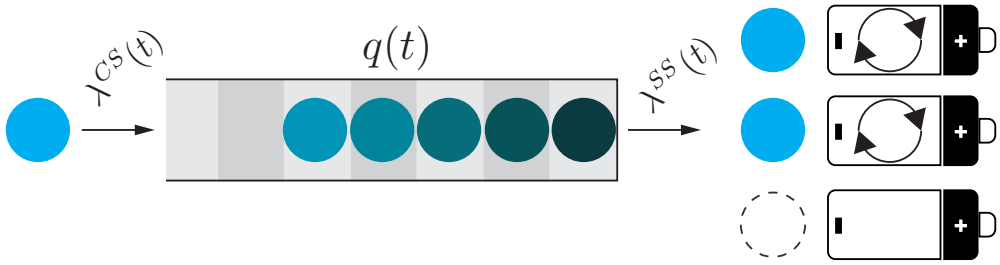

Figure 5.2: Demand rate considerations

$$\sum_{\tau=1}^{t\in T}(\lambda^{BSS}(\tau) - \lambda^{SS}(\tau)) = nEV_Q(\tau) \tag{5.1}$$

$$nEV_Q(t+1) = nEV_Q(t) + \lambda^{BSS}(t) - \lambda^{SS}(t) \tag{5.2}$$

where $nEV_Q(t)$ represents the number of EVs within the queue at time t and $\lambda^{SS}(\tau) \leq nSS$.

5.2 Battery Swapping Station

A BSS consists basically in a certain number of batteries and swapping spaces; and the objective is having enough full charged batteries to serve the customers arriving. Both figures (number of batteries and swapping spaces) determine the BSS size and will be tightly related to the amount of energy the BSS can serve.

The own nature of this configuration entails some particular features. For instance the swapping operation duration is fixed and can not be adapted, the customers can not request a personalized SoC since the charging process is completed

before the customers arrival, and precisely because of that, its well performance is conditioned by the demand prediction accuracy.

The fact of the BSSs not being obligated to fast-charge batteries makes them able to apply smoother control signals or event sell the energy stored if it results beneficial. That gives to the BSSs a great deal more suitable configuration to adapt its energy consumption if convenient.

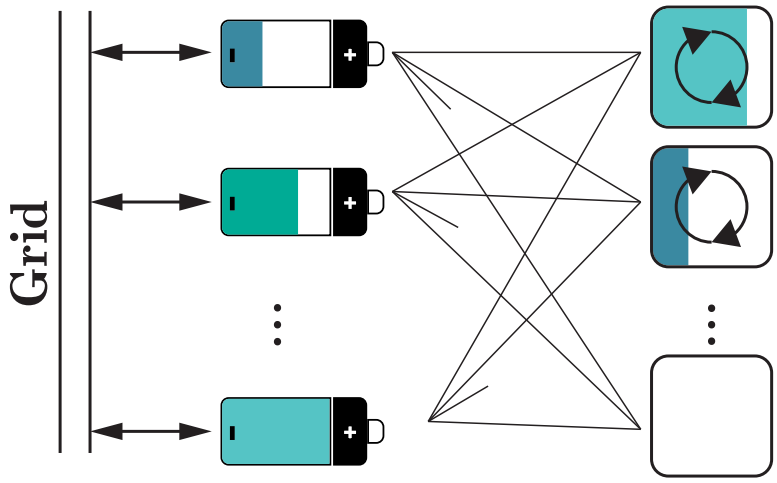

Figure 5.3: BSS scheme.

As it can be seen in figure 5.3, the batteries are assumed to be connected directly to the grid. When a new customer arrives, one of the most charged battery is assigned to him. This selection could be random or take into consideration some criteria such as the batteries number of cycles.

Parameters

As it has been commented, the size of a BSS is given by the number of batteries it owns ($nBat \in \mathbb{N}^+$), and the number of swapping spaces ($nSS \in \mathbb{N}^+$) available. The charging process is defined by the maximum power flow that can be applied to charge/discharge the batteries ($P^M_{Ch} \in \mathbb{R}$ kW), the maximum power flow the BSS can consume (P^M_{BSS} kW), the battery capacity (E^M_{Bat} kWh) and the time the swapping process entails ($TSwap$ min). Table 5.1 shows the typical values used for those parameters in this work.

Parameter	Value
$nBat$	5
nSS	4
P^M_{Ch}	80 kW
P^M_{BSS}	160 kW
E^M_{Bat}	30 kWh
$TSwap$	15 min

Table 5.1: Parameters typical value

System State

The state of the system comes defined by the SoC of the batteries in the BSS ($SoC_i = \frac{E_i}{E^M_{Bat}} \forall i \in \mathbb{N}^+[1, nBat]$ with E_i being the energy stored in battery-i) and its evolution is modeled by Equation 5.3.

$$SoC(t+1) = SoC(t) + \frac{P_b \Delta t}{E^M_{Bat}} \tag{5.3}$$

Where P_b is the power applied to the battery-b and Δt the sampling time.

The number of vehicles within the arrival queue is $nEV_Q(t) \in \mathbb{N}^+$ and the battery swapping operation progress is calculated as $Swap_j = \frac{SS^{cont}_j}{TSwap} \forall j \in (1, nSS)$ where SS^{cont}_j is a counter associated with the SS -j. Besides, some binary states have been introduced: a first binary variable ($Y_{b,j} \in \{0, 1\}$) which shows if the battery b is being swapping in the SS -j (1) or not (0) and a second binary variable that is activated if the SoC of battery-b is under the minimum desirable ($SoC^{LB} \in \{0, 1\}$).

Control Signals

Two sets of control signal can be differentiated. One set which commands the charging/discharging battery process $U_b \in \mathbb{R}[0, 1]$ and a second one which triggers a swapping operation involving the battery b and the swapping space j ($X_{bj} \in \{0, 1\}$).

The control signal U_b represents a normalized value of the power used to charge the battery-b in such a way that the power applied is equal to $P_b(t) = U_b(t) P^M_{Ch}(t)$

External Input

Finally, the BSS customers arrival rate $\lambda^{BSS}(t) \in \mathbb{N}^+$ is considered an external input which is related to the SS customer arrival rate $\lambda^{SS}(t) \in \mathbb{N}^+$ through the queue state (Section 5.1).

Chapter 6 Battery Swapping Station control

The objective of a BSS controller consists in managing the batteries (dis)charging, triggering the swapping process, as well as generating the battery assignation to each SS at the beginning of each swapping operation. This work proposes two methods for doing it. On the one hand, inspired by [17], an *event driven protocol* where only current information is used in the making decision process is presented in Section 6.1. On the other hand, a *MPC* is formulated in Section 6.2 as an extension of the optimization problem presented in [6] .

6.1 Event driven protocol

This strategy is mainly described by the flow chart in Figure 6.2. It considers that the number of full charged batteries in reserve must be, at least, equal to the number of swapping spaces in the BSS and if not, that status has to be reached as quickly as possible. The criteria followed to charge the rest of the batteries is based on the spot price and the mean price expected in the foreseeable future.

To implement the protocol the set of batteries Ω is split in two sets: a high priority one $\Omega^{HP} \subseteq \Omega$ and a regular one $\Omega^{LP} \subseteq \Omega$. Ω^{HP} contains the n_{SS} batteries with the highest SoC and Ω^{LP} the rest.

$$\Omega^{HP} = \left\{ i \in \Omega | \text{SoC}_{\ i} \geq \text{SoC}_{\ j \in \Omega^{LP}}, |\Omega^{HP}| = n_{SS} \right\} \tag{6.1}$$

$$\Omega^{LP} = \Omega \backslash \Psi \tag{6.2}$$

The control signal value depends on the battery priority. Regarding the high priority group:

$$U_{i \in \Omega^{HP}} = \min \left(1, \frac{\text{SoC}_{\ i}}{\sum_{k \in \Omega^{HP}} \text{SoC}_{\ k}} \frac{P_{BSS}^{M}}{P_{Ch}^{M}} \right) \tag{6.3}$$

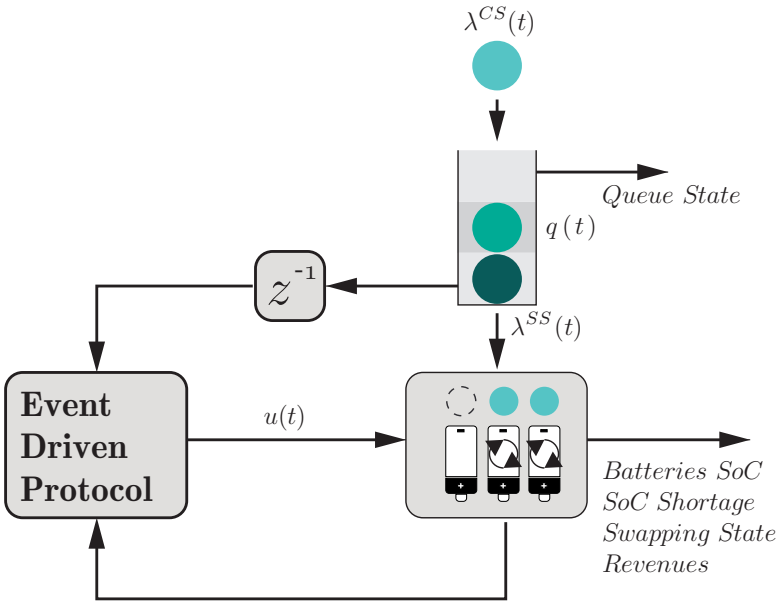

Figure 6.1: BSS control scheme for Event Driven protocol

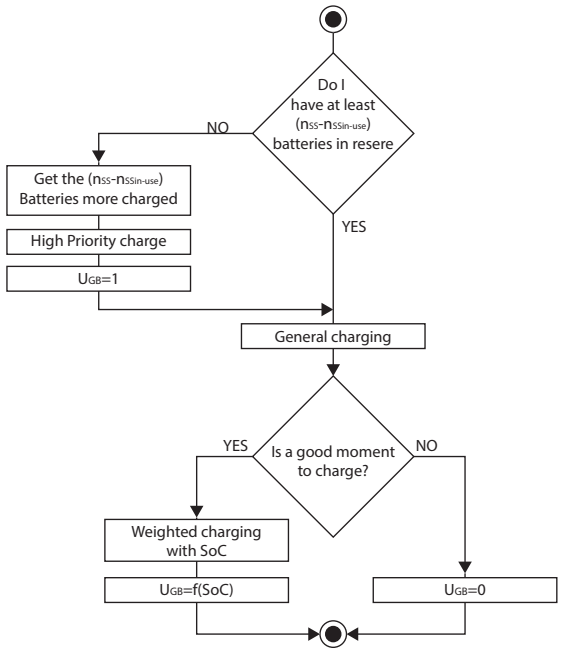

Figure 6.2: BSS Discrete Strategy Flow Chart

While if the priority is low, the control signal value takes into account the spot

price.

$$U_{i\in\Omega^{LP}} = \begin{cases} 0 & \text{if } pr(t) > pr(t+N_2) \\ \frac{\text{SoC}_{\ i}}{\sum_{k\in\Omega^{LP}}\text{SoC}_{\ k}} \frac{P^M_{BSS} - \sum_{i\in\Omega^{HP}} U_i P^M_{Ch}}{P^M_{Ch}} & \forall i \in \Omega^{LP} \end{cases} \tag{6.4}$$

6.2 MPC

In contrast to the protocol presented above, the MPC formulated makes use of a demand forecasting $\hat{\lambda}^{SS}(t)$. That information is used to determine the number of batteries that have to be full charged at each moment. Obviously, the same optimization problem with different demand forecasting accuracies results in different control performance. This conditions allow to motivate different prediction alternatives in Chapter 7.

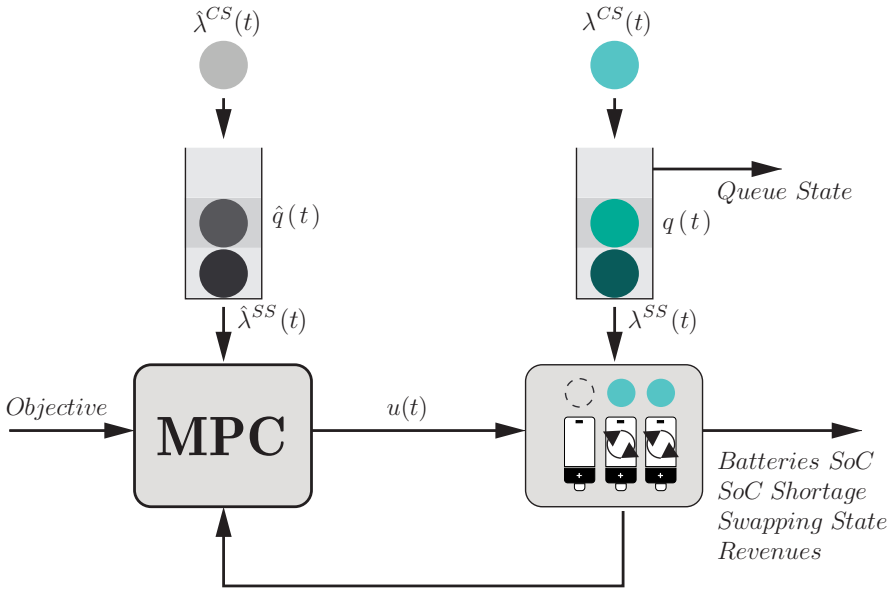

Figure 6.3: BSS control scheme for MPC

The optimization problem formulated here is based in the one presented by Mushfiqur R. Sarker et al. in [5]. The formulation has been changed to simplify some aspects (such as the existence of different types of batteries) and to include others (such as the duration of the swapping operation, a minimum SoC desirable

for every battery etc). The optimization problem proposed is:

Maximize

$$-(\sum_{t\in T}\sum_{b\in B}\left(x_{b,t}-SoC_{b,t}^{\text{Short}}\right)-\sum_{t\in T}pr_t\left(e_t\right)-200(\sum_{t\in T}D_t-\sum_{b\in B}x_{b,t})-9\sum_{t\in T}\sum_{b\in B}SoC_{b,t}^{Low} \tag{6.5}$$

Subject to

$$SoC_{b,t}=\left(SoC_{b,t-1}+\frac{TP_b^M}{E_b^M}\left(u_{b,t}^{ch}-u_{b,t}^{ds}\right)\right)\left(1-x_{b,t}\right)+SoC_{b,t}^{ini}x_{b,t}\ \forall b\in B,t\in T \tag{6.6}$$

$$SoC_{b,t-1}+SoC_{b,t}^{\text{short}}\geq x_{b,t}\ \forall b\in B,t\in T \tag{6.7}$$

$$\sum_{b\in B}x_{b,t}+bat_t^{\text{short}}=\hat{\lambda}_t^{SS}\ \forall t\in T \tag{6.8}$$

$$e_t^{\text{buy}}-e_t^{\text{sell}}=TP_{Ch}^M\sum_{b\in B}\left(u_{b,t}^{\text{ch}}-u_{b,t}^{\text{ds}}\right)\ \forall t\in T \tag{6.9}$$

$$y_{b,t}\leq\sum_{t-\text{TSwap}}^{t}x_{b,t} \tag{6.10}$$

$$y_{b,t}\geq\frac{1}{\text{TSwap}}\sum_{t-\text{Swap Time}}^{t}x_{b,t} \tag{6.11}$$

$$0\leq u_{b,t}^{\text{ch}}\leq\left(1-y_{b,t}\right)\ \forall b\in B,t\in T \tag{6.12}$$

$$0\leq u_{b,t}^{\text{ds}}\leq\left(1-y_{b,t}\right)\ \forall b\in B,t\in T \tag{6.13}$$

$$SoC_{b,t}^{Low}\leq\left(1-SoC^{LB}\right)+SoC_{b,t} \tag{6.14}$$

$$SoC_{b,t}^{Low}\geq SoC_{b,t}-1-SoC^{LB} \tag{6.15}$$

$$P_{Ch}^{\text{M}}\sum_{b\in B}u_{b,t}^{\text{ch}}\leq P_{BSS}^M \tag{6.16}$$

$$0\leq SoC_{i,t}\leq 1\ \forall b\in B,t\in T \tag{6.17}$$

$$0\leq SoC_{i,t}^{\text{short}}\leq 1\ \forall b\in B,t\in T \tag{6.18}$$

$$u_{b,t}^{\text{ch}}\leq 1\alpha_{b,t}\ \forall b\in B,t\in T \tag{6.19}$$

Constraint 6.6 corresponds to the battery model where the binary variable $x_{b,t}$ is used to reset the battery SoC each time that a swapping operation takes place. Constraints 6.7 and 6.8 are used to quantify the lack of energy in the partially charged batteries being swapped and the battery shortage if a customer is not served respectively. Equation 6.9 registers the amount of energy bought/sold. Constraints 6.10 and 6.11 relate the binary variable y, which shows that the battery is begin swapped, to the swapping operation triggering signal $x_{b,t}$. To

take into account the swapping operation itself, during which the battery being swapped can not be (dis)charged or been reassigned, constraints 6.12 and 6.13 are introduced. Constraints 6.14 and 6.15 activate the binary variable $SoC_{b,t}^{Low}$ when a battery SoC is under the security level previously established. Equation 6.17 ensures that the total power flow used is under the maximum level retailed by the BSS . Finally, constraints 6.17, 6.18 and 6.19 state the upper and lower bounds for the decision variables $u_{b,t}$, $SoC_{b,t}$ and $SoC_{b,t}^{\text{Short}}$.

The objective function 6.5 penalizes the non-fully charged battery that have been served, the amount of energy bough/sold, and battery shortage, as well as the number of battery whose SoC has been under the "security" level during the prediction horizon while maximize the perceived revenues.

The problem as it has been formulated is a Mixed integer nonlinear programming (MINLP) problem where the non linearity is introduced by constraint 6.6. In this case, the problem can be converted in a Mixed integer linear programming (MILP) by modifying equation 6.6 introducing new intermediate variables $V_{b,t}^1, V_{b,t}^2, V_{b,t}^3$ (following [18]). The new equation is rewritten as follows:

$$SoC_{b,t} = SoC_{b,t-1} + TP_b^{\text{M}} \left(u_{b,t}^{\text{ch}} - u_{b,t}^{\text{ds}}\right) - V_{b,t}^1 - TP_b^{\text{M}} \left(V_{b,t}^2 - V_{b,t}^3\right) + SoC_{b,t}^{ini} x_{b,t} \quad (6.20)$$

Where V values will be constrained in the next way:

$$V_{b,t}^1 \leq SoC_{b,t-1} \quad (6.21)$$
$$V_{b,t}^1 \geq SoC_{b,t-1} - M(1 - x_{b,t}) \quad (6.22)$$
$$V_{b,t}^1 \leq M x_{b,t} \quad (6.23)$$

$$V_{b,t}^2 \leq u_{b,t}^{\text{ch}} \quad (6.24)$$
$$V_{b,t}^2 \geq u_{b,t}^{\text{ch}} - M(1 - x_{b,t}) \quad (6.25)$$
$$V_{b,t}^2 \leq M x_{b,t} \quad (6.26)$$

$$V_{b,t}^3 \leq u_{b,t}^{\text{ds}} \quad (6.27)$$
$$V_{b,t}^3 \geq u_{b,t}^{\text{ds}} - M(1 - x_{b,t}) \quad (6.28)$$
$$V_{b,t}^3 \leq M x_{b,t} \quad (6.29)$$

Optimization resolution

The problem formulated could be solver with Matlab since it provides some solvers able to solve *MILP* problems. However, in case of using it directly, it is needed

to rewrite the problem in a standard form 6.30.

$$\min_x f^T x \text{ subject to } \begin{cases} x(\text{intcon}) \text{ are integers} \\ Ax \leq b \\ A_{eq}x = b_{eq} \\ lb \leq x \leq ub \end{cases} \tag{6.30}$$

Alternatively a tool that allows to solve optimization problems by describing them in a high level way can be used. Concretely the language used is *YALMIP* [19] that is an open-source parser compatible with a widely set of external solvers. Among which, the one used in this thesis is *Cplex*.

As an illustrative example, after defining the size of the different decision variables, the constraints and the objective function for this optimization problem are written as follows.

```
%objective function
    obj = -( 250*sum(sum(X-SoCShort))-sum(pr.*(sum(Uch-Uds,1)*
      DT*P))-(200*sum((Dem_Pred - sum(X,1)))))-9*sum(sum(BLOW));

%Constraints
    Constraints = [SOC==([Socini, SOC(:,1:(end-1))]+DT*P*(Uch-
      Uds)/EBat-V1-P*DT*(V2-V3)+0.1*X ), ...
    [Socini, SOC(:,1:(end-1))]+SoCShort>=X , ...
    Uch<=(1-X), Uch>=0, ...
    Uds<=(1-X), Uds>=0, ...
    SOC >=0 , SOC<=1, ...
    SoCShort>=0 , SoCShort<=1, ...
    V1<=[Socini, SOC(:,1:(end-1))] , V1>=[Socini,SOC(:,1:(end
      -1))]-(1-X) , V1<=X, ...
    V2<=Uch , V2>=Uch-(1-X) , V2<=X, ...
    V3<=Uds , V3>=Uds-(1-X) , V3<=X, ...
    (Dem_Pred - sum(X,1))>=0,V1>=0,V2>=0,V3>=0,...
    Uch<=(1-Y),Uds<=(1-Y),X<=(1-Y),...
    P*sum(Uch)<=PCS,...
    Y <=[Xini,X(:,1:(end-1))]*AUX, Y>=1/Swap_Time*[Xini,X(:,1:(
      end-1))]*AUX;
    BFULL<=0.20001+SOC, BFULL>=SOC-0.8,...
    BLOW<=0.80001+SOC, BLOW>=SOC-0.2];
```

To be in position of really solving the problem, it is necessary to clarify some aspects about the term $\hat{\lambda}_t^{SS}$ presented in 6.8 and it is done in the next chapter.

Chapter 7 Demand

This chapter describes the forecasting methods whose performance and results will be discussed in Section 8.2. The demand prediction plays a key role in the BSS performance. Its accuracy can result in improved market strategies, better QoS , batteries managing etc. This project proposes using ITS as a tool to estimate it accurately. The fact of having real-time information available about EV SoC , BSS congestion, neighboring BSS prices etc makes more interesting the study of advanced demand forecasting tools. This section presents three prediction strategies that will be tested in Section 8. First, a *blind* strategy which does not use any kind of external information, a second one that uses historical data to generate a likely arrival pattern; and finally a third one which uses real time information about the SoC and traffic congestion to get accurate and flexible predictions.

It is worthy stressing that the importance of $\lambda^{BSS}(t)$ forecasting accuracy decreases with the number of customers in the queue $nEV_Q(t)$ given that:

- The SS arrival rate uncertainty is upper bounded by the value $\max(0, SS(t) - q(t))$
- $\lambda^{SS}(t)$ turns deterministic in the foreseeable future if there are enough customers waiting in the queue.

7.1 Blind strategy

The simplest option regarding the BSS customers arrival estimation is considering it constant. The lack of information in that sense could lead a BSS manager to operate its facility by imposing the constraint of having at least as many full charged batteries as the number of SS , that corresponds to consider that nSS

customers are arriving shortly.

$$\lambda_{Bl}^{BSS} \in \mathbb{R}^{1\times N_2} | l_i^{BSS} = 0 \ \forall i \neq j, l_j^{cs} = nSS \tag{7.1}$$

where N_2 is the prediction horizon considered and j is the customer arrival time supposed. That strategy is precisely the implicitly used in the *event driven control* addressed in Section 6.1.

7.2 Historic Data

A second option consists in using historical data to generate a likely customer arrival pattern $\lambda_{HD}^{BSS} = [l_i^{cs,hd}]$. Given a register with N^{Reg} samples of the customer arrival experienced during a simulation period $\lambda_{Reg\#i}^{BSS} = [l_j^{cs,reg\#i}] \ \forall i \in [1, \cdots, N^{Reg}] \ \forall j \in [1, \cdots, N_2]$, the historical pattern elements are given by:

$$l_i^{cs,hd} = \max(l_j^{cs,rg\#i}) \ \forall i \in (1, \cdots, N^{Reg}) \tag{7.2}$$

Where the pattern is generated by considering the maximum arrival rate experienced at each time in order to be conservative and attempting to assure the QoS level.

7.3 ITS approach

From the data provided by the ITS proposed in Section 4.4, the number of customers arriving in the foreseeable future could be approximated. As commented before, the information gathered within each cell is:

$$SoC_{Cell} = \frac{\sum SoC}{nEV_{Cell}} \tag{7.3}$$

$$Ev_{Cell} = \frac{nEV_{Cell}}{nEV_{Tot}} \tag{7.4}$$

The problem to solve is estimating the arrival rate $\lambda^{BSS}(t+k)$ for a BSS using the information in each cell. Given a cell, it is possible to obtain a SoC range ($[SoC_m, SoC_M]$) such as, a customer with its battery within that range could reach the BSS at time $t+K$. Once the range has been obtained, an upper bound of the number of potential customers in the cell within that range can be estimated.

SoC Range

Given a cell, a SoC range associated with each future instant K can be calculated. Assuming the speed at which the EVs are moving, the prediction instant of interest can be turned into a distance (d_{path} m).

$$d_{path} = K \cdot vel \tag{7.5}$$

Thus, d_{path} represents the distance that a customer has to be able to drive for arriving at $t + K$. Assuming that the EVs only drive in straight line (which is an assumption suitable for this particular case), the set of points such that the sum of the distances up to the BSS considered and up to the cell position is equal to d_{path} comes determined by an ellipse (Figure 7.1). The ellipse represents the points where the trajectory changes, and for the scenario considered in this works, each trajectory changing corresponds with a decision of going to charge.

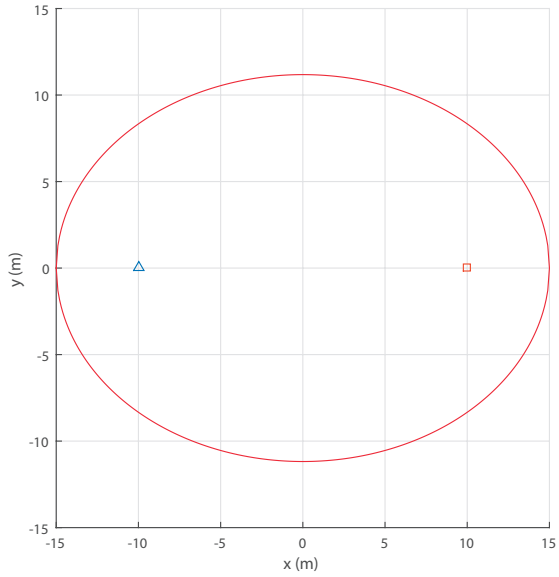

Figure 7.1: Ellipse representing the points where the decision of going to charge must be making in order to reach the BSS considered at the future instant of interest.

Taking into account the ellipse polar form relative to a focus (Equation 7.6), the SoC_m and the SoC_M that result in making the decision of going to charge in the nearest and furthest ellipse point from the cell position can be calculated (Equations 7.8 and 7.8).

$$r(\theta) = \frac{a(1 - e^2)}{1 + e\cos(\theta)} \tag{7.6}$$

$$SoC_m = \min_{\theta} R^{CELL}(\theta) \tag{7.7}$$

$$SoC_M = \max_{\theta} R^{CELL}(\theta) \tag{7.8}$$

The closest and furthest point from the cell position can be easily calculated by doing $\frac{dr(\theta)}{d\theta} = 0$, and the points resulting are $(0, a)$ for the closest and $(0, -a)$ for the furthest. With that in mind, the next can be written:

$$SoC_m = SoC_{Charge} + (a - \frac{dist(BSS, CELL)}{2})\frac{1}{Max\_Range} \tag{7.9}$$

$$SoC_M = SoC_{Charge} + \frac{a + dist(BSS, CELL)}{Max\_Range} \tag{7.10}$$

Maximum potential customers

Before considering the SoC range, the potential number of users associated with a single target SoC is obtained. Knowing the mean SoC registered in the cell and the number of EV within it, one can obtain the maximum potential number of customers in the cell with a desired SoC . Concretely, for a target SoC = SoC^* the maximum number of EV within the cell ($nEV^M_{SoC^*}$) is:

$$\begin{aligned} nEV^M_{SoC^*}(SoC_{Cell} - SoC^*) &\leq (nEV_{Cell} - nEV^M_{SoC^*})(1 - SoC_{Cell}) \\ nEV^M_{SoC^*} &\leq \frac{nEV_{Cell}(1 - SoC_{Cell})}{1 - SoC^*} \end{aligned} \tag{7.11}$$

if $SoC^* \leq SoC_{Cell}$ and

$$\begin{aligned} nEV^M_{SoC^*}(SoC^* - SoC_{Cell}) &\leq (nEV_{Cell} - nEV^M_{SoC^*})SoC_{Cell} \\ nEV^M_{SoC^*} &\leq \frac{nEV_{Cell}SoC_{Cell}}{SoC^*} \end{aligned} \tag{7.12}$$

if $SoC^* \geq SoC_{Cell}$.

Figure 7.2 shows the upper bound calculated given a SoC_{Cell} (vertical dashed lines) and a nEV_{Cell} (horizontal dashed line).

When a target SoC range is being considered, the maximum number of potential customer in the cell within the range can be upper bounded calculating the potential customers for each range's limit, and taking the biggest one. The limit that will report the greatest result changes according to the three cases shown in Figure 7.3.

1. SoC_m if $SoC_m > SoC_{Cell}$ and $SoC_M > SoC_{Cell}$.
2. SoC_{Cell}if $SoC_m < SoC_{Cell}$ and $SoC_M > SoC_{Cell}$.
3. SoC_Mif $SoC_m < SoC_{Cell}$ and $SoC_M < SoC_{Cell}$.

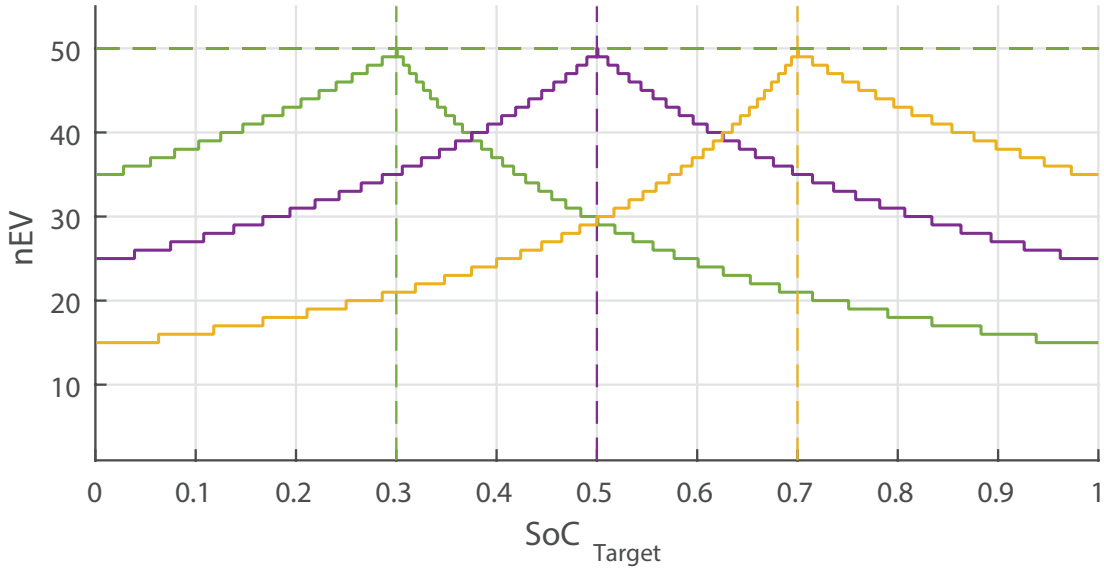

Figure 7.2: Maximum potential number of EVs within a cell according the target SoCs (x-axis) and different SoC_{Cell} (vertical dashed lines).

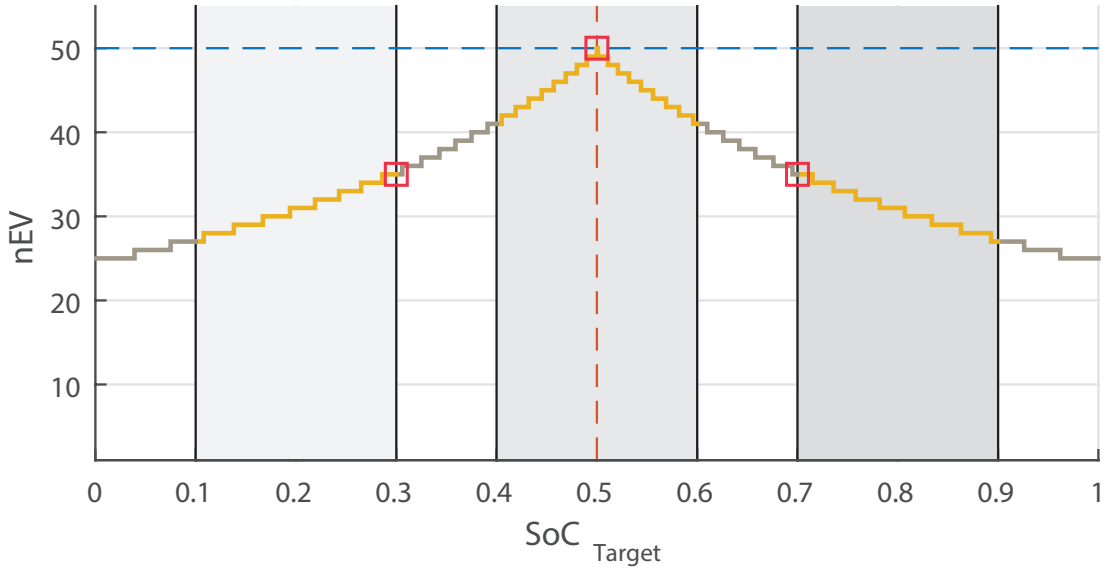

Figure 7.3: Cases according to the position of the range's limits.

Additional considerations

There are some aspects that have to be taken into account regarding to this method. On the one hand, for some BSSs , it is possible that the ellipse aforementioned will contain points out of the influence area (Figure 7.4) denoting by

influence area the map extension whose closest BSS is the one considered. Those points have to be neglected since an EV making a decision in that points will not select the BSS evaluated.

On the other hand the discussion presented is applicable for users whose SoC is greater than SoC_{Charge}. Those with $SoC \leq SoC_{Charge}$ and being within the influence region, are directly assigned.

Finally, it has to be noticed that, in general, a user within the region could describe different paths before driving towards the BSS and thus, a user could reach the BSS at different instants in the future. That means that, the prediction can result oversize as a result of overlapping ellipses. Figure 7.5 shows two pairs of ellipses, one pair with overlapping and other one without it.

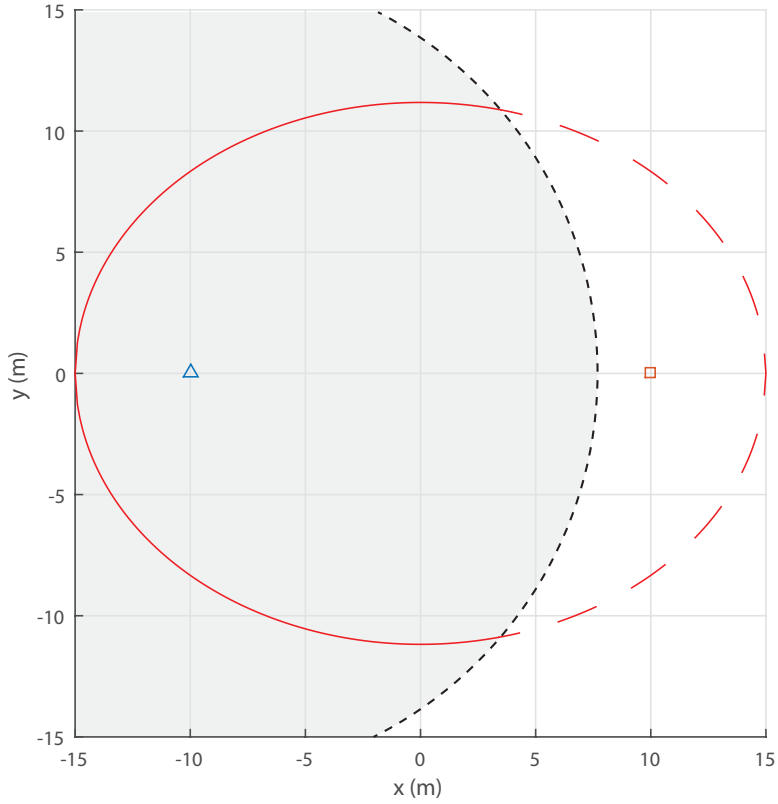

Figure 7.4: Ellipse out of range case

A solution for this issue is selecting a set of ellipses avoiding overlapping, or what is the same, quantizing the future instants for which the demand can be estimated. The relation between the suitable ellipses (or better said, the future predicted instant) with the $dist(BSS, CELL)$ is.

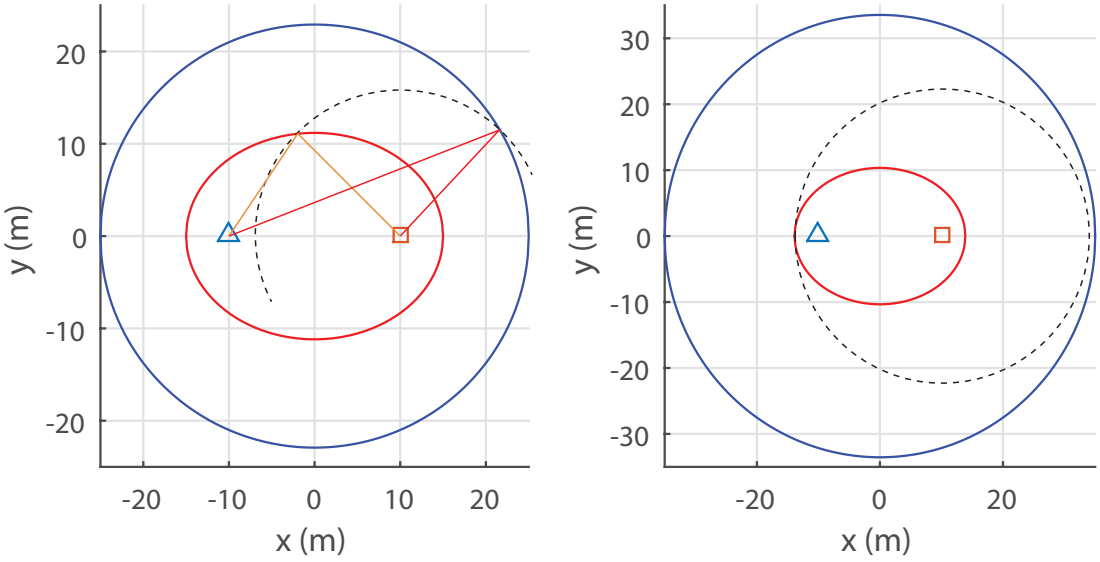

Figure 7.5: Ellipse overlapping

$$a_{ellipse\ j+1} = a_{ellipse\ j} + dist(BSS, CELL) \tag{7.13}$$

$$T_j = T_{j-1} + \frac{2dist(BSS, CELL)}{vel} \tag{7.14}$$

The steps followed to implement this algorithm are:

1. Get distance $dist(BSS, CELL)$
2. If $CELL$ is within the influence region.

   Get the arrival time, and the potential number of users with $SoC \leq SoC_{Charge}$.
3. Get time sample vector.
4. Get SoC_m, SoC_M for each future instant.
5. Get nEV^* associated with each range.
6. Assign the result to the demand forecast vector.

ITS cell size influence

It is important to point out that ITS has a limitation regarding the nearest prediction possible that is given by the ITS $_{size}/(2vel)$ s. But from the point of

view of the implementation, considering the first prediction instant equals to that value results not having the necessity of having any full charged battery since the algorithm think that it has ITS $_{size}/(2vel)$ to manage it. The solution is applying a temporary offset of precisely that value.

Additionally, it has to be noticed that the larger the cell size, the greater the prediction uncertainty.

Chapter 8 Results

This Chapter shows the results for seeing how each algorithm here presented works. First, Section 8.1 presents some simulations for stressing the main working differences between the *event driven control* (Section 6.1) and the MPC (Section 6.2) proposed for the BSS being managed. Then, Section 8.2 explores and compares the two demand forecasting methods addressed in Chapter 7. Finally, Section 8.3 compares the control algorithms performance when using different demand prediction methods supported by the information extracted from the simulator developed in Chapter 4.

8.1 BSS Management

This sections shows the practical differences between the control techniques presented in Chapter 6. Both the price and the demand evolution have been generated synthetically. The price profile corresponds to the one shown in Figure 8.1 and its shape has been conceived to clearly see the price influence over the solution. Regarding the congestion level, four cases are tested: (i) a non-customers case, (ii) a low congested, (iii) a medium congested and (iv) a high congested case whose demand profiles are shown in Figure 8.2, 8.3, 8.4 and 8.5 correspondingly. The result charts interpretation is the next: if one of the results Figures is observed (for instance 8.8) you will see a gray line corresponding to the battery control signal, a blue line showing the SoC and a red-dashed line which is the binary control signal that triggers the swapping operation.

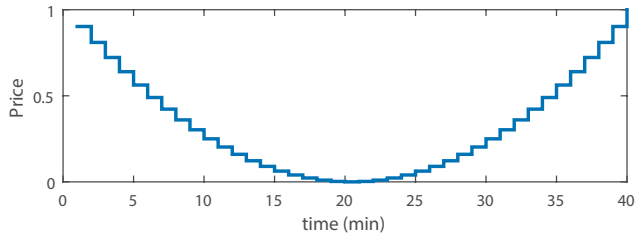

Figure 8.1: Price

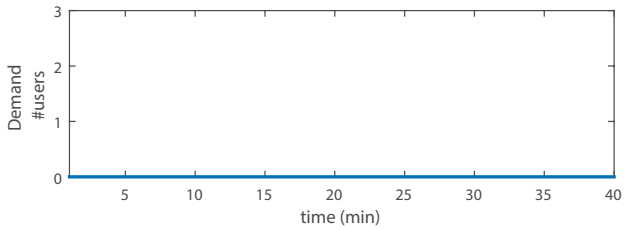

Figure 8.2: Non-customer case demand profile.

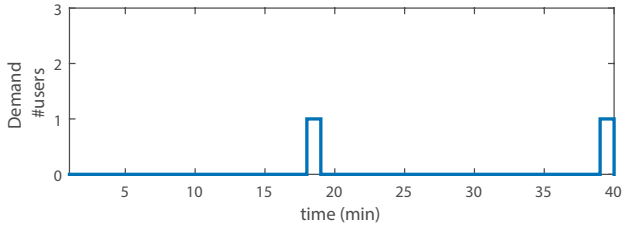

Figure 8.3: Low congestion case demand profile.

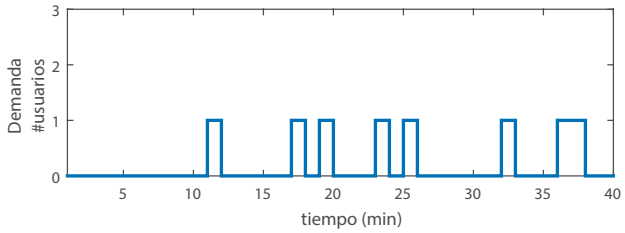

Figure 8.4: Medium congestion case demand profile

Event Driven Protocol

The results of applying the event driven protocol with the demand curves presented above are shown in Figures 8.6, 8.7, 8.8 and 8.9. The non-customers case (Figure 8.6) shows how the algorithms charge nSS batteries as soon as possible and then, when the price is low, it charges the rest. Both the low and medium

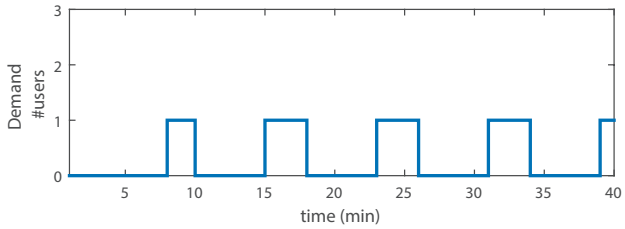

Figure 8.5: High congestion case demand profile

congested cases shows how it manages to serve full charged batteries and how, during the $Tswap$ minutes the swapping operation lasts, the batteries are blocked.

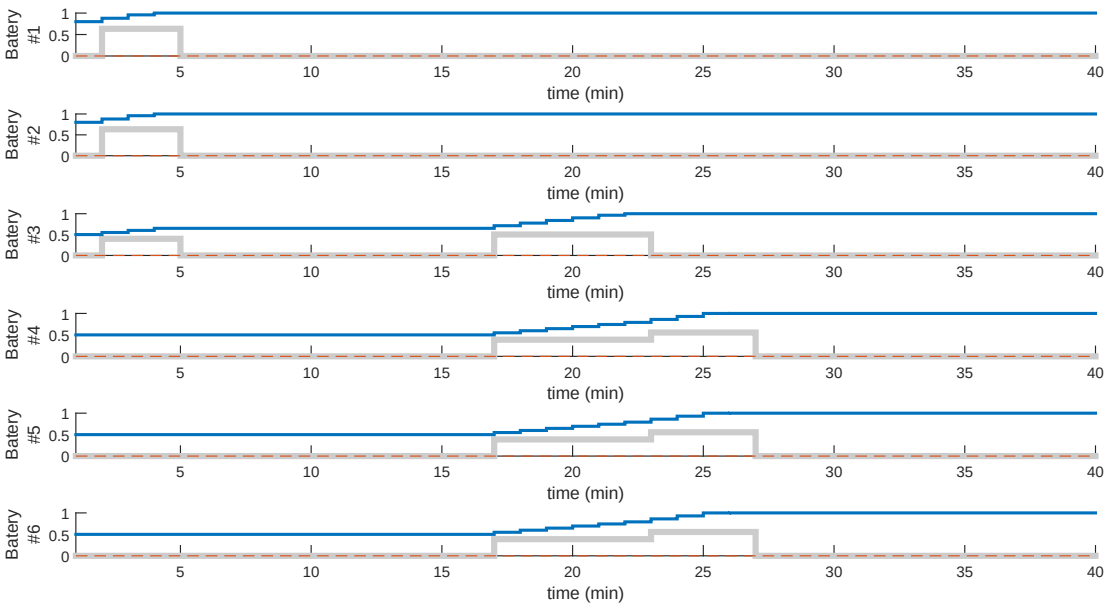

Figure 8.6: Disc Cong Level None Batteries SoC

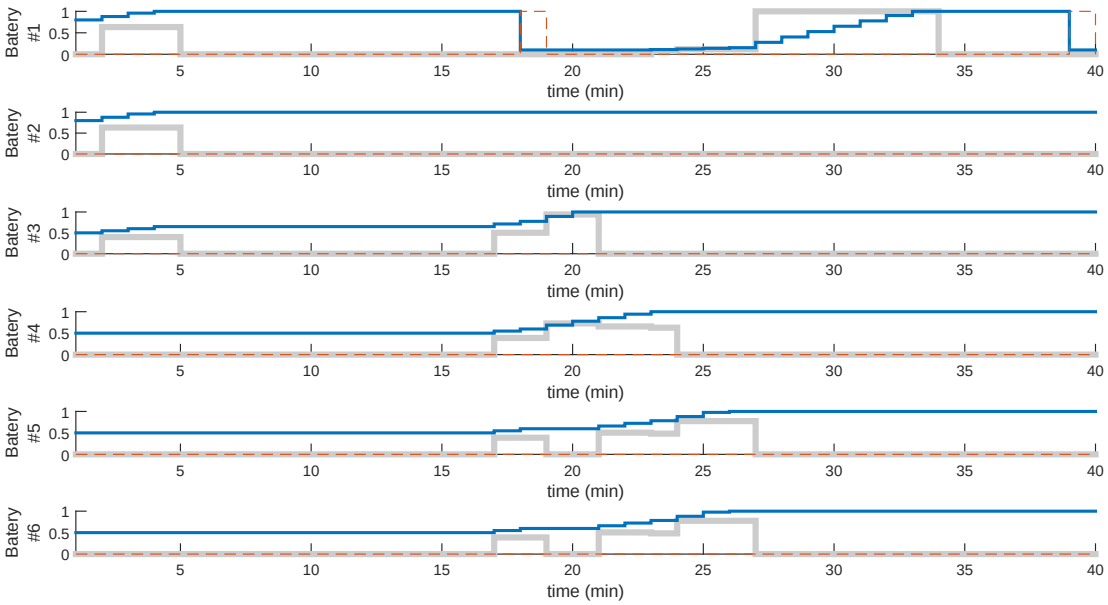

Figure 8.7: Disc Cong Level Low Batteries SoC

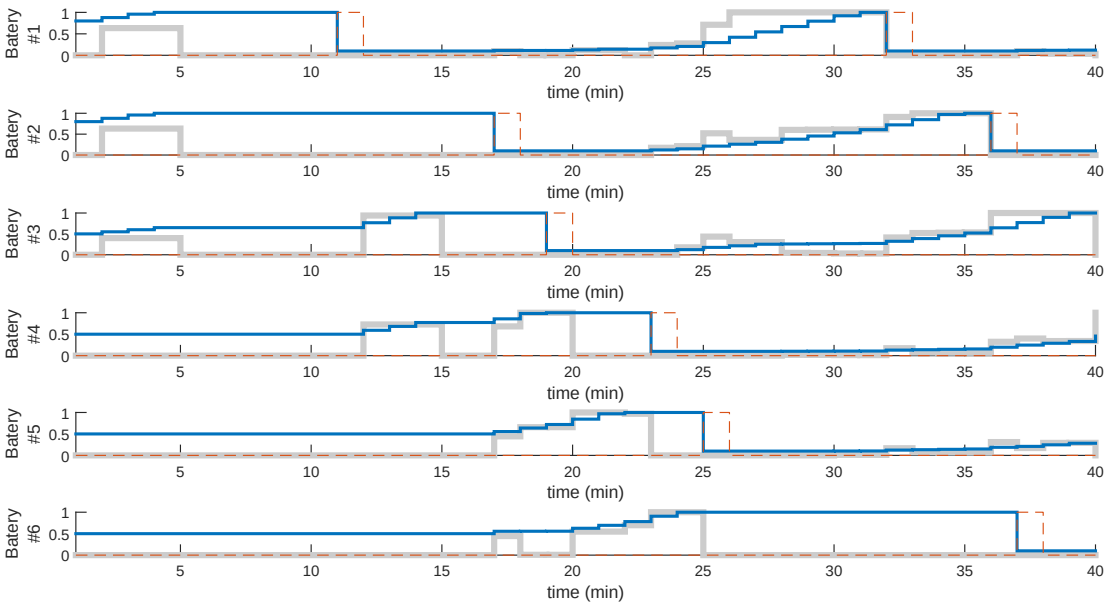

Figure 8.8: Disc Cong Level Medium Batteries SoC

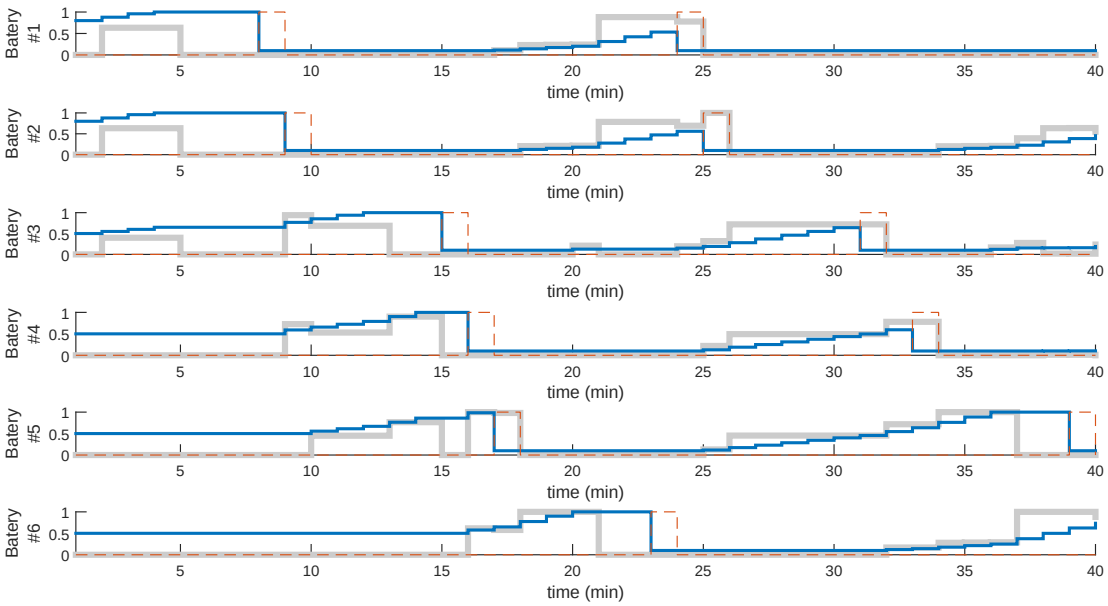

Figure 8.9: Disc Cong Level High Batteries SoC

8.1.1 Optimization

When the optimization problem presented in Section 6.2 is solved for the input signals presented at the beginning of this section, the results shown in Figures 8.10, 8.11, 8.12 and 8.13 are obtained.

In the case where there is no customers, the control signal manages to maximize the revenues. As it can be seen in Figure 8.10, the algorithm charges the batteries when the price is low, and sell the energy stored at the end of the simulation when the price is higher.

Figure 8.11 shows the result in the second case. Now, there are only two costumers arriving in the time considered and the algorithm chooses to serve them with Batteries number 1 and 6. With this congestion level, the algorithm works perfectly since there is not any kind of problem regarding power boundary or lack of batteries.

If the number of users is increased a little more, the algorithm begins to show some problems regarding the computational time needed. In Figures 8.12 and 8.13, it can be seen how the algorithm optimizes the SoC of the batteries to be swapped although, in certain moments, the imposed power boundary makes impossible to fully charge them in time. After each swapping event, the battery SoC is reduced to the SoC that the battery of the customers being served have. Since the congestion used is a prediction, that SoC is unknown beforehand and it is assumed to be 0.1.

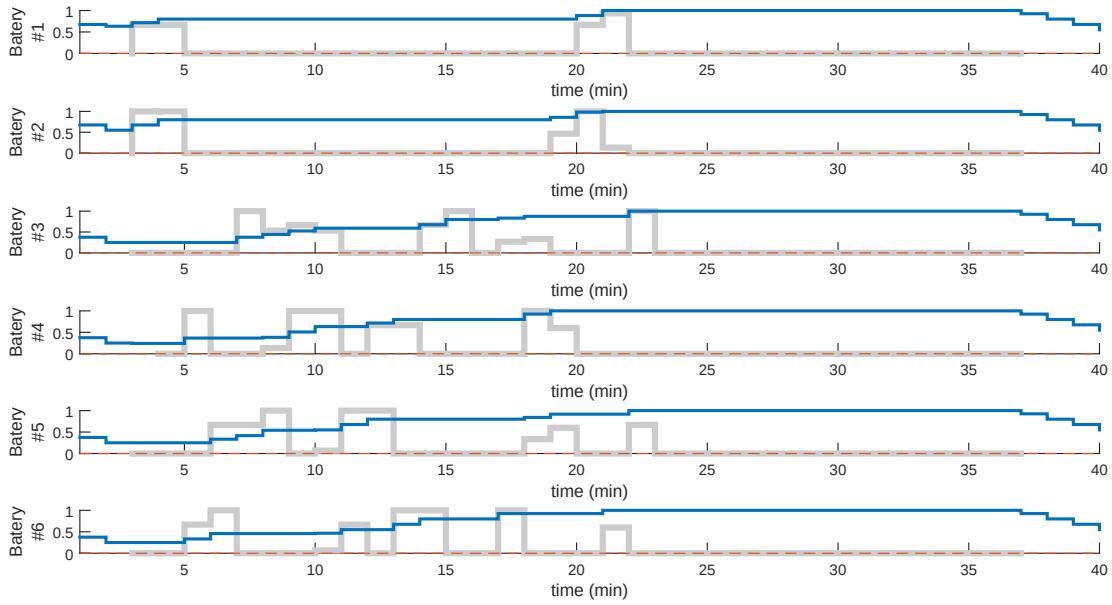

Figure 8.10: Batteries SoC

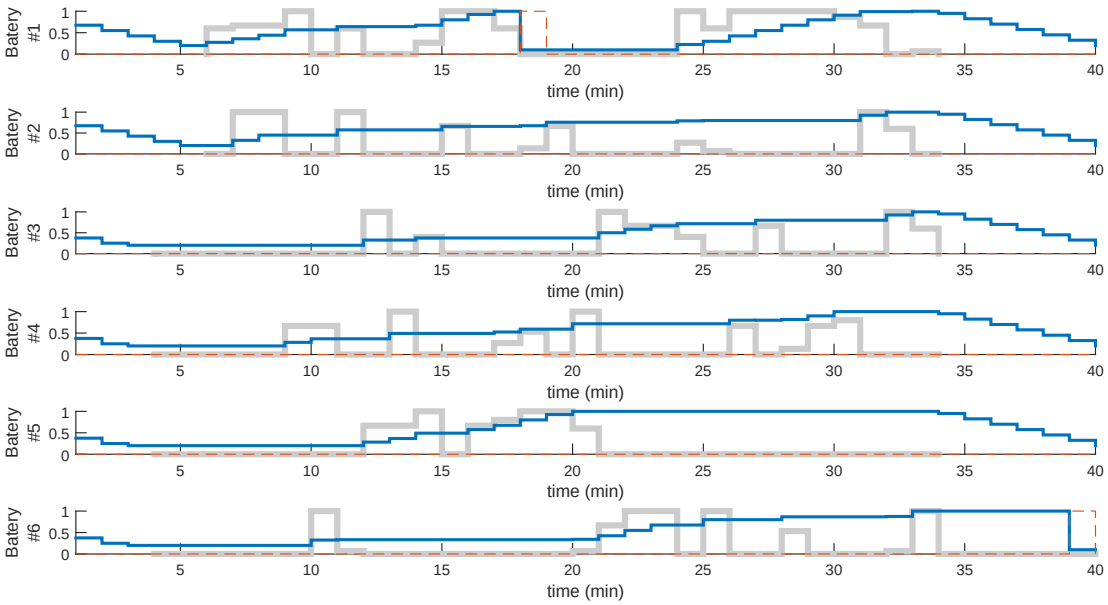

Figure 8.11: Batteries SoC

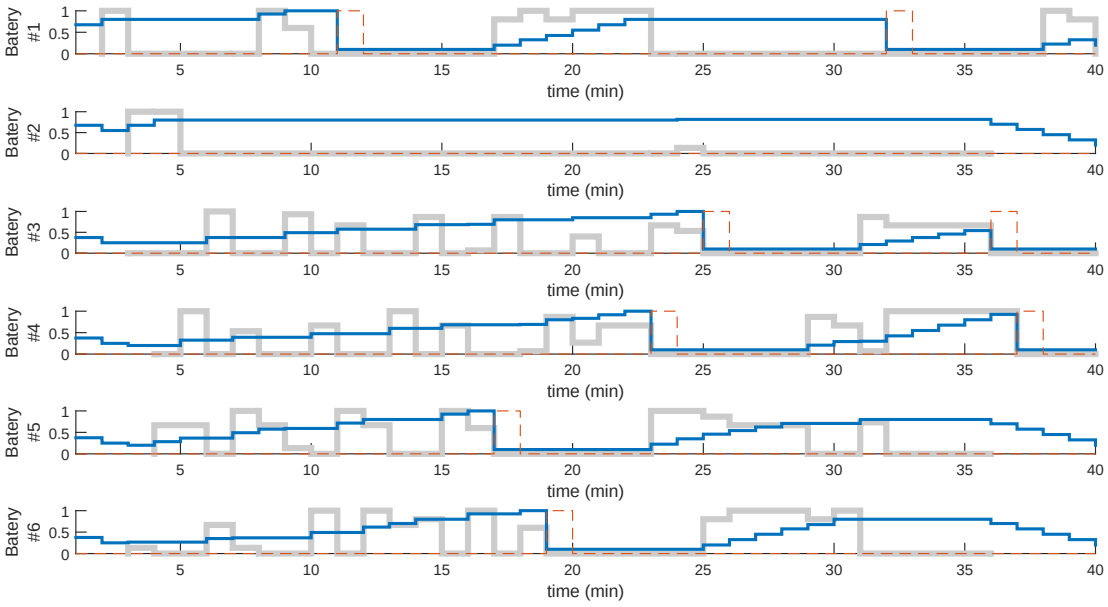

Figure 8.12: Batteries SoC

Computational time

Figure 8.14 shows an experimental relation between the computational time and the number of arriving customers considered for a temporal horizon of N_2 =

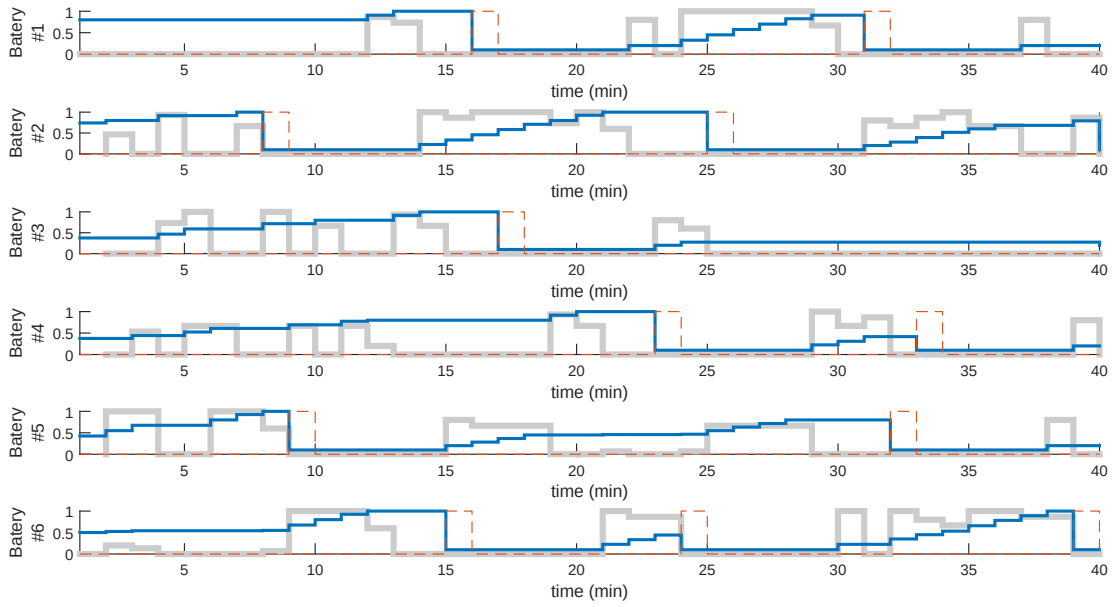

Figure 8.13: Batteries SoC

40min.

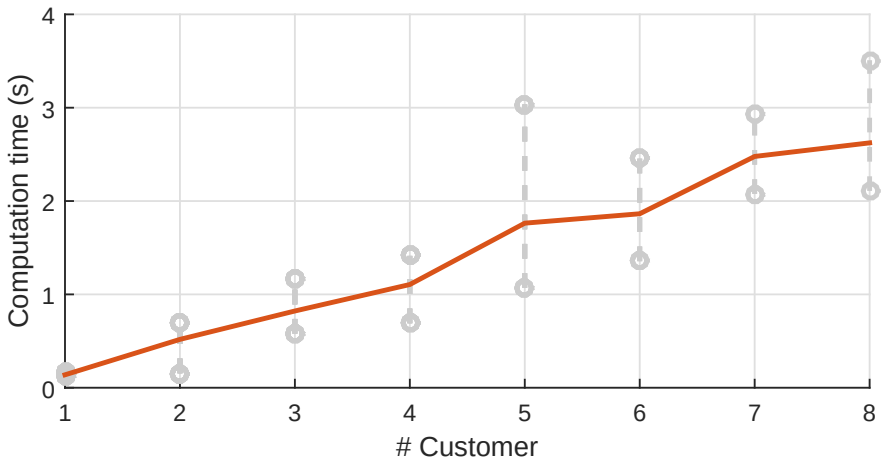

Figure 8.14: Computational time

8.2 Demand Forecasting

To illustrate the different demand forecasting alternatives presented in Chapter 7, both predictions techniques are going to be compared. The scenario where they have been tested is defined by the parameters in table 8.1 and it can be previewed in Figures 8.15 and 8.16.

Parameter	Value
nEV	100
Scenario Size	$500 \times 500\ m$
BSS Spacing	$500\ m$
Sample time	$1\ min$
Ev Vel	$20\ m/s$
Ev Bat Capacity	$30kWh$
Ev Bat Max Range	$8000\ m$
RT Resolution	$500\ m$
Ev Max P Charge	$60kW$
BSS nSS	4
BSS nBat	6
Swapping time	$15min$
BSS Max Power	$80kW$

Table 8.1: Scenario Parameters

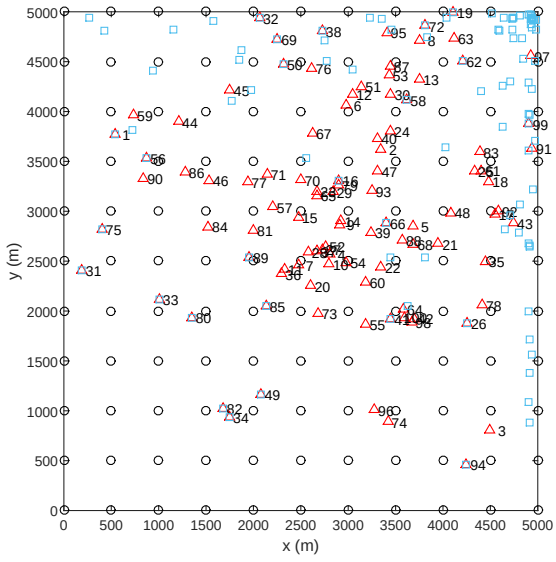

Figure 8.15: Scenario Preview

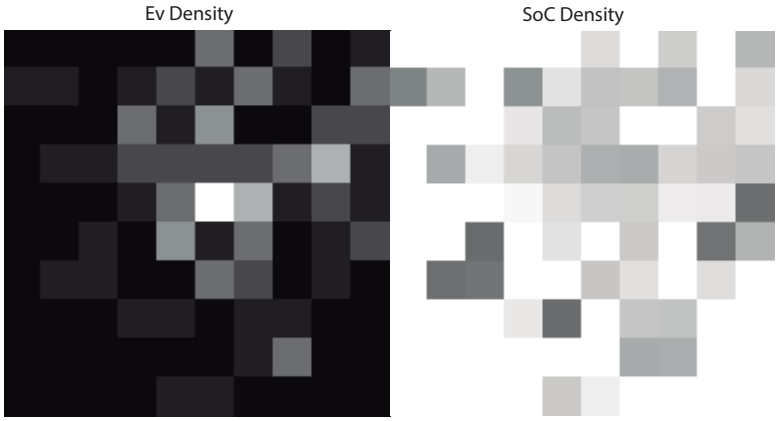

Figure 8.16: Scenario Density Preview

Fixed Pattern

As it was commented, getting a fixed likely demand pattern requires a previous training. For that propose, the simulator has been used to generate a training set of 50 simulations in total.

ITS approach

The demand prediction which makes use of an ITS manages to extract a more accurate prediction without any training stage. It is worthy commenting that this strategy calculates at each time t a prediction up to $t + N_2$. That means that for any moment t^* there are N_2 different predictions according to the instant in which it was done $\lambda^{BSS}(t|t-k)\ k \in \mathbb{N}^+ : (0, N_2)$. For being able to compare this strategy with the fixed pattern, the last points of each prediction have been neglected and the first points are used to generate an ITS demand profile.

Comparison

To discuss the differences between the methods, some BSSs with different congestion levels are going to be selected and its demand will be predicted and compared with the exact arrival events registered. In case of BSSs placed in low traffic congestion areas (Figures 8.17 and 8.18) both predictions result very conservative and thus, none of them receive any unexpected customer. The main difference resides in the false-positive predictions. Fixed pattern approach takes into account the arrival events registered in the past and because of that it can not adapt its prediction to new conditions. When no customers arrive, ITS approach observes that the surrounding region does not contain any potential customer while the

fixed pattern remembers that sometime in the past, it received some customers and hence, it keeps some batteries ready.

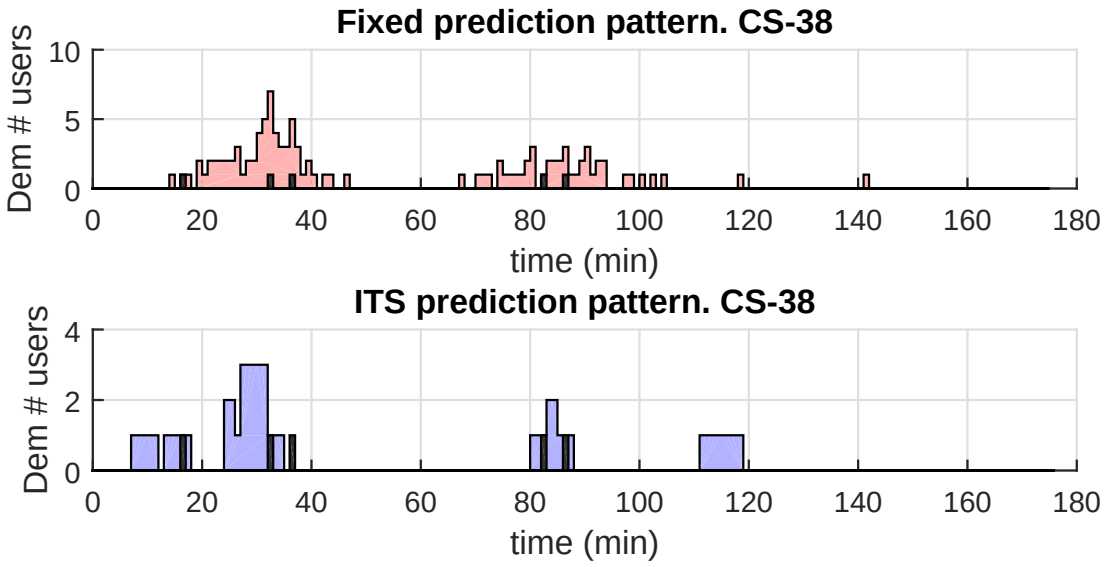

Figure 8.17: Demand prediction methods comparison with a little congested BSS .

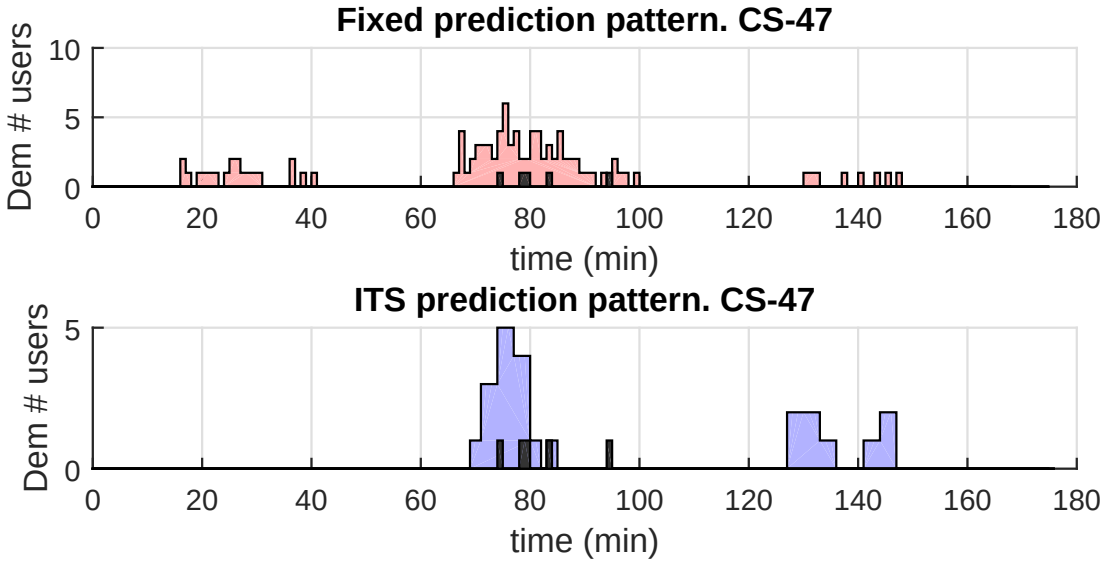

Figure 8.18: Demand prediction methods comparison with a little congested BSS .

When the traffic level of the area grows (Figures 8.19 and 8.20), the same

discussion can be applied. Besides, it can be seen how ITS starts to overestimate the number of users arriving given that it considers all the vehicles driving close to it.

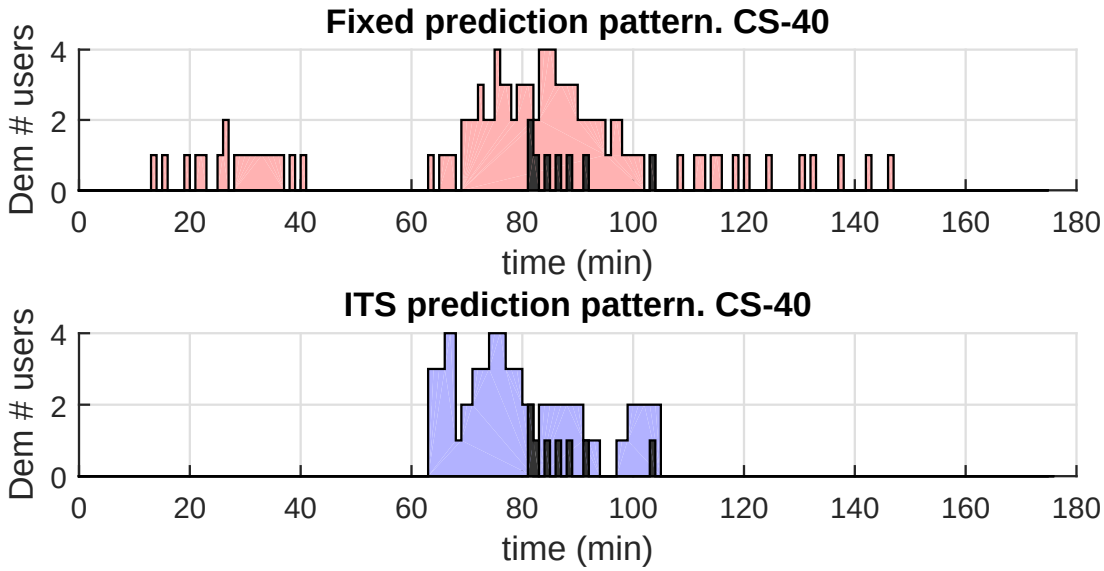

Figure 8.19: Demand prediction methods comparison with a medium congested BSS .

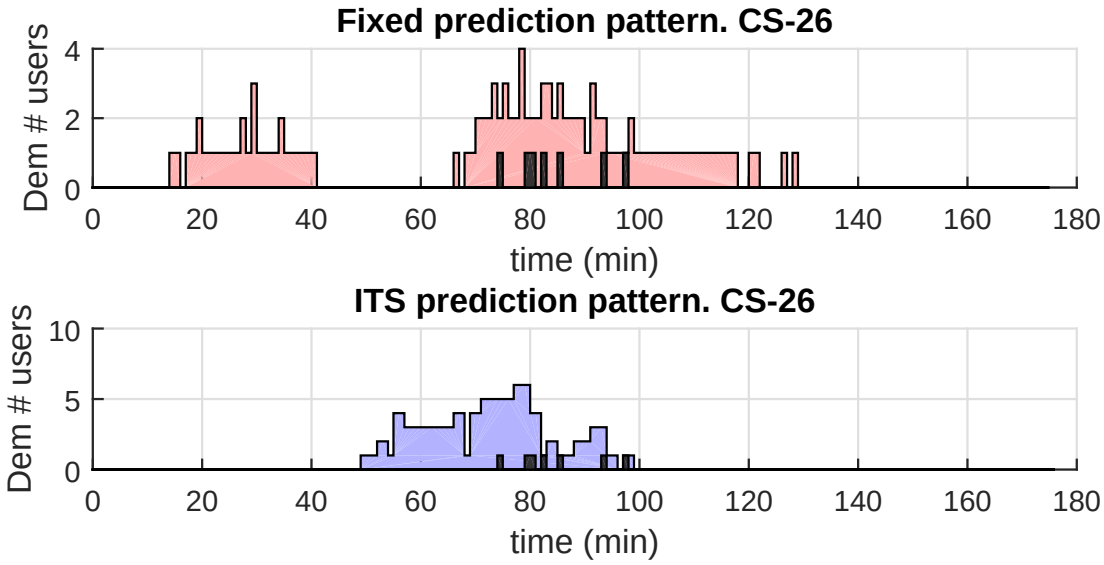

Figure 8.20: Demand prediction methods comparison with a medium congested BSS .

Finally, BSS placed in high congested areas (Figures 8.21 and 8.22) leads to the same discussion regarding the fixed pattern prediction. In relation to the ITS approach, a new effect appears. It corresponds to the final part of the charts and it is produced by the near parked vehicles. The interpretation is simple, the algorithm considers the SoC of the parked vehicles and attempts to keep some battery charged to cover a possible arrival.

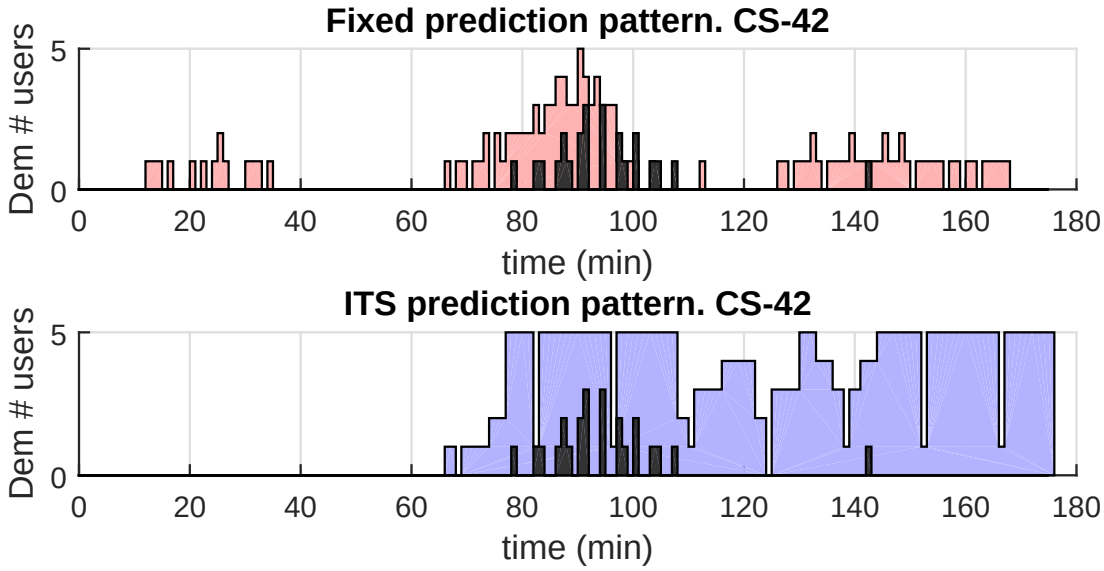

Figure 8.21: Demand prediction methods comparison with a high congested BSS .

Both ITS effects (parked vehicles and prediction overestimation) have good implications in terms of QoS and not so good in terms of business profitability since there are batteries that can not be operated. A possible solution is attempting to detect both situations and applying rules to make the effect decreases. In the particular case of oversize prediction, a good option is upper bounding its value according to the number of SS and taking into account that the existence of a queue makes that considering ten or four customers arriving have the same effect over the optimized solution.

To compare numerically both addresses, the prediction margin and error are going to me measure in each case. Both the error and the margin are calculated as the mean error/margin registered during the simulations (Equations 8.2 and 8.1).

$$DF_{cs}^{Error} = \overline{\lambda(t) - DFPattern} \tag{8.1}$$

$$DF_{cs}^{Margin} = \overline{DFPattern - \lambda(t)} \tag{8.2}$$

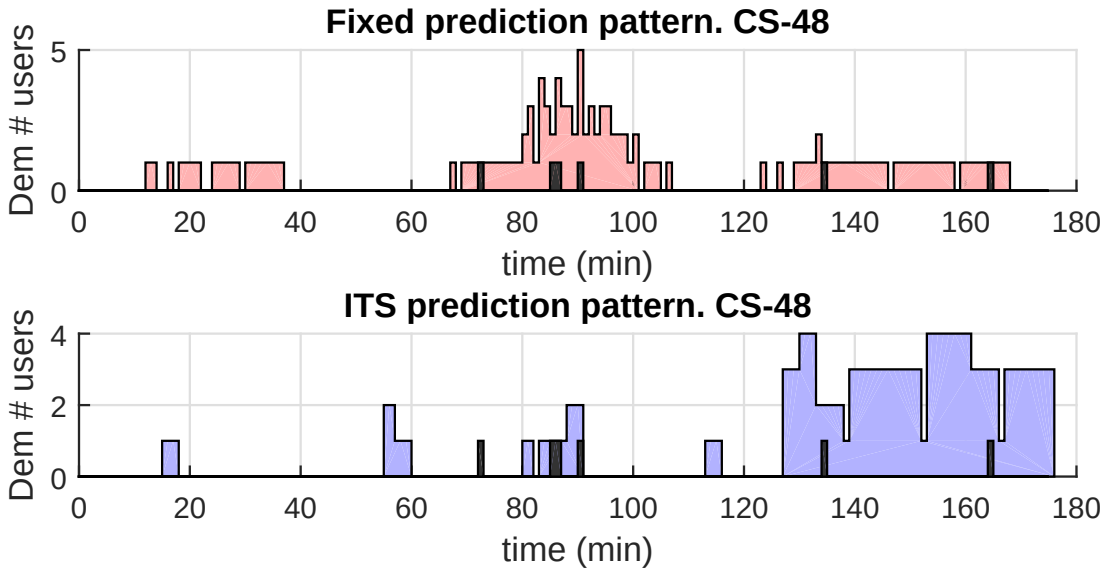

Figure 8.22: Demand prediction methods comparison with a high congested BSS .

Table 8.2 gathers the mean errors and margins measured for different congested BSSs . As it can be seen, the ITS prediction approach manages to avoid unexpected arrivals (what is denoted as *error*) while the margin decreases in low congestion level conditions and increases in high congested BSSs . Those figures are consistent with the effects observed in the preceding figures.

Fixed Pattern		
Congestion Level	**Error**	**Margin**
Low	0.341	4.046
Medium	0.25	1.770
High	1	1.397
ITS approach		
Congestion Level	**Error**	**Margin**
Low	0	2.399
Medium	0	3.607
High	0	9.135

Table 8.2: Error/Margin registered for each congestion level

8.3 BSS Simulator Test

To conclude with the results, some BSS simulations are carried out by considering the two control approaches and demand predictions. From now on, the possible combinations of control and prediction methods will be denoted as shown in Table 8.3. In that way, it is denoted as *blind strategy* the direct application of the discrete control approach (Section 6.1), as *myopic* the combination of the MPC with the fixed pattern prediction method, as *Observer* the application of the MPC and the ITS prediction method and *optimal* if the exact future demand is known.

Control method	Prediction approach	Combination name
Discrete (Section 6.1)	none	Blind
MPC (Section 6.2)	Fixed Pattern	Myopic
MPC (Section 6.2)	ITS	Observer
MPC (Section 6.2)	Exact	Optimal

Table 8.3: Methods combination notation

Each strategy will be applied over three BSSs placed in spots with different traffic congestion levels. The comparison is based on the revenues obtained at the end of the simulation by taking into account the QoS turned in economic penalties.

Figures 8.23, 8.24, 8.25 and 8.26 show the performance of each combination related to a BSS where all the interesting effects worthy of being commented can be seen. On the one hand, Figure 8.24 shows how the lack of adaptability that *myopic* combination presents can result in a swapping operation involving a partially charged battery, something that does not happen with others control combinations. On the other hand, it can be seen a direct relation between the number of charging cycles applied when there is no customer arrival and the prediction accuracy. In that sense, the *observer* combination shows a behavior closer to the *optimal* one than the *myopic*. Figures 8.27, 8.28, 8.29 and 8.30 show the evolution of a BSS placed in a more congested area where the same discussion is valid. Table 8.4 gathers the total revenues considering the whole system as well as the mean value for the BSSs for each combination. The advantage of the *observer* approach can be clearly seen since it reports better results in both cases.

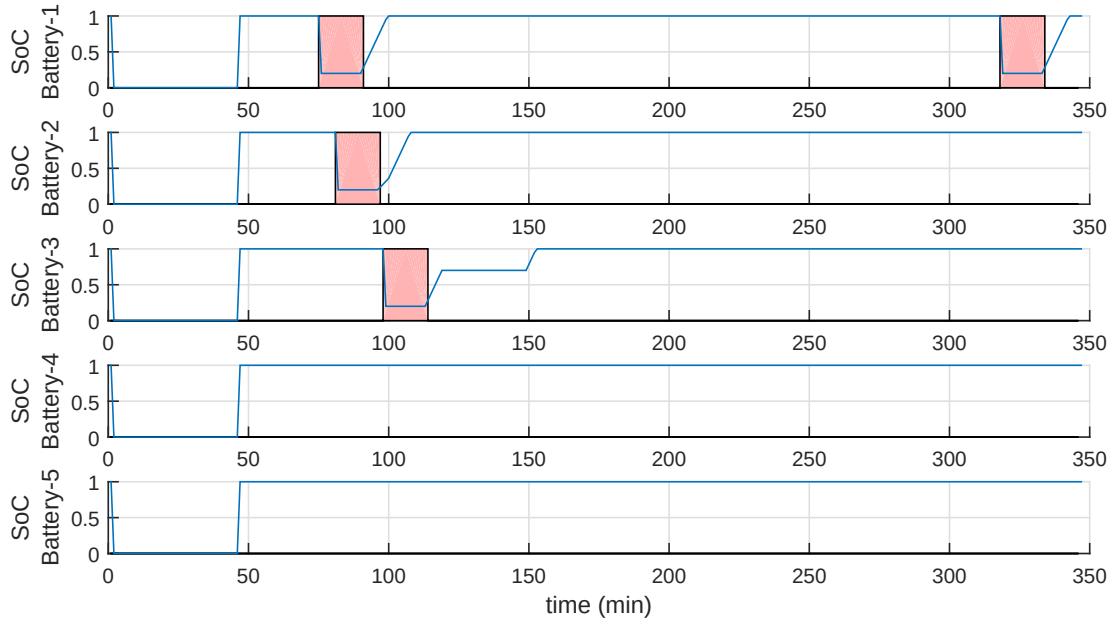

Figure 8.23: *Blind* combination applied over a BSS placed in a low congested area. Case 1

Value	Combination	Revenues
Total	Blind	510
	Myopic	613
	Observer	638
	Optimal	670
Mean	Blind	51
	Myopic	68
	Observer	70
	Optimal	75

Table 8.4: Numeric comparison between considered combinations

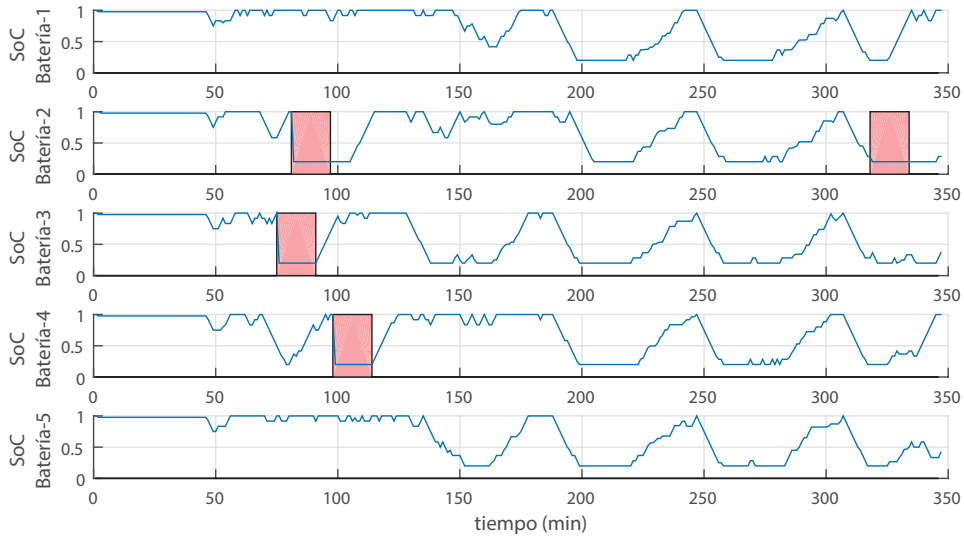

Figure 8.24: *Myopic* combination applied over a BSS placed in a low congested area. Case 1

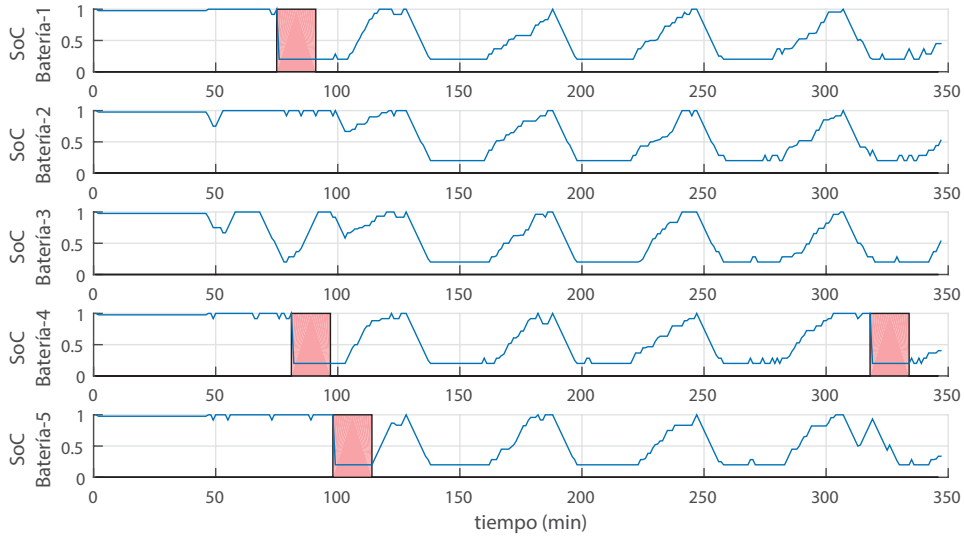

Figure 8.25: *Observer* combination applied over a BSS placed in a low congested area. Case 1

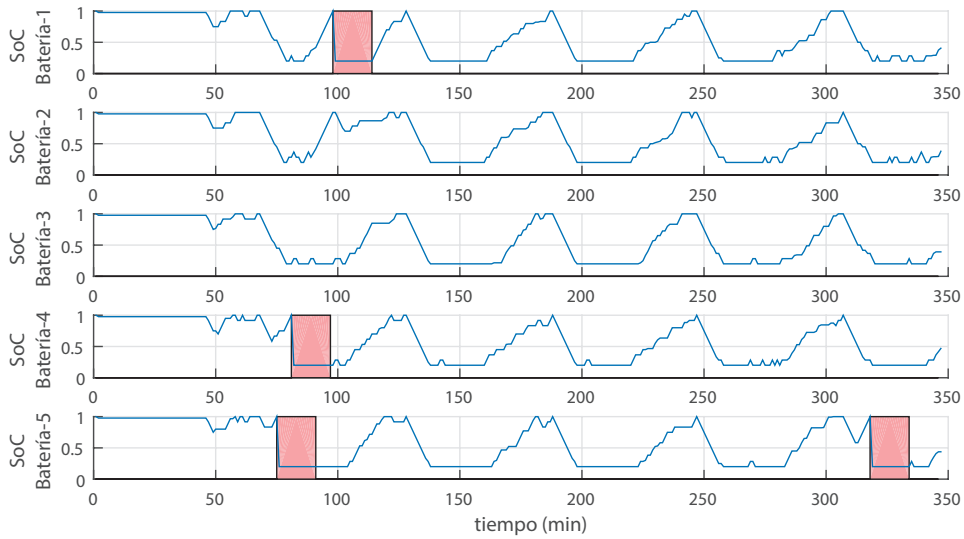

Figure 8.26: *Optimal* combination applied over a BSS placed in a low congested area. Case 1

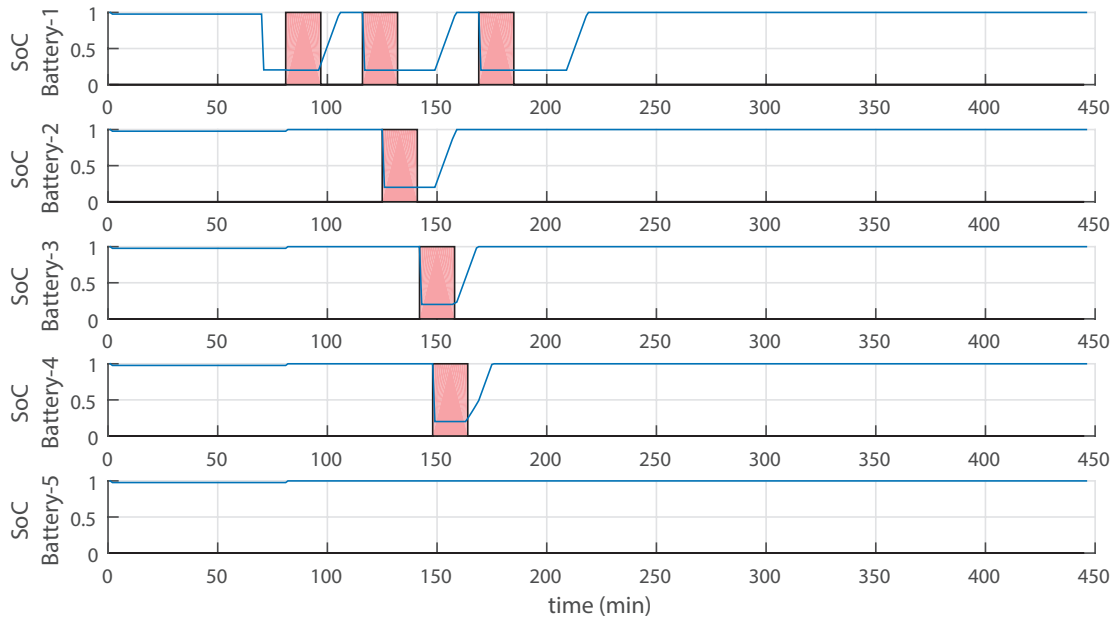

Figure 8.27: *Blind* combination applied over a BSS placed in a low congested area. Case 2

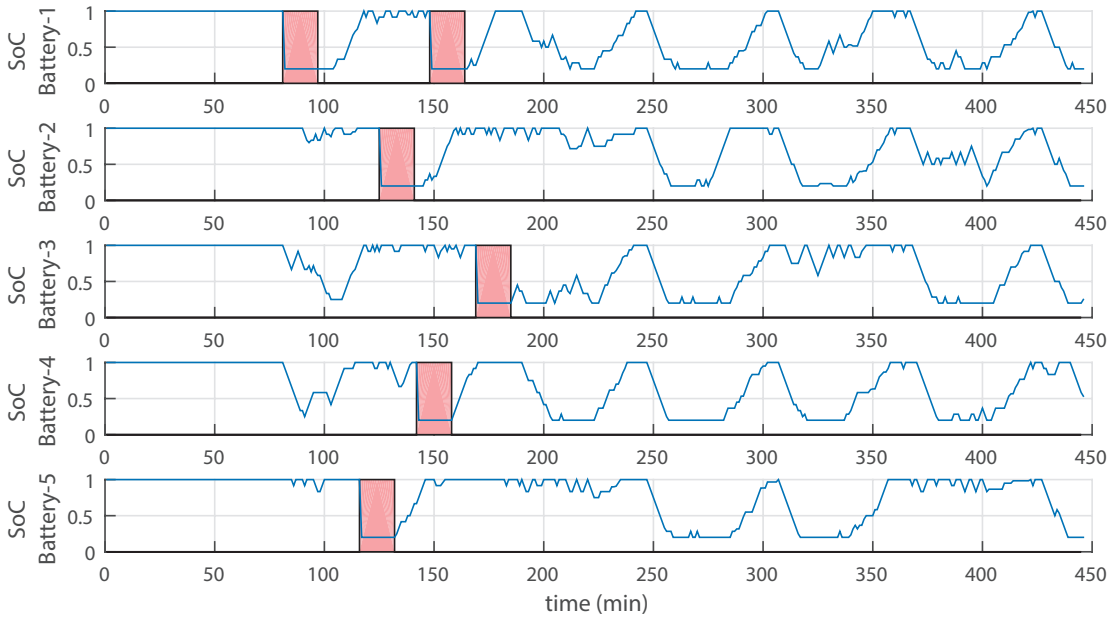

Figure 8.28: *Myopic* combination applied over a BSS placed in a low congested area. Case 2

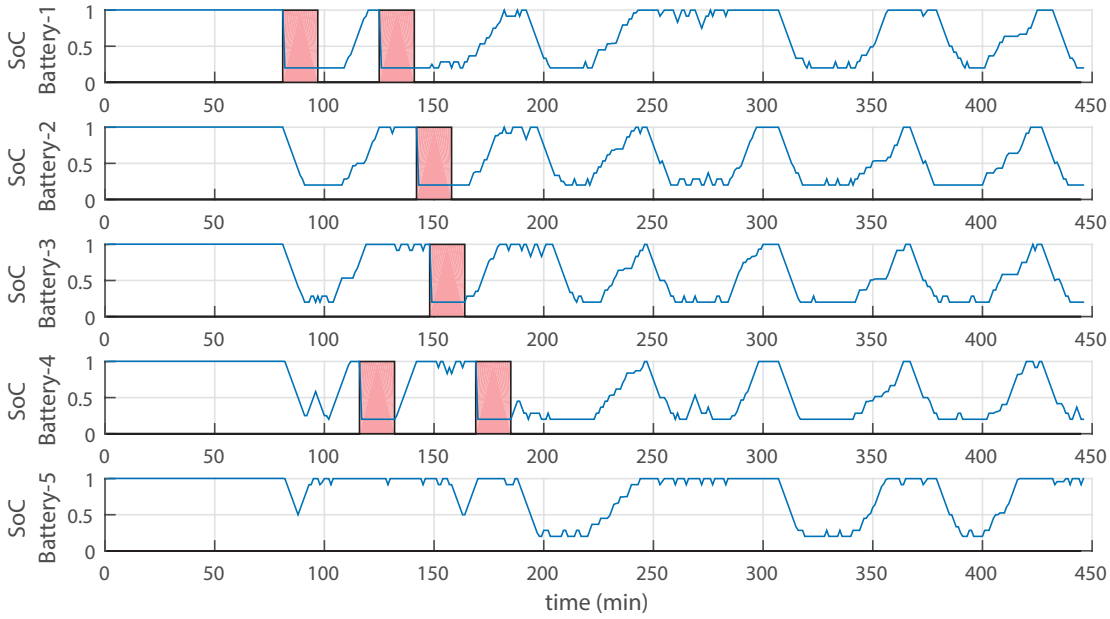

Figure 8.29: *Observer* combination applied over a BSS placed in a low congested area. Case 2

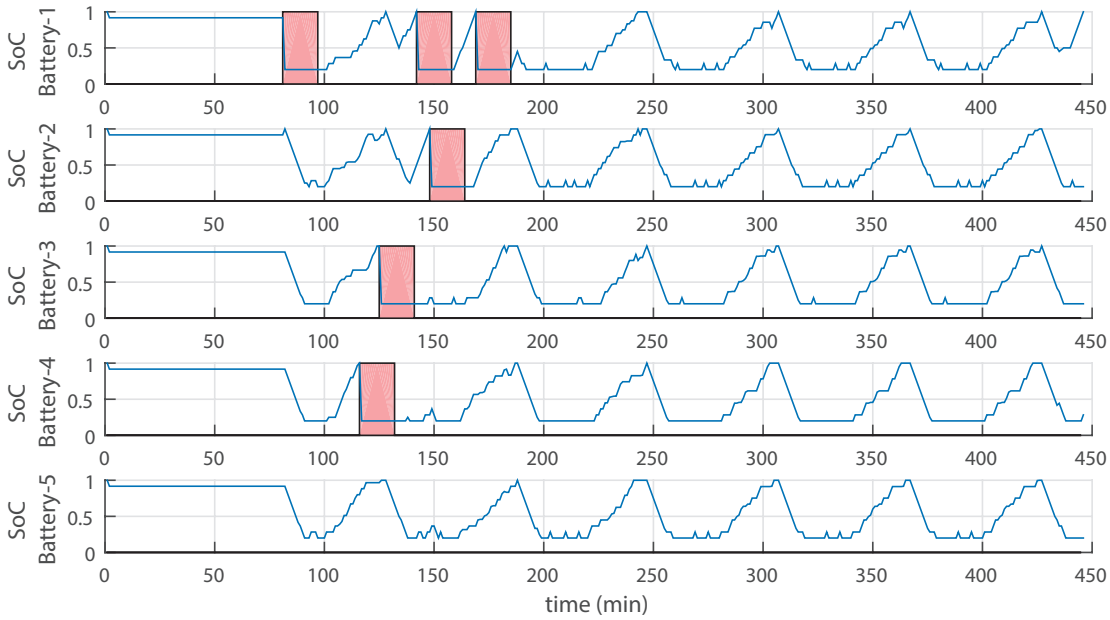

Figure 8.30: *Optimal* combination applied over a BSS placed in a low congested area. Case 2

Chapter 9 Conclusions and future work

This work presents a brief study about BSS operation and demand prediction effects. First, an artificial environment is developed in order to use it as a tool for testing charging strategies. After having detailed the system components and performance, an MPC to operate the BSS in the most profitable way is presented. Subsequently, the key aspects of demand forecasting are discussed. The main contributions of this works comprise the optimization problem proposed as well as the result regarding the importance of the demand forecasting accuracy. The latest shows how, when a queue that decouples the BSS arrival rate and the SS arrival rate exists, the demand forecasting accuracy is more important in situations of low congestion than in high congestion scenarios. Besides, ITS concept materialized as information about the SoC and traffic density on the road, has been presented as a promising tool for managing properly a BSS , and the implications of its resolution have been discussed. Finally, the performance of different combinations of control and demand prediction strategies (*Blind*, *Myopic*, *Observer* and *Optimal*) is measured in terms of revenues and QoS . The application of the MPC together with the ITS demand prediction approach, reports the best value of both indicators.

Several future works can be built on this thesis. Regarding the *simulation tool* used, a more complex rational behavior and road-map could be included as well as demand response mechanisms. Regarding the own *system architecture* it could be though that a likely future scenario could comprises EVs supporting both, charging and swapping batteries operation. In those terms, it would be interesting analyzing the advantages of having a Hybrid Charging Station (HCS) able to serve energy to EVs by swapping their batteries already charged and by charging the customers' batteries directly from the grid. That feature would suppose a good way to serve unexpected customer arrivals.

The own mathematical programming optimization could be extended to take into account some desirable effects that have not been included. For instance the number of cycles applied over the batteries could be bounded including a cost to each cycle, different charging/discharging performances could be considered, the switching frequency between charging and discharging states could be limited, several types of batteries could be included, the power used to manage the batteries could be penalized in order to apply high power flow only when necessary etc.

Associated with this work, one could consider the option of studying Demand Response Management mechanisms in order to reach some target. For instance, a BSS could be interested in varying the charging prices in order to reduce/increase the congestion level during some periods. Such a thing could be done by including a demand response model and the swapping price in the optimization problem, giving to the algorithm certain influence over the future demand. A further extension could consists in considering the BSSs able to transmit information and to make decisions about their prices in order to reach a common objective.

Since the algorithm proposes manages to handle a battery farm that, eventually, has defined its plugging time, it could be used to manage big parking places and long-term stay customers. The interesting thing here would be to include Vehicle to Grid (V2G) operations.

In relation with the demand forecasting, the first thing to improve could be providing mechanisms for detecting and correcting the undesirable effects entailed by the ITS method (parked car influence and the oversize prediction). Furthermore, an alternative way to reduce the prediction error could be considering that customers have the possibility of booking its charging/swapping time before hand by defining their arrival time.

Last but not least, the information provided by the ITS could be modified in order to reduce the uncertainty. For instance, instead of using the mean value of the SoC or the center of each ITS cell as the real position, the SoC_{Cell} could be generated by a weighted sum giving more importance to the slow SoCs ($SoC_{Cell} = \sum_i w_i(SoC_i)SoC_i$) and the cell position could be substituted by the cell barycenter.

Bibliography

[1] F. Malandrino, C. Casetti, and C.-F. Chiasserini, "The role of its in charging opportunities for evs," in *Intelligent Transportation Systems-(ITSC), 2013 16th International IEEE Conference on*, pp. 1953–1958, IEEE, 2013.

[2] Y. Zheng, Z. Y. Dong, Y. Xu, K. Meng, J. H. Zhao, and J. Qiu, "Electric vehicle battery charging/swap stations in distribution systems: comparison study and optimal planning," *Power Systems, IEEE Transactions on*, vol. 29, no. 1, pp. 221–229, 2014.

[3] J. Yang and H. Sun, "Battery swap station location-routing problem with capacitated electric vehicles," *Computers & Operations Research*, vol. 55, pp. 217–232, 2015.

[4] X. Tan, B. Sun, and D. H. Tsang, "Queueing network models for electric vehicle charging station with battery swapping," in *Smart Grid Communications (SmartGridComm), 2014 IEEE International Conference on*, pp. 1–6, IEEE, 2014.

[5] M. R. Sarker, H. Pandzic, and M. A. Ortega-Vazquez, "Optimal operation and services scheduling for an electric vehicle battery swapping station," 2014.

[6] M. R. Sarker, H. Pandzic, and M. A. Ortega-Vazquez, "Electric vehicle battery swapping station: business case and optimization model," in *Connected Vehicles and Expo (ICCVE), 2013 International Conference on*, pp. 289–294, IEEE, 2013.

[7] S. Yang, J. Yao, T. Kang, and X. Zhu, "Dynamic operation model of the battery swapping station for ev (electric vehicle) in electricity market," *Energy*, vol. 65, pp. 544–549, 2014.

[8] L. Xinyi, L. Nian, H. Yangqi, Z. Jianhua, and Z. Nan, "Optimal configuration of ev battery swapping station considering service availability," in *Intelligent Green Building and Smart Grid (IGBSG), 2014 International Conference on*, pp. 1–5, IEEE, 2014.

[9] B. Sun, X. Tan, and D. H. Tsang, "Optimal charging operation of battery swapping stations with qos guarantee," in *Smart Grid Communications (SmartGridComm), 2014 IEEE International Conference on*, pp. 13–18, IEEE, 2014.

[10] P. Xie, B. Qian, D. Shi, J. Chen, and L. Zhu, "Supplementary automatic generation control using electric vehicle battery swapping stations," in *Power and Energy Society General Meeting (PES), 2013 IEEE*, pp. 1–5, IEEE, 2013.

[11] Q. Dai, T. Cai, S. Duan, and F. Zhao, "Stochastic modeling and forecasting of load demand for electric bus battery-swap station," 2014.

[12] E. Xydas, C. Marmaras, L. Cipcigan, A. Hassan, and N. Jenkins, "Forecasting electric vehicle charging demand using support vector machines," in *Power Engineering Conference (UPEC), 2013 48th International Universities'*, pp. 1–6, IEEE, 2013.

[13] A. Nkoro and Y. Vershinin, "Current and future trends in applications of intelligent transport systems on cars and infrastructure," in *Intelligent Transportation Systems (ITSC), 2014 IEEE 17th International Conference on*, pp. 514–519, IEEE, 2014.

[14] S. C. Alessandro Di Giorgio, Francesco Liberati, "Iec 61851 compliand electric vehicle charging control in smartgrids," 2013.

[15] J. Johnson, M. Chowdhury, Y. He, and J. Taiber, "Utilizing real-time information transferring potentials to vehicles to improve the fast-charging process in electric vehicles," *Transportation Research Part C: Emerging Technologies*, vol. 26, pp. 352–366, 2013.

[16] I. P. Safak Bayram, George Michailidis and M. Devetsikiotis, "Decentralized control of electric vehicles in a network of fast charging stations," 2013.

[17] T. K. X. Z. Shengjie Yang, Jiangang Yao, "Dynamic operation model of the battery swapping station for ev (electric vehicle) in electricity market," 2014.

[18] C. Guéret, C. Prins, and M. Sevaux, "Applications of optimization with xpress-mp," *contract*, p. 00034, 1999.

[19] J. Lofberg, "Yalmip: A toolbox for modeling and optimization in matlab," in *Computer Aided Control Systems Design, 2004 IEEE International Symposium on*, pp. 284–289, IEEE, 2004.